CHAPTER 3

PRE-OPTIMIZATION OF BACTERIAL CELLULOSE PRODUCTION: INVESTIGATING KEY FACTORS AFFECTING YIELD AND PROPERTIES

3.1 Abstract

Bacterial cellulose (BC) is a high-value biopolymer with broad applications in food, biomedical, and material sciences. However, its production is constrained by the high cost of traditional culture media. This study explores the use of Thai tea kombucha as a low-cost and culturally relevant medium for BC production, with the goal of identifying favorable conditions for subsequent process optimization. The study was conducted under static conditions at 30 °C for 15 days using a commercial SCOBY as the inoculum. Four types of tea—Chinese Black Tea (RBTH), *Assamica* Black Tea (BTC), Thai Green Tea (GTC), and Thai Red Tea (RTC)—were evaluated. Among them, RTC produced the highest wet BC yield (168.00 ± 2.93 g/L), making it the most promising substrate. To further explore yield enhancement, RTC-based media were supplemented with various additives (ethanol, pure coffee, yeast extract, soy protein isolate, and vitamin C) and different carbon source combinations. The highest yield was obtained with ethanol supplementation (RTC-EtOH, 218.36 ± 12.85 g/L) and the sucrose-glucose combination (RTC-SGlu, 259.54 ± 8.92 g/L), though not significantly different from RTC-sucrose-dextrose. Further investigation of basic fermentation parameters—including initial pH, tea concentration, cultivation duration, and harvesting frequency—revealed that unadjusted pH (~5.20), tea concentrations of 2%, and bi-weekly harvesting over four weeks yielded the best results (368.22 ± 28.33 g/L cumulative). Characterization of the resulting BC using SEM, FTIR, XRD, TGA/DTG, and nanoindentation confirmed acceptable physical and chemical properties, including good fiber structure, crystallinity, thermal stability, and mechanical strength. This

preliminary study establishes the suitability of Thai red tea kombucha as a viable fermentation medium. It provides essential baseline data to guide the statistical optimization in the next phase of research.

Keywords: Bacterial nanocellulose, Thai tea, kombucha, mechanical properties, nano-indentation

3.2 Introduction

Bacterial cellulose (BC) is a sustainable and multifunctional biomaterial distinguished by its exceptional mechanical strength, high crystallinity, purity, and biocompatibility (Lin et al. 2020). Unlike plant-derived cellulose, BC is extracellularly synthesized by *Komagataeibacter* spp. as a nanofibrillar network, free of lignin and hemicellulose contaminants (Gorgieva and Trček 2019). Its unique properties have enabled diverse applications in the food industry, where it serves as a food ingredient, fat replacer, dietary fiber, thickening agent, and stabilizer in emulsions (Reiniati 2017; Lin et al. 2020). BC has also been incorporated into functional foods and traditional desserts, as well as employed as a carrier for bioactive compounds such as antioxidants, probiotics, and enzymes (Khan et al. 2018; Azeredo et al. 2019a; Li et al. 2021).

Despite these advantages, commercial BC production remains limited due to the high costs associated with conventional media, which typically utilize purified glucose and refined nutrients (Revin et al. 2018; El-Gendi et al. 2022; Kamal et al. 2022). In response, research has focused on exploring low-cost substrates such as agricultural by-products, food industry residues, and waste biomass to reduce production costs (Tsouko et al. 2015; Waghmare et al. 2018; Akintunde et al. 2022). Among these, kombucha fermentation—employing a symbiotic culture of bacteria and yeast (SCOBY)—has gained attention as an eco-friendly, scalable, and cost-effective system for BC production (Dhali et al. 2021) (Mehrotra et al. 2023). Using simple ingredients like tea and sugar, kombucha fermentation can produce BC with properties comparable to those obtained from synthetic media. However, BC yield and quality in

this system are highly sensitive to multiple variables, including tea type, sugar composition, fermentation conditions, and microbial dynamics.

Thailand offers a wide diversity of tea products, such as black tea, green tea, and Thai red tea, that present promising substrates for BC production. Variations in tea processing methods lead to differences in nutrient composition, potentially influencing microbial metabolism and BC yield (Shevchuk et al. 2020; Deka et al. 2021). Thai red tea, often a blend of black tea with herbs, spices, and colorants, may introduce unique bioactive compounds not present in other teas. While some studies have investigated black and green teas for BC production, systematic comparisons across diverse Thai teas remain limited.

Beyond tea type, numerous studies have shown that additives and carbon source variations can further enhance BC yield and tailor its properties. Additives such as vitamin C (VC) act as antioxidants and metabolic cofactors, improving crystallinity and yield (Keshk 2014; Cielecka et al. 2021; Leonarski et al. 2021a). Nitrogen sources like yeast extract (YE) and soy protein isolate (SPI) supply essential nutrients for bacterial growth (Aswini et al. 2020; Almihyawi et al. 2024) (Wen et al. 2024). Ethanol can optimize metabolic pathways, increasing glucose utilization and cellulose biosynthesis (Kazemi et al. 2015; Agustin and Padmawijaya 2018; Montenegro-Silva et al. 2024). Similarly, coffee-based additives rich in phenolic compounds serve as stimulants and alternative carbon sources (De Souza et al. 2021; Jiménez-Sánchez et al. 2024).

The selection and combination of carbon sources also critically influence BC production. Different substrates are metabolized via distinct pathways, affecting both yield and productivity. Glucose and dextrose are quickly utilized through glycolysis, while fructose contributes via both glycolysis and the TCA cycle (Wang et al. 2018; Trevino-Garza et al. 2020). Glycerol not only serves as a carbon source but also promotes microbial viability as an osmoprotectant (Aswini et al. 2020). Various studies have reported that glycerol consistently enhances BC yield compared to other sugars,

while optimal sucrose concentrations and honey have also shown promising results (Kalifawi 2018; Trevino-Garza et al. 2020; De Souza et al. 2021; Amorim et al. 2024).

In addition to substrate composition, process parameters such as initial pH, fermentation time, tea concentration, and cultivation method play crucial roles in determining BC productivity and characteristics. Moderate acidity (around pH 5) generally favors BC synthesis, while extreme pH levels can inhibit microbial growth (Tsouko et al. 2015). Extended fermentation time allow thicker BC pellicle formation but may ultimately reduce quality due to nutrient depletion and microbial senescence (Lin et al. 2013). Tea provides essential bioactive compounds—including polyphenols, caffeine, and minerals—that stimulate microbial activity, but excessive concentrations may disrupt fermentation balance (Mann et al. 2017). Cultivation methods also influence production outcomes: static culture produces high-quality BC but at lower yields, whereas dynamic systems (agitation or shaking) often enhance yield and homogeneity at the potential cost of reduced mechanical properties (Wang et al. 2019b; Gao et al. 2020; Lahiri et al. 2021; Akintunde et al. 2022).

This study investigated key factors influencing BC productivity with the aim of identifying conditions conducive to further optimization. The variables examined include the type of Thai tea—Chinese Black Tea (RBTH), *Assamica* Black Tea (BTC), Thai Green Tea (GTC), and Thai Red Tea (RTC); various additives—vitamin C (VC) as a metabolic enhancer, yeast extract (YE) and soy protein isolate (SPI) as nitrogen sources, ethanol (EtOH) as a metabolic modulator, and pure coffee (PC) as a phenolic stimulant; combinations of carbon sources—sucrose (control), sucrose-glucose (S-Glu), sucrose-dextrose (SD), sucrose-fructose (SF), and sucrose-glycerol (SGLy); as well as initial pH, fermentation duration, tea concentration, and cultivation method. The findings are expected to contribute to the development of optimized and cost-effective strategies for enhanced BC production.

3.3 Materials and Methods

The materials used in this study include a commercial kombucha starter (SCOBY) from Neo Cold Brew Shop (Thailand), sucrose, various teas (red tea-vanilla flavor (*ChaTraMue*, RTC), green tea mix (*ChaTraMue*, GTC), black tea (*ChaTraMue*, BTC), and Chinese black tea (Three Horses brand No. 3, RBTH)), Various of additives (yeast extract (Merck), ethanol absolute anhydrous (Carlo Erba), commercial vitamin C (Bright Aromatic and Chemical, Thailand), commercial soy protein isolate (KME Mart, Thailand), and commercial pure coffee (Nescafe gold brand)), and various carbon sources (D-glucose (UniVAR, Merck), D-fructose (Carlo Erba), sucrose (ACI Labscan), dextrose monohydrate (KC, Bangkok Chemical), and glycerol (Merck). Other chemicals include sodium hydroxide (NaOH, Q RëC™) and hydrochloric acid 37% (HCl, Q RëC™). Water sources included reverse osmosis (RO) and deionized (DI) water.

Equipment used consisted of a cheesecloth, coffee filter, glass jar, funnel, autoclave (Biobase), laboratory glassware, biosafety cabinet (Cryste, Puricube Neo), analytical balance (AE Nimbus NBL 84E), incubator, pH meter (Oakton pH 700), refractometer, oven dryer (XUE058, France-Etuves), FT-IR (Bruker VERTEX 70), XRD (Bruker D8 Advance), SEM (Zeiss AURIGA, Germany), nanoindenter (NanoTest Vantage, Micro Materials Limited, UK), and HPLC (Hitachi Chromaster: RI detector 5450, column oven 5310, auto sampler 5260, and pump 5110).

3.3.1 Experimental Design

This study was designed to systematically evaluate the key factors influencing BC production in a kombucha-based fermentation system. The primary objective was to identify the most effective conditions for maximizing BC yield. In addition to measuring BC yield, selected physicochemical properties of the resulting BC were characterized, along with kombucha culture parameters to support a more comprehensive understanding of the fermentation process. The experimental framework consisted of four main studies, each targeting a different set of variables, as outlined below:

1) Effect of Different Thai Tea Types on BC Yield and Characteristics

This experiment aimed to evaluate the impact of different Thai tea substrates on BC production through kombucha fermentation. Four commercially available Thai teas with distinct compositions were selected, including traditionally used teas—such as Assam-type black tea and Chinese black tea—and flavored blends that are less common in conventional kombucha fermentation. The selection was guided by practical considerations, including local availability, affordability, and insights from previous scientific studies. Market surveys, both online and offline, indicated that some teas were more accessible and cost-effective, making them suitable candidates for reducing production costs. All samples were fermented under identical conditions to assess their influence on BC yield and properties. Detailed descriptions of the tea types and their compositions are provided in **Table 3.1.**

Table 3.1 Thai tea type variations and their compositions used as substrates in kombucha fermentation for BC production

Variation of tea	Samples Code	Composition of tea*
Chines Black Tea (Three Horses Brand No. 3)	RBTH	Dried Chinese tea leaves (100%).
Assamica Black Tea (ChaTraMue Brand)	BTC	Black tea powder (Assam) (100%).
Assamica Green Tea Mix (*ChaTraMue* Brand)	GTC	Green tea powder (Assam) (94%), sugar (5%), nature identical flavor, FD&C Yellow No. 5 (INS 102), FD&C Yellow No. 6 (INS 110), FD&C Blue No. 1 (INS 133)
Assamica Red Tea Powder-Vanilla Flavor (*ChaTraMue* Brand)	RTC	Red tea powder (Assam) 94%, sugar 5%, artificial flavors, FD&C Yellow No. 6 (INS 110)

**Based on product label information available on the packaging.*

The fermentation broth was characterized for pH, total soluble solids (°Brix), and sugar composition before and after fermentation using standard analytical methods. The BC produced was evaluated for wet and dry yield, water holding capacity (WHC), visual appearance, and color. Surface morphology was examined using scanning electron microscopy (SEM), and chemical functional groups were identified through Fourier-transform infrared spectroscopy (FTIR). Crystallinity and crystallite size were determined using X-ray diffraction (XRD), while thermal behavior was assessed by thermogravimetric analysis (TGA). Mechanical properties of the BC were measured using nanoindentation.

2) Effect of Different Types of Additives on BC Yield and Characteristics

This study examined the effects of five different additives—selected for their distinct nutritional and functional properties—on the productivity and characteristics of BC. Thai red tea (RTC), identified as the optimal substrate from the previous experiment, was used as the fermentation medium. The additives were chosen based on prior studies indicating their potential to enhance microbial growth, stimulate BC biosynthesis, or improve product quality. Each additive was incorporated at predetermined concentrations, as detailed in **Table 3.2**.

Table 3.2 Types of additives incorporated into the fermentation medium for BC production in Thai tea-based kombucha fermentation

Type of additive	Samples code	Concentration	References
Control*	RTC-C	-	-
Soy protein isolate	RTC-SPI	0.5% (w/v)	-
Ethanol	RTC-EtOH	1% (v/v)	(Kazemi et al. 2015; Cielecka et al. 2021; Fei et al. 2023)
Vitamin C	RTC-VC	0.5% (w/v)	(Keshk 2014)
Yeast extract	RTC-YE	0.5% (w/v)	(Aswini et al. 2020)
Puree coffee	RTC-PC	0.8% (w/v)	(De Souza et al. 2021)

**) The tea used in this study is based on a previous study, i.e. Thai red tea (ChaTraMue Brand)*

The objective of the study was to assess how these supplemental ingredients affect BC yield, structural attributes, and overall production efficiency, thereby providing insights for optimizing BC fermentation conditions. Each sample was fermented using the same set of conditions. The characterization parameters for both the fermentation broth and the BC in this experiment were consistent with those used in the previous experiment, including pH, total soluble solids (°Brix), sugar composition, wet and dry yield, WHC, surface morphology, chemical functional groups, crystallinity, thermal behavior, and mechanical properties. Due to the insignificant changes in color after purification, BC color analysis was not performed

3) Effect of Carbon Source Combinations on BC Yield and Characteristics

This study systematically evaluated five carbon source formulations to optimize BC production (**Table 3.3**) in Thai red tea fermentation as the selected tea for BC production. The experimental design leveraged distinct metabolic advantages of each component: while sucrose (hydrolyzed to glucose and fructose) served as the foundational carbon source, dextrose and glucose were included to boost UDP-glucose precursor supply for cellulose polymerization. Fructose supplementation targeted enhanced energy generation through TCA cycle activity, whereas glycerol provided dual benefits as both a carbon source and an osmoprotectant. The fermentation conditions were consistent across all samples.

The characterization parameters for both the fermentation broth and the BC in this experiment were consistent with those used in the previous study, including pH, total soluble solids (°Brix), sugar composition, wet and dry yield, WHC, surface morphology, chemical functional groups, crystallinity, thermal behavior, and mechanical properties. BC color analysis was not included in this experiment, as purification resulted in minimal variation.

Table 3.3 Carbon source combinations tested for BC production in in Thai tea-based kombucha fermentation.

Carbon source	Code	Total carbon source (g/100 ml)
Sucrose (S)*	RTC-C	10
Sucrose (S) + Fructose (F)	RTC-SF	5 + 5
Sucrose (S) + Dextrose (D)	RTC-SD	5 + 5
Sucrose (S) + Glycerol (Gly)	RTC-SGly	5 + 5
Sucrose (S) + Glucose (Glu)	RTC-SGlu	5 + 5

** Sucrose as control treatment*

4) Effect of Process Parameters: initial pH, Harvesting Time, Tea Concentration, and Cultivation Method on BC yield and WHC

This multifactorial study examined the influence of key fermentation parameters on BC yield, using the following experimental variations. This experiment utilized the optimal tea i.e. Thai red tea.

- **Effect of Different Initial pH on the BC Yield and WHC**

This experiment investigated the impact of different initial pH on BC yield and WHC. The pH of the fermentation medium was adjusted to target values of 5, 6, and 7 by adding either 0.1 N NaOH or 0.1 N HCl until the desired pH was reached. A control group was included without pH adjustment, maintaining the natural pH of the medium at approximately 5.2. Prior to and after fermentation, the broth of each sample was analyzed for pH and total soluble solids (°Brix). Additionally, the yield of BC and its WHC were measured for each treatment.

- **Effect of Different Harvesting Period on BC Yield and WHC**

This experiment investigated the effect of different harvesting periods on BC yield and WHC. Samples were divided into four harvesting groups: 1st week, 2nd week, 3rd week, and 4th week. After the initial harvest, the 1st, 2nd, and 3rd week samples were allowed to continue fermenting and were harvested again along

with the 4th week group. For the 1st, 2nd, and 3rd week samples, total BC yield was calculated by summing the *wet weight after purification* and the *dry weight after drying* from both the first and second harvests. The 4th week samples were harvested only once. Before and after fermentation, pH and °Brix values of the sample broths were measured. BC yield and WHC were subsequently determined for each treatment group. The experimental design related to the harvesting period variations is summarized in **Table 3.4.**

Table 3.4 Experimental design of harvesting period for BC production

Treatment	Harvesting time			
Harvest 1st week	7th day	-	-	28th day
Harvest 2nd week	-	14th day	-	28th day
Harvest 3rd week	-	-	21st day	28th day
Harvest 4th week	-	-	-	28th day

- **Effect of Different Tea Concentration on BC Yield and WHC**

To evaluate the impact of varying tea concentrations on BC yield and WHC, a study was conducted using concentrations of 1%, 2%, and 3% (w/v). Broth samples were analyzed for pH and total soluble solids (°Brix) both before and after fermentation. The resulting BC yield and WHC were also determined for each treatment.

- **Effect of Different Cultivation Methods on BC Yield and WHC**

The study on various cultivation methods, including static, shaking, and agitated cultures, was conducted to investigate their effects. Static cultivation served as the control method, while shaking cultivation was performed using an orbital shaker at 150 rpm, and agitated cultivation was conducted in a bottle with a magnetic stirrer at 150 rpm (Zywicka et al. 2015). Broth samples were analyzed

for pH and total soluble solids (°Brix) at both pre- and post-fermentation stages. The resulting BC yield and WHC were also measured for each treatment.

3.3.2 Bacterial Cellulose Production

1) Medium Preparation

In general, the fermentation medium was prepared as follows: a total of 20 g of sucrose and tea extract (at a concentration of 10 g/L) were added to a 480 mL glass jar. The tea extract was prepared by brewing 2 g of tea leaves in 180 mL of hot deionized water (~90 °C) for approximately 15 minutes. After brewing, the tea was filtered and combined with sucrose in the jar. The mixture was then adjusted to a final volume of approximately 180 mL using deionized water, stirred until homogeneous, covered, and sterilized by autoclaving (121 °C, 15 minutes, 1 psi). After sterilization, the medium was cooled to room temperature (~30–35 °C).

To study the effect of different tea types, the tea component was substituted with various tea variants (see **Table 3.1**) at the same concentration (10 g/L). Thai red tea (RTC) was identified as the most effective and was subsequently used in all following experiments using the same formulation (1% tea concentration), except in experiments investigating the effect of different tea concentrations. For the study on the harvesting period, the general formulation was also used prior to evaluating its impact.

For the additive effect study, selected additives were incorporated into the medium based on the formulations provided in **Table 3.2.** Yeast extract (YE), soy protein isolate (SPI), and peptone casein (PC) were added prior to sterilization, whereas ethanol (EtOH) and vitamin C (VC) were added after cooling, immediately before inoculation.

For the study on carbon source effects, the carbon sources were varied according to the combinations detailed in **Table 3.3.** The general formulation was also used as the base medium for experiments investigating the effects of initial

pH, fermentation time, and cultivation method. In the initial pH variation study, the pH was adjusted to 5, 6, and 7 using 0.1 N HCl or 0.1 N NaOH, while the control (unadjusted) had an initial pH of approximately 5.20. Acid or base was added dropwise prior to sterilization, with pH monitored concurrently.

To examine the effect of tea concentration, tea infusions were prepared at concentrations of 1%, 2%, and 3% using the same brewing method described in the general procedure. Each sample was adjusted to a final volume of approximately 180 ml.

2) Regeneration of Kombucha Starter

In the first experiment, designed to study the effect of different tea types, kombucha cultures were prepared using four types of tea: RTC, GTC, BTC, and RBTH. The kombucha cultures were prepared in accordance with the tea types used in the fermentation media. Each sterilized tea medium was inoculated with 20 mL of commercial kombucha starter, mixed thoroughly, covered with two layers of cheesecloth, and fermented for 14 days at approximately 30 ℃. Based on the results, Thai red tea (RTC) was selected as the optimal tea. Therefore, in all subsequent experiments, kombucha cultures were consistently prepared using RTC and regenerated every two weeks to maintain experimental consistency. Kombucha culture regeneration was carried out separately for each experimental treatment or study design.

3) Kombucha Fermentation for BC Production

The sterilized media, prepared according to each experimental design, were inoculated with 20 mL (10% (v/v)) of regenerated kombucha starter and gently shaken to ensure thorough mixing. The jars were covered with two layers of cheesecloth and incubated for 15 days at approximately 30 ℃. In the experiment examining different tea types, a control consisting of a 10% sucrose solution without tea was included under the same conditions. For all subsequent experiments, a medium containing Thai red tea (RTC) with 10% sucrose was used as the control for

BC production. Each experiment was conducted independently and simultaneously in triplicate, following its respective design.

4) Harvesting and Purification of BC

After around 15 days of fermentation, the BC was separated by lifting it using tweezers and drained for ±10 minutes. The BC was then heated in boiling water for about 30 minutes and drained for about 10 minutes. The BC is then heated (~90oC) in the alkaline solution (NaOH, 2%) for 120 minutes and rinsed with RO water, then soaked and changed repeatedly with RO water until the pH is neutral (Yanti et al. 2018; Aswini et al. 2020).

3.3.3 Culture Medium Characterization

The culture media were analyzed both before and after fermentation to assess key parameters, including °Brix, pH, and sugar composition (sucrose, glucose, and fructose), depending on the specific experimental design. °Brix was measured using a refractometer, while pH was determined with a pH meter. Sugar composition was analyzed using high-performance liquid chromatography (HPLC).

Sugar composition analysis was performed using an HPLC system (Hitachi Chromaster) equipped with a refractive index (RI) detector (model 5450), column oven (model 5310), auto sampler (model 5260), and pump (model 5110). Separation was achieved using an Aminex HPX-42A column with filtered deionized water (0.22 μm) as the mobile phase, operating at a flow rate of 0.6 mL/min. The column temperature was maintained at 45°C, with an acquisition time of 22 minutes and an injection volume of 20 μL. The standard solution for calibration was prepared by mixing sucrose, glucose, and fructose at a concentration of 60 g/L, resulting in a final concentration of 20 g/L for each sugar. A standard curve was constructed using a series of concentrations: 0, 3, 6, 9, 12, and 15 g/L. Samples were diluted by combining 0.1 mL of the sample with 0.9 mL of DI water in Eppendorf tubes. Both standard solutions and diluted samples were filtered through a 0.22 μm syringe filter prior to HPLC analysis. Before analyzing the standards and samples, the HPLC system was

stabilized to ensure a steady baseline. All measurements were conducted in triplicate to ensure accuracy and reliability.

3.3.4 Bacterial Cellulose Characterization

1) Yield and Water Holding Capacity

After the BC was purified and drained for about 10 minutes, it was weighed to determine the net wet weight. Further, for dry samples, the BC sample was dried using an oven at a temperature of 40°C until it reached a constant weight (Aswini et al. 2020). WHC was determined by calculating the mass of water lost during drying, expressed as the ratio of removed water to the dry weight of the cellulose (g of water per g of dry sample) (Schrecker and Gostomski 2005). The samples were made in three replications.

2) The Color of BC

The appearance of wet BC before and after purification was observed directly and measured using a colorimeter. Observation and analysis was carried out on the sample after it was boiled in RO water and after it was purified using NaOH and neutralization. The purified sample was then compared to the commercial nata de coco (NDC) as a control. The color investigation was determined with a portable digital colorimeter using the CIELAB color parameters L* (luminosity), a* (-green to +red), and b* (-blue to +yellow). The details of the method are mode measurement: RSEX, path length of cell: (-), port size: 0.375 inch, and scale: CIE Lab. The analysis was made in three repetitions.

3) Morphology Analysis Using Scanning Electron Microscope (SEM)

The surface morphology of BC was analyzed using a scanning electron microscope (SEM). After the BC samples were dried, the BC sheets were cut to a size of approximately 5×5 mm, positioned on a sample stage, and coated with gold. The fiber diameter was determined by analyzing SEM images with Image J software (Volova et al. 2022). The number of data points taken for fiber diameter analysis was 50.

4) Fourier Transform Infrared Spectroscopy Analysis

The functional group of the sample was analyzed using FT-IR spectroscopy. The spectral data was collected at a wavelength of around 400–4000 cm^{-1}. The resolution was 4 cm^{-1}, the background and sample scan times were 64, and the result spectrum was transmittance. The measurements were carried out at room temperature.

5) X-Ray Diffraction (XRD) Analysis

Crystal characteristics, primarily the 2θ diffraction peaks and crystallinity index (CI), were analyzed using a Bruker D8 Advance X-ray diffractometer. The measurements were conducted in Coupled Theta/2Theta scan mode with Continuous PSD Fast acquisition. A Cu Kα radiation source (λ = 1.5418 Å) was used, operating at 40 kV and 40 mA (power = 1600 W). The detector employed was a LYNXEYE 1D position-sensitive detector. Data were collected over a 2θ range of 10° to 60° with an increment of 0.0204°, a step count of 2446, and a time per step of 0.400 seconds, resulting in a total scan time of approximately 1035.2 seconds. Crystallinity index was calculated using **Equation 3.1**, and average crystallite size was determined by the Scherrer equation (**Equation 3.2**), with data processing performed in *OriginLab* and *Microsoft Excel*.

$$CI = \frac{Total\ Area\ of\ Crystalline\ Peak}{Total\ Area\ of\ Crystalline\ and\ AmporphousePeak}\ x\ 100\% \quad \text{.....(Eq. 3.1)}$$

$$d = \frac{K\lambda}{\beta \cos\theta} \quad \text{.....(Eq. 3.2)}$$

where *CI* is the crystallinity index, *d* is the crystallite size, *K* is the Scherrer constant (0.89), λ is the wavelength of the X-ray radiation (1.5418 Å for Cu Kα), β is the full width at half maximum (FWHM) of the diffraction peak in radians, and θ is the Bragg angle corresponding to the peak position (in radians, i.e., half of the 2θ value) (Sardjono et al. 2019).

6) Thermogravimetric (TGA/DTG) Analysis

The dynamic weight loss and thermal decomposition behavior of the BC samples were analyzed using a thermogravimetric analyzer (Mettler-Toledo, Model TGA/DSC1). The samples were heated on an alumina sampling pan from 28°C to 600°C at a rate of 10°C/min under nitrogen (N_2) gas purging with a flow rate of 30 mL/min. The TGA/DTG data was processed using *OriginLab* software, and the TDA/DTG graph was made in *MS Excel* software.

7) Mechanical Properties analysis Using Nanoindentation

A nanoindenter was used to evaluate the mechanical properties of BC films, including penetration depth at a maximum load of 50 mN, hardness, reduced modulus, elastic recovery parameter (ERP), and Young's modulus. Samples were prepared by cutting them into circular shapes with a diameter of 0.8 cm and mounted flat on a clear acrylic holder using white glue (adhesive latex), without additional treatment. Indentation tests were performed at loading and unloading rates of 0.40 mN/s, with a maximum load of 50 mN. Each BC film was measured at six different points to calculate average surface property values. Young's modulus was determined using the equation presented in **Equation 3.3.**

$$E = \frac{(1-v^2)}{\left(\frac{1}{E_r} - \frac{(1-v_i^2)}{E_i}\right)} \quad \text{(Eq. 3.3)}$$

Where E = Young's Modulus of the sample, ν = Poisson's ratio of BC sample (0.3), E_r = Reduced modulus of BC sample, ν_i = Poisson's ratio of the indenter (0.07) and E_i = Young's Modulus of the indenter (1141 GPa) (Roberts et al. 1994; Rabbani et al. 2022).

3.3.5 Statistical Analysis

Analysis of variance was carried out using Ms. Excel software. The differences between the mean values were analyzed using least significant difference (LSD) test and the significance level was set at $P < 0.05$.

3.4 Results and Discussion

3.4.1 Effect of Thai Tea Types on Bacterial Cellulose Yield and Characteristics

1) Tea Profile Composition

The term "tea" refers to products derived from the leaves of plants in the Camellia family. In Thailand, the commercially produced tea cultivars *include Camellia sinensis* var. *Assamica* and *Camellia sinensis* var. *Sinensis*, commonly known as Chinese cultivars (Theppakorn et al. 2014). The same fresh tea leaves can yield various types of dried tea depending on the processing method, including black, green, oolong, white, and Thai red tea. These processing methods result in distinct chemical compositions and nutritional (Naveed et al. 2018; Shevchuk et al. 2020; Deka et al. 2023). The general composition of the teas used in this study was obtained from the tea packaging labels, as detailed in **Table 3.1,** in the design experiment section.

Different types of tea have distinct nutritional compositions. For example, the dried Chinese black tea contains approximately 16.79–23.68% protein, 5.02–7.23% water, 2.67–2.90% volatiles, and 5.43–6.10% ash, while dried Chinese green tea contains 28.66–41.36% protein, 3.23–6.60% water, 2.41–2.67% volatiles, and 5.06–6.09% ash (Czernicka et al. 2017). Additionally, Chinese green tea generally has higher levels of Ca, K, Na, Mg, Zn, and Mn, but lower levels of Al and caffeine compared to black tea, with similar phosphorus content (Czernicka et al. 2017). Green tea infusion also contains higher total phenolic content (110.73±22.46 mg/100 mL) compared to black tea (69.36±16.66 mg/100 mL) (Klepacka et al. 2021). Moreover, dried green tea has higher levels of epigallocatechin (21.91–37.46 mg/g) and caffeine (21.3–47.47 mg/g) than dried black tea, which contains 3.5–8.3 mg/g of epigallocatechin and 20.58–24.22 mg/g of caffeine (Wang et al. 2022b).

Comprehensive data on the nutritional composition of Assam black and green teas remain limited. Nonetheless, a comparative study on carbohydrate content reported that Assam black tea contains approximately 6.87 ± 2.68 mg/g of

fructose, 1.04 ± 0.16 mg/g of maltose, 9.41 ± 1.75 mg/g of inositol, 6.83 ± 4.73 mg/g of sucrose, and 3.95 ± 1.19 mg/g of glucose—values slightly higher than those observed in Chinese black tea (Shevchuk et al. 2020). In addition to traditional teas, Thai red tea is widely consumed in Thailand. This type of tea is typically derived from black tea and blended with various spices, such as star anise, cardamom, and crushed tamarind seed, as well as food colorants (Devje 2022; Thegreencreator.com 2022).

The distinct nutritional profiles and bioactive compound compositions of different tea types may significantly influence BC production during kombucha fermentation. For example, caffeine has been identified as a potential stimulant for BC synthesis (Fontana et al. 1991). Black tea, in particular, serves as an important source of caffeine in kombucha fermentation and contributes to the overall metabolic activity of the microbial consortium involved (Miranda et al. 2016).

2) The Change of pH and Total Soluble Solid (TSS)

The changes in fermentation parameters, including pH and total soluble solids (TSS), were systematically evaluated in this study to monitor microbial activity and substrate utilization. Before inoculation, the pH of the tea-based media ranged from 5.02 to 5.37, depending on the type of tea used. After inoculation with the starter culture, the pH dropped to 3.05 to 3.57, due to the introduction of an acidic inoculum typically rich in organic acids from prior fermentation. After 15 days of fermentation, the pH further decreased to 2.33 to 2.70, primarily due to the microbial production of organic acids such as acetic acid and gluconic acid, which are commonly generated by acetic acid bacteria (Aswini et al. 2020; Lee et al. 2021). Other organic acids such as glucuronic, lactic, malic, tartaric, citric, and succinic acids may also be produced, contributing to the overall pH reduction (Neffe-Skocińska et al. 2017).

The extent of pH reduction can vary depending on the type of tea used, as different teas contain varying levels of polyphenols, caffeine, amino acids, and other bioactive compounds that affect microbial growth and metabolism. For instance, teas richer in polyphenols and free amino acids may support higher

metabolic activity, accelerating acid production. **Table 3.5** and **Figure 3.1** (left side) illustrate the progression of pH throughout the fermentation process.

Table 3.5 The change of pH and degree of °Brix during kombucha fermentation of different types of Thai tea for BC production.

Tea	The Change of the pH			The Change of the °Brix		
Sample	Medium	Before	after	Medium	Before	after
WT	5.31±0.01^{c}	3.05±0.00^{a}	2.33±0.03^{a}	10.50±0.00^{a}	10.40±0.00^{a}	10.40±0.00^{c}
RTC	5.15±0.01^{b}	3.53±0.00^{c}	2.47±0.02^{b}	10.80±0.00^{b}	10.60±0.00^{c}	8.57±0.10^{a}
BTC	5.02±0.00^{a}	3.57±0.00^{d}	2.53±0.02^{c}	10.90±0.00^{c}	10.50±0.00^{b}	8.50±0.15^{a}
GTC	5.37±0.01^{d}	3.53±0.00^{c}	2.70±0.03^{d}	10.80±0.00^{b}	10.47±0.05^{b}	9.30±0.09^{b}
RBTH	5.06±0.02^{a}	3.47±0.00^{b}	2.53±0.04^{c}	10.90±0.08^{c}	10.70±0.00^{d}	9.20±0.23^{b}

Different lowercase letters within a column indicate significant differences among the five tea samples (LSD test: $P < 0.05$).

TSS, expressed in °Brix, serves as an indicator of the sugar content in the fermentation medium. Prior to inoculation, TSS values ranged from 10.50 to 10.90 °Brix, depending on the tea base and sugar concentration. After fermentation, TSS decreased to a range of 8.57 to 10.40 °Brix. This reduction reflects microbial consumption of sugars during fermentation. Although ethanol and organic acid contents were not directly measured in this study, previous research has shown that such reductions are typically associated with the conversion of sugars into ethanol and organic acids by yeast and acetic acid bacteria (Muzaifa et al. 2022).

The rate of TSS reduction is also influenced by the tea composition. Teas with higher levels of fermentable sugars or compounds that stimulate yeast activity may experience a more rapid decline in TSS. For example, Zubaidah et al. (2019) reported that the TSS of snake fruit kombucha dropped from 13.30–14.08 °Brix to 12.43–12.97 °Brix, while cascara kombucha TSS declined from 10.97 °Brix on day two to 9.97 °Brix by day eight (Muzaifa et al. 2022). The decrease in TSS is mainly due to the hydrolysis of sucrose into glucose and fructose, which are then utilized for

microbial growth and secondary metabolite production (Sinamo et al. 2022). **Table 3.5** and **Figure 3.1** (right side) present the changes in TSS before and after fermentation.

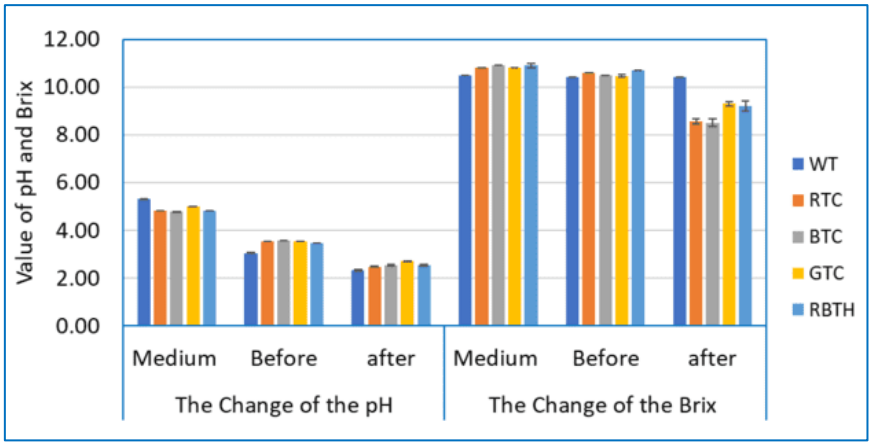

Figure 3.1 The change of pH and degree of °Brix during kombucha fermentation of different types of Thai tea for BC production.

3) The Change of Sugar Composition

Sugar composition, especially sucrose, glucose, and fructose, was evaluated before and after fermentation using HPLC. The result showed that there were changes in the concentration of the sugar components before and after fermentation, as is demonstrated in **Figure 3.2** and **Table 3.6.** The microbial (SCOBY) used the sucrose in the kombucha as a carbon source. Microbes often require carbon sources for growth and product formation, among other activities (Shu 2007). Numerous yeasts and bacteria, including *Saccharomyces cerevisiae*, *Schizosaccharomyces*, *Zygosaccharomyces rouxii*, *Torulaspora delbrueckii*, *Acetobcter xylinum*, and *Gluconobacter*, are found in SCOBY (Greenwalt et al. 2000). Before fermentation, the concentration of sucrose, glucose, and fructose was 9.03 to 9.58 %, 0.21 to 2.53 %, and 0.05 to 1.19 %, respectively. The presence of glucose and fructose prior to fermentation may be attributed to both the use of kombucha starter culture and the partial hydrolysis of sucrose during the autoclaving process. Ball (1953) reported that autoclaving a 3% sucrose solution resulted in the formation of approximately 0.7% to 0.9% glucose, indicating that thermal processing can induce sucrose breakdown. Similarly, de Lange (1989) demonstrated through a

semiquantitative test that sucrose in an autoclaved medium at pH 2 could be fully hydrolyzed into glucose and fructose. This hydrolysis was also found to occur, albeit to a lesser extent, at pH levels between 5 and 7.

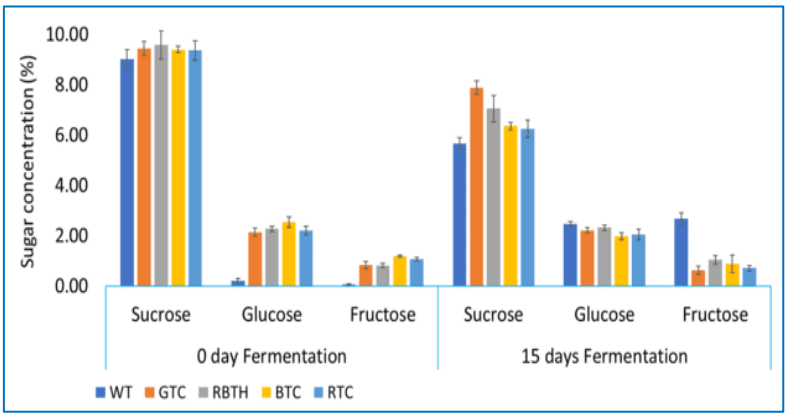

Figure 3.2 The change of sugar composition (sucrose, glucose, and fructose) of kombucha broth before and after fermentation

In the early stages of kombucha fermentation, microbial cells hydrolyze the sucrose into glucose and fructose. The subsequent metabolism of glucose and fructose yields carbon dioxide and ethanol (Wang et al. 2022a). In BC production, bacteria use some of the available glucose and fructose to synthesize cellulose. At the end of the fermentation, the concentration of sucrose decreases to the range of 5.67 to 7.88%. For all the different tea kombucha samples, there are significant differences in sucrose concentration before and after fermentation. Before fermentation, the concentration of sucrose in all the samples was not significantly different ($P > 0.05$). However, after fermentation, the concentrations of sucrose in the samples are different. **Table 3.6** provides details about the differences in concentrations of glucose and fructose before and after fermentation. Neffe-Skocińska et al. (2017) found that after 10 days of Kombucha fermentation at 30°C, the concentrations of glucose and fructose increased from 0.09% to 0.1% and from 0.07 to 0.87%, respectively, while the concentration of sucrose decreased from 9.97% to 0.74%.

Table 3.6 The change of sugar composition during kombucha fermentation with different types of teas

Sample	Before fermentation			After fermentation		
	Sucrose	Glucose	Fructose	Sucrose	Glucose	Fructose
WT*	9.03±0.36$^{a, B}$	0.21±0.08$^{a, A}$	0.05±0.03$^{a, A}$	5.67±0.23$^{a, A}$	2.47±0.08$^{c, B}$	2.67±0.23$^{c, B}$
GTC	9.43±0.28$^{a, B}$	2.15±0.16$^{b, A}$	0.82±0.14$^{b, A}$	7.88±0.27$^{d, A}$	2.22±0.11$^{b, A}$	0.62±0.16$^{a, A}$
BTC	9.40±0.13$^{a, B}$	2.53±0.21$^{c, B}$	1.19±0.05$^{d, A}$	6.35±0.16$^{b, A}$	1.98±0.14$^{a, A}$	0.87±0.35$^{ab, A}$
RBTH	9.58±0.56$^{a, B}$	2.27±0.10$^{b, A}$	0.82±0.08$^{b, A}$	7.05±0.52$^{c, A}$	2.32±0.11$^{bc, A}$	1.03±0.18$^{ab, A}$
RTC	9.36±0.38$^{a, B}$	2.21±0.16$^{b, A}$	1.06±0.07$^{c, B}$	6.24±0.36$^{b, A}$	2.04±0.20$^{a, A}$	0.71±0.11$^{ab, A}$

**Sample without tea as a control. Different lowercase letters within a column indicate significant differences among the five tea samples (LSD test: P, 0.05); different uppercase letters in the same row indicate the significant differences between the same sugar before and after fermentation (LSD test: P, 0.05).*

4) BC Productivity and Water Holding Capacity (WHC)

Figure 3.3 shows the BC production results from kombucha with various types of Thai tea. It showed that the generated BC has varying wet yields, dry yields, and WHC. The wet yields (g/L) of BC from WT, GTC, RBTH, BTC, and RTC are 61.25±10.25, 73.47±9.94, 74.82±16.14, 158.56±17.30, and 168.00±16.59, respectively. RTC and BTC produced the highest wet yields, significantly different from WT, GTC, and RBTH ($P<0.05$). The wet yields from WT, GTC, and RBTH are not significantly different from one another ($P > 0.05$). The dry yield results (g/L) of WT, GTC, RBTH, BTC, and RTC are 0.38±0.08, 0.87±0.08, 0.76±0.11, 1.49±0.08, and 1.36+0.10, respectively. The dry yield from WT is the lowest, and it is significantly different from GTC and RBTH ($P < 0.05$). GTC and RBTH are not significantly different from each other; however, they are significantly different from BTC and RTC. BTC and RTC have the highest dry yield, and both are not significantly different ($P > 0.05$).

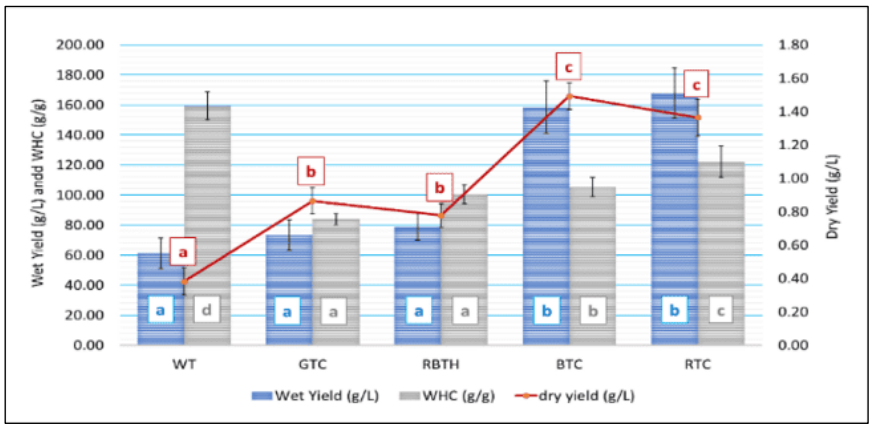

Figure 3.3 Wet yield (g/L), dry yield (g/L), and WHC (g water/g cellulose) from BC produced from kombucha with different types of Thai tea. Different lowercase letters indicate significant differences between the five BC sample (LSD test: $P < 0.05$).

The low BC yield observed in the WT (water treatment) sample is likely due to the lack of essential nutrients in the medium. As shown in **Table 3.6,** there was a marked decrease in sucrose content alongside an increase in glucose and fructose levels, indicating that while sucrose hydrolysis occurred, the conversion of available carbon into BC was inefficient. The absence of tea in the WT medium meant it lacked key compounds such as polyphenols, nitrogen, caffeine, and minerals, all of which are important for supporting microbial activity and efficient BC production. In the case of the GTC (green tea) sample, the relatively lower BC yield may be attributed to green tea's lower ash content, which suggests a limited supply of certain minerals essential for microbial growth and cellulose biosynthesis (Czernicka et al. 2017). Likewise, the RBTH sample exhibited reduced BC production compared to BTC, possibly because Chinese black tea contains lower amounts of sucrose, fructose, and glucose than Assam black tea (Shevchuk et al. 2020). Furthermore, the RBTH used in this study was grade 3, which included dried stems along with leaves, potentially influencing its overall nutrient composition. In contrast, the RTC sample had the highest BC yield, likely due to its richer nutritional profile. Unlike pure black tea, Thai red tea often contains added spices, which enhance its vitamin, mineral, and amino

acid content, creating a more favorable environment for microbial growth and BC production.

In the previous studies, several BC production results have been reported, including BC production in a 0.4% black tea solution with 20 g/L sucrose. The result was 17.63±0.50 g/L for wet yield and 3.06±0.21 g/L for dry yield after 10 days of fermentation (Hamed et al. 2023). Kombucha fermentation using a solution of 10 g/L black tea and 100 g/L sucrose for 14 days produced wet BC with a yield of 63.58 g/L (Al-Kalifawi and Hassan 2014). In green tea fermentation using kombucha culture with fermentation times of 7, 14, and 30 days, the dry weight yield of BC relative to the amount of sugar, where BC has not been purified with NaOH, is 0.9, 3.9, and 6.5 g/L (Charoenrak et al. 2023). Treviño-Garza et al. (2020) reported the results of wet-based BC produced from kombucha green tea using a microbial consortium coded Cor and CFr, producing between 195.39–301.81 g/L and 126.79–300.74 g/L. BC was made using coconut water with the addition of 10 g/L sucrose and 5 g/L yeast extract, using *G. xylinum* bacteria, and fermented for 14 days at 30°C. This production produces BC of 250.00±0.21 g/L (Gayathry 2015). In one study, BC was produced in Hestrin-Schramm medium using selected bacteria, *A. senegalensis* MA1. Fermentation was carried out at optimum conditions, namely pH 4.5 and temperature 33.5°C, for 30 days, and BC was produced with a wet weight of 469.83 g/L (Aswini et al. 2020). The amount of BC generated may be higher or lower than previously reported. These disparities in outcomes can be attributed to both internal and external factors. Several factors can influence BC productivity, including differences in nutrient source and concentration, as well as other conditions such as pH, temperature, volume, and container surface area (Al-Kalifawi and Hassan 2014; Villarreal-Soto et al. 2018b). However, in this situation, the BC findings of kombucha tea with BTC and RTC samples demonstrate high potential, and productivity may be increased through production optimization.

The WHC of BC from WT, GTC, RBTH, BTC, and RTC samples were 159.26±9.30, 83.99±3.73, 98.10±7.65, 105.21±6.36, and 122.20±10.33, respectively. The

WT sample has the highest WHC and is significantly different from all the other samples. The BC samples from the WT sample did not form BC sheets properly, and the dry yield was also very low. It may be due to the lack of nutrition content in the broth sample during kombucha fermentation. The WHC from GTC and RBTH are not significantly different from one another. However, they are significantly different and have a lower WHC than BTC and RTC samples. These results, in general, follow the reports from several previous studies, except for BC from the WT samples. The BC made from fermented coconut water (NDC) has a WHC value of around 87.14 g/g (Gayathry 2015). NDC produced with different pH, sucrose, and ammonium sulfate concentrations had WHC values ranging from 38.7±0.6 to 88.1±2.7 g/g (Jagannath et al. 2008). BC from distillery wastewater media had a WHC value of 98.5 g/g (Wu and Liu 2013). The WHC value of BC from those studies is comparable to the WHC value of BC samples from GTC and RBTH. The WHC of BC with different media fermentation of waste products from biodiesel and confectionery industries had WHC values ranging from 102 to 138 g/g (Tsouko et al. 2015). BC from kombucha fermentation with black tea media has a WHC of 114.01 g/g (Avcioglu et al. 2021). Those WHC values are comparable to the BC samples from BTC and RTC.

5) The Appearance and Colors of Bacterial Cellulose

The BC sample from the WT medium was quite thin, had a very high-water content, and had a very low dry weight. It also did not form a proper pellicle layer on the surface. Hence, we did not include the BC sample in the WT sample for further characterization. **Figure 3.4** displays the BC sample from the WT medium.

Figure 3.4 The appearance of BC from WT sample in a medium fermentation and after drained

The BC from various Thai tea kombucha fermentations has distinct hues. After harvesting, RTC produced red-orange BC, GTC produced green BC, and BTC and RBTH produced brownish white BC (**Figure 3.5.a**). Then, after boiling in RO water for 30 minutes at ±90oC, the color of BC slightly faded (**Figure 3.5.b**). The BC color becomes translucent white after purifying it with 2% sodium hydroxide and rinsing it with RO water until the pH is neutral (refer to **Figures 3.5.c and 3.5.d**). **Figure 3.5.e** displays the appearance of BC after oven drying at 40 °C until a consistent weight was achieved. We compared the characteristics of BC produced through the fermentation of kombucha tea with BC from commercial NDC. The studies of BC production using green tea reported a picture of BC with a greenish-white color (Fahim and Montazer 2020) and a brownish color (Treviño-Garza et al. 2020). The BC from kombucha fermentation using black tea has a brownish-white color (Sharma et al. 2021). None of the studies reported BC production using Thai red tea. In this study, the BC from green tea kombucha exhibited a more pronounced green color compared to previous studies, likely due to the presence of coloring agents such as FD&C Yellow No. 5 (INS 102), FD&C Yellow No. 6 (INS 110), and FD&C Blue No. 1 (INS 133). In some previous studies, the color of BC from black tea kombucha was similar to that of BC from black tea in this study. The BC from Red Thai Tea Kombucha might have a red-orange color due to the presence of the coloring agent FD&C Yellow No. 6 (INS 110).

The color of BC samples after boiling in RO water (P1) and after purification with NaOH (P2) was analyzed using the CIELAB Lab* system. L* indicates lightness (<50: dark, >50: light), a* represents red (+) to green (–), and b* represents yellow (+) to blue (–) (hunterlab.com, 2023). We then compared the four purified samples to the NDC control by calculating the ΔE value using **equation 3.4**. The summary results of the color analysis are shown in **Table 3.7**.

$$\Delta E = \sqrt{\Delta L^{*2} + \Delta a^{*2} + \Delta b^{*2}} \quad \text{.....(Eq. 3.4)}$$

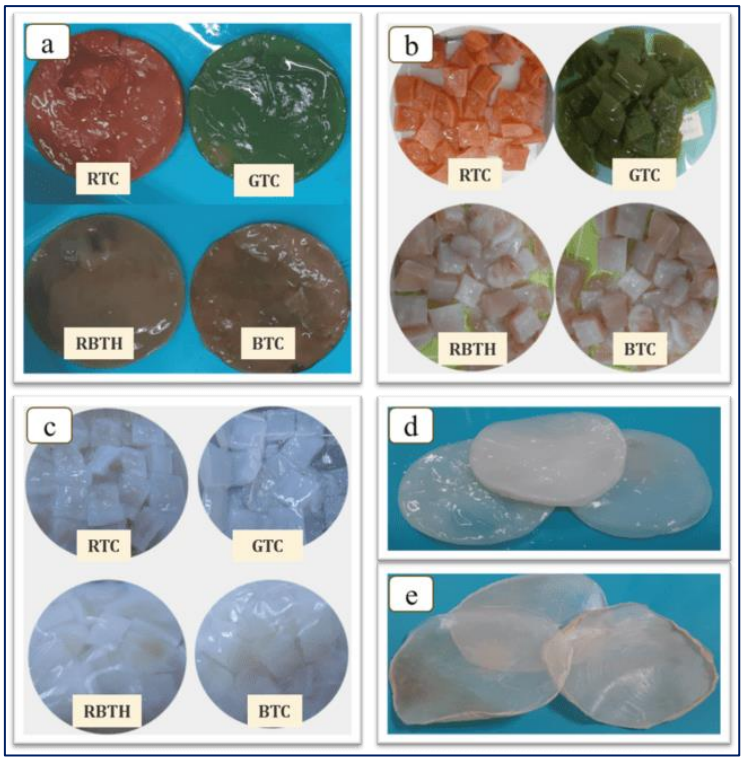

Figure 3.5 The appearance of BC (a) BC after harvesting, (b) sliced BC after harvesting and boiling in RO water, (c) sliced BC after purification using NaOH and RO water, (d) BC sheet after purification using NaOH and RO water, and (e) dried BC sheet.

Before purification, the BTC-P1 and RBTH-P1 samples had similar colors and were not significantly different (P<0.5). The L* and b* values in the RTC-P1 sample are not significantly different; however, the value of a* is greater and significantly different when compared to BTC-P1 and RBTH-P1 (P<0.5). The GTC-P1 sample exhibited significantly different L*, a*, and b* values than the RTC-P1, BTC-P1, and RBTH-P1 samples (P<0.5). After purification, the color values of the BTC-P2 and RBTH-P2 samples did not differ significantly (P<0.5). Sample RTC-P1 contains a* and b* values that are not significantly different, but L* values that are greater and significantly different from BTC-P2 and RBTH-P2 (P<0.5). The GTC-P2 sample shows significantly different L* and a* values, but the b* value is not statistically different when compared to the RTC-P1, BTC-P1, and RBTH-P1 samples (P<0.5). "We compared the ΔE values of four purified BC samples with the NDC as a control. According to Minaker et al. (2021),

a ***ΔE*** value between 0 and 1.0 is imperceptible to the human eye, while a ***ΔE*** between 1 and 2 is noticeable upon close inspection, and a ***ΔE*** between 2 and 10 is easily noticeable at a glance (Minaker et al. 2021). The BC samples BTC-P2 and RBTH-P2 have ***ΔE*** values below 2, indicating a subtle difference visible only upon close observation. In contrast, the ***ΔE*** values for RTC-P2 and GTC-P2 are 3.18 and 8.78, respectively, making them readily distinguishable.

Table 3.7 Summary of BC color investigation of kombucha with various types of tea before and after purification.

Samples Code	Results			
	L*	a*	b*	ΔE***
Before purification				
RTC-P1	42.53±2.07^{b}	11.16±0.87^{c}	9.2 ±1.01^{a}	-
BTC-P1	42.45±3.40^{b}	2.36±1.14^{b}	7.41±2.30^{a}	-
RBTH-P1	41.80±0.53^{b}	3.29±0.22^{b}	9.09±0.62^{a}	-
GTC-P1	28.37±0.99^{a}	-5.52±0.68^{a}	12.02±1.07^{b}	-
After purification				
NDC**	47.96±1.16^{b}	-1.62±0.22^{a}	-10.38±0.31^{a}	control
RTC-P2	51.07±2.98^{c}	-1.95±0.09^{a}	-9.79±0.57^{ab}	3.18
BTC-P2	46.64±3.24^{b}	-1.81±0.17^{a}	-9.02±0.45^{b}	1.90
RBTH-P2	47.34±2.64^{b}	-1.77±0.10^{a}	-8.72±0.38^{bc}	1.78
GTC-P2	39.27±0.78^{a}	-1.06±0.43^{b}	-9.24±0.99^{b}	8.78

Different lowercase letters within a column indicate significant differences among the five BC samples (LSD test: P < 0.05).

Previous research has provided limited information on the color of BC or NDC before drying. One study investigated how different carbon sources—glucose, sucrose, mannitol, and fructose—affected the color of wet BC, reporting L*, a*, and b* values ranging from 24.7 to 48.48, -4.29 to 0.95, and -21.59 to 1.67, respectively (Shim and Kim 2019). These values are similar to those found in this study.

Other research has focused on the color of BC after drying. For example, Amorim (2022) reported that untreated BC had L*, a*, and b* values of 51.5±3.5, 14.8±0.6, and 31.5±2.1, respectively, while alkaline-treated BC had values of 83.6±1.0, 1.5±0.4, and 13.1±0.7 (Amorim et al. 2022).

6) Morphology Analysis

The morphology of BC samples produced from kombucha fermentation media with various types of tea, along with commercial NDC samples, was analyzed using SEM. **Figures 3.6.(a.1)** to **3.6(e.2)** present each sample at magnifications of 10,000x and 30,000x. Higher magnifications of 50,000x and 100,000x were applied to the RTC samples (**Figure 3.6.(e.3)** and **3.6.(e.4**)) to observe the cellulose fiber arrangement in greater detail. Fiber diameters were measured using ImageJ software, and their size distribution is illustrated in **Figure 3.7.**

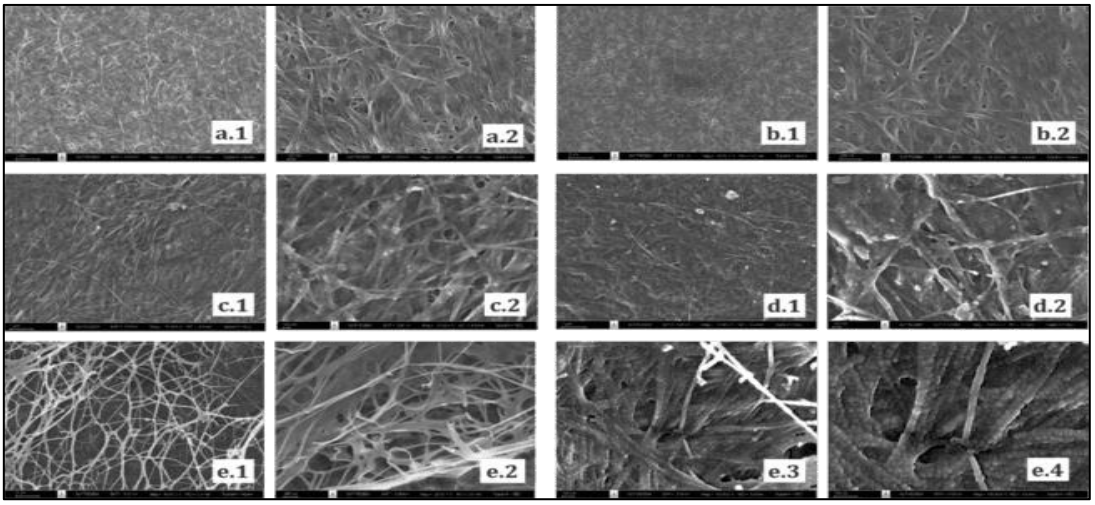

Figure 3.6 The SEM images of BC samples: (a) NDC; (b) GTC; (c) BTC; (d) RBTH; and (e) RTC. The images are shown at varying magnifications: (1) 10,000x; (2) 30,000x; (3) 50,000x; and (4) 100,000x.

Overall, the BC samples exhibit a consistent fiber pattern, aligning with the findings of Brandes et al. (2020), Nguyen and Nguyen (2022), and Illa et al. (2019) (Illa et al. 2019; Brandes et al. 2020; Nguyen and Nguyen 2022). However, in the samples of **Figure 3.6.c** (BTC) and **3.6.d** (RBTH), residues or insoluble materials persist after alkali purification, as also reported by Amorim et al. (2023) (Amorim et al. 2023).

This residual material obscures the fiber arrangement, particularly in **Figures 3.6.c.2** and **3.6.d.2**. In the RTC samples, magnified at 50,000x and 100,000x, the detailed arrangement of cellulose fiber units is more distinctly observed.

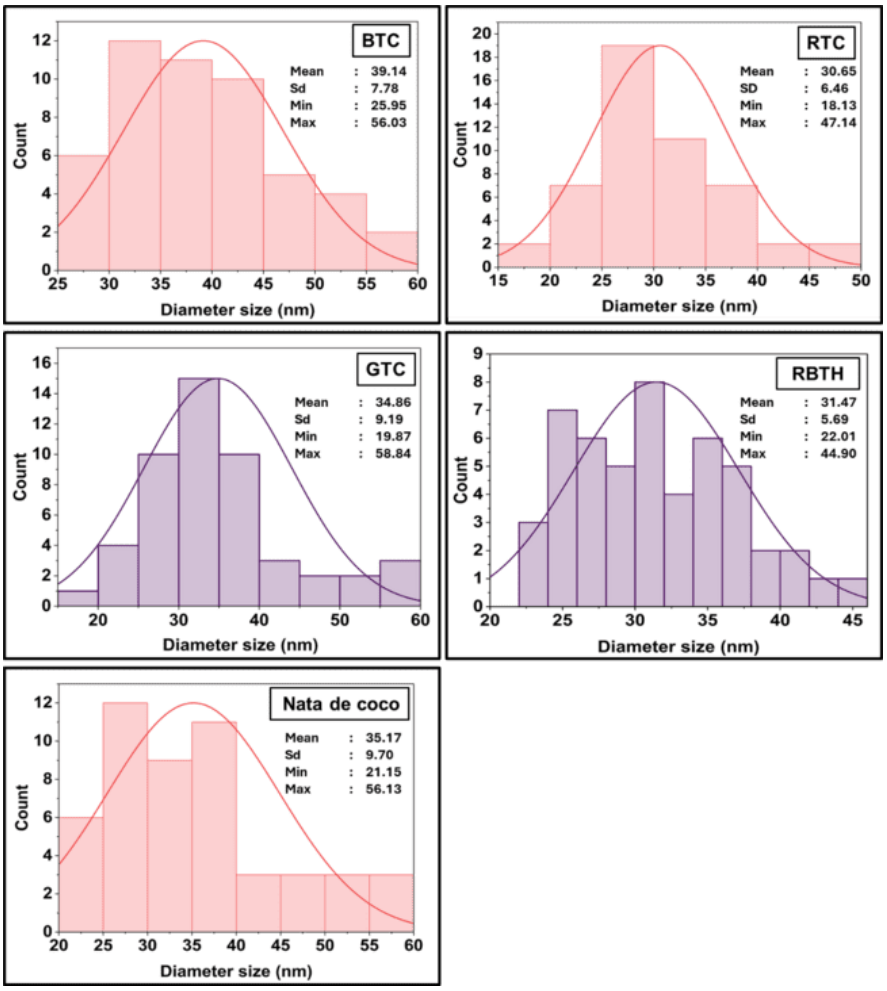

Figure 3.7 Graph of poly distribution diameter size of BC samples from NDC, RTC, GTC, BTC, and RBTH.

The polydistribution graphs of BC fiber diameters (**Figure 3.7**) revealed that fiber sizes range from 18.13±6.46 nm to 58.84±9.19 nm, with average diameters between 30.65±6.46 nm and 39.14±7.78 nm. The diameters of RTC, GTC, BTC, and RBTH are 30.65±6.46, 34.86±9.19, 39.14±7.78, and 31.47±5.70 nm, respectively. The fiber diameters of BC produced from kombucha tea are comparable to those of NDC (35.17±9.70). These results are consistent with the findings of Illa et al. (2019), who reported that BC produced by *K. hansenii* 23769 (ATCC) and an isolated

cellulose-producing strain from grape juice (GBHS) exhibited fiber diameters ranging from 10 to 60 nm (Illa et al. 2019). Specifically, oven-dried BC from the ATCC strain had an average diameter of 28.9±5.6 nm, while the GBHS strain had an average diameter of 28.6±6.7 nm. Similarly, BC produced by *A. pasteurianus* MGC-N8819 using lotus rhizome as a culture medium showed fiber diameters ranging from 28±1.5 nm to 57±1.2 nm (Nie et al. 2022). Furthermore, BC produced by *K. saccharivorans* MD1 using HS medium supplemented with palm date exhibited fiber diameters ranging from 10 to 90 nm (Abol-Fotouh et al. 2020).

7) Fourier Transform Infrared Spectroscopy

Figure 3.8 presents the FTIR spectra of BC samples obtained from different tea-based kombucha fermentations. Overall, all BC samples exhibit similar spectral bands. However, a noticeable difference is observed in the BC sample from GTC, which displays a distinct peak at approximately 1725.95 cm^{-1}.

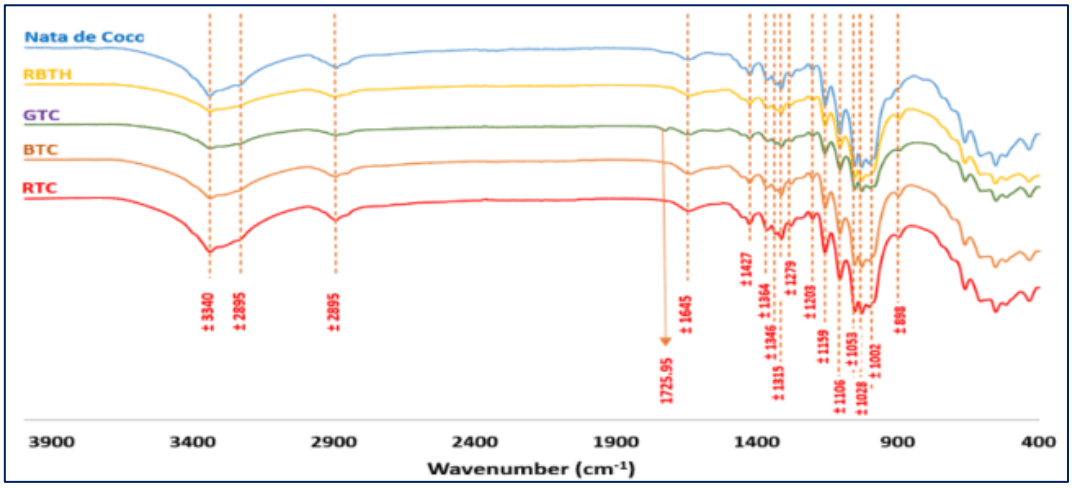

Figure 3.8 FTIR spectra of BC produced from different Thai tea kombucha fermentations

The FTIR spectra analysis is divided into two regions: the feature region and the fingerprint region. The feature region corresponds to high-frequency wavenumbers between 4000 and 1330 cm^{-1}. Meanwhile, the fingerprint region covers wavenumbers between 1330 and 500 cm^{-1} (Liu et al. 2023). The FTIR spectra of the BC

samples reveal the following key features: In the first spectral region, peaks were observed at wavenumbers around 3340, 3232, and 2895 cm^{-1}. The strong, broad bands at wavenumbers of approximately 3340 and 3232 cm^{-1} indicate the presence of O-H stretching, while the band near 2895 cm^{-1} corresponds to C-H stretching vibrations (Amorim et al. 2023). In the second spectral region, we observed a weak peak at around 2330 cm^{-1}, suggesting the presence of functional groups associated with triple bonds, specifically C≡C and C≡N (Srivastava and Mathur 2022). The third region in our FTIR spectra was observed between 1350 cm^{-1} and 2000 cm^{-1}, with absorption peaks at 1364 cm^{-1}, 1427 cm^{-1}, 1644 cm^{-1}, and 1725 cm^{-1}. The bands at 1360–1363 cm^{-1} correspond to C-H symmetric bending vibrations, while the peak at 1427 cm^{-1} represents CH_2 symmetric bending, and the peak at 1644 cm^{-1} indicates C=O stretching vibrations for the glucose carbonyl group (Liu et al. 2023). **Figure 3.8** also shows a peak at 1725 cm^{-1}, which appears exclusively in the FTIR spectrum of the BC sample from green tea kombucha (GTC). This peak may correspond to carbonyl stretching vibrations typically associated with aldehydes (1720–1740 cm^{-1}), ketones (1705–1725 cm^{-1}), or carboxylic acids (1700–1725 cm^{-1}) (Yao et al. 2015). The presence of this peak in the GTC sample could be attributed to specific compounds originating from green tea or intermediate metabolites produced during fermentation. Alternatively, it may indicate residual compounds or impurities that were not fully removed during purification. Further analysis would be required to determine the exact origin of this absorption peak.

In the fingerprint region, several peaks were observed at 1336 cm^{-1}, 1315 cm^{-1}, 1279 cm^{-1}, 1203 cm^{-1}, 1159 cm^{-1}, 1106 cm^{-1}, 1053 cm^{-1}, 1028 cm^{-1}, 1002 cm^{-1}, and 898 cm^{-1}. According to Liu et al. (2023), the peak at 1336 cm^{-1} corresponds to OH in-plane bending, while the peak at 1315 cm^{-1} is attributed to CH_2 wagging at C-6. The peak at 1159 cm^{-1} represents C-O-C antisymmetric bridge stretching vibrations, and the one at 1106 cm^{-1} is associated with ring asymmetric stretching vibrations. The 1053 cm^{-1} peak corresponds to C-O-C and C-O-H stretching vibrations of the sugar ring,

and the 1028 cm^{-1} peak represents C-O stretching vibrations (Liu et al. 2023). The band observed at 898–894 cm^{-1} may be associated with stretching vibrations of the C-O-C bond in the β-1,4-glycosidic linkages, indicating an amorphous absorption band (Ciolacu et al. 2011).

8) X-Ray Diffraction (XRD) Analysis

Figure 3.9 presents the X-ray diffraction (XRD) patterns of various BC samples, with a commercial NDC product used as a reference. It shows that the three distinctive peaks appear consistently in all samples at 2θ values of approximately 14.78°, 16.89°, and 22.90°. This indicates the crystalline structure of all the BC samples (Said Azmi et al. 2023). These XRD profiles are consistent with those reported for BC by Said Azmi et al. (2023), Jittaut et al. (2023), and Revin et al. (2018) (Revin et al. 2018; Jittaut et al. 2023; Said Azmi et al. 2023). While the X-ray patterns confirm the same cellulose chemical structure across all samples, they reveal variations in diffraction intensities. The highest intensity peak at around 23° corresponds to cellulose type I (Said Azmi et al. 2023; Hossen et al. 2024). Gaspar et al. (2014) identified that the peaks at 2θ values of 14.7°, 16.8°, and 22.7° correspond to the 100, 110, and 200 crystallographic planes of monolithic cellulose type I. This is typical of native cellulose (Gaspar et al. 2014). The variation in relative peak intensity likely reflects small differences in chain orientation among the samples (Said Azmi et al. 2023). This finding suggests that BC produced from different tea kombucha fermentations maintains a well-ordered crystalline structure, essential for its mechanical strength and WHC.

The data from the XRD analysis were then used to calculate the crystallinity index (CI) and crystallite size of BC samples. The CI of BC samples from BTC, GTC, RBTH, and RTC were 84.17%, 86.50%, 83.01%, and 85.36%, respectively, closely matching the CI of NDC, which was 86.66%. These results align with other studies, such as BC from pineapple peel waste fermentation with a CI of 87% (Sardjono et al. 2019), BC from pineapple waste solution fermentation at 82.2% (Pham and Tran

2023), BC produced from citrus processing waste or discarded fruits with a CI of 86.9% (Andritsou et al. 2018), and BC from HS-medium with varying carbon sources, which exhibited crystallinity ranging from 57% to 85% (Heydorn et al. 2023). BC can exhibit a high crystallinity index (CI), typically ranging from 84% to 90%, due to the absence of non-cellulosic components that may disrupt the crystalline structure (Cazón and Vázquez 2021). Further analysis of the average crystallite size of the BC samples revealed values of 2.60, 2.13, 3.34, 3.15, and 3.54 nm for BTC, RBTH, GTC, RTC, and NDC, respectively. For comparison, BC produced by *G. xylinus* InaCC B404 in HS medium was reported to have a crystallite size of 3.06 nm (Agustin et al. 2021). Additionally, BC derived from black tea kombucha after 3 and 5 days of fermentation showed crystallite sizes of 3.29 nm and 4.80 nm, respectively (Balistreri et al. 2024).

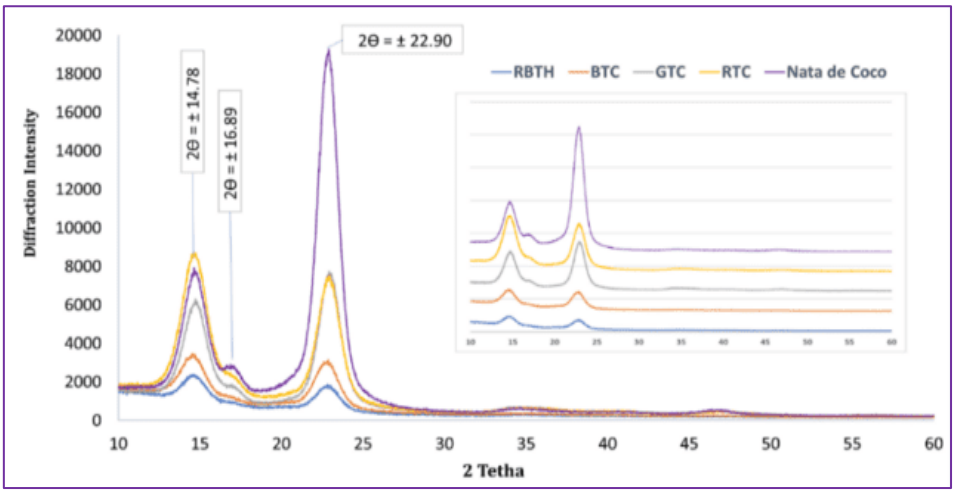

Figure 3.9 XRD spectra of BC produced from different types of tea kombucha fermentation

Differences in diffraction intensity and crystallite size (2.13–3.54 nm) suggest slight variations in molecular structure, likely influenced by fermentation conditions and tea type. The GTC sample had the highest CI (86.50%) and a larger crystallite size (3.34 nm), indicating improved crystallinity. Overall, the XRD results confirm that BC from kombucha tea fermentations has a highly crystalline structure, similar to commercial NDC. This makes it suitable for applications like food packaging,

biomedical materials, and nanocomposites. Further research on fermentation conditions could help enhance BC properties for specific uses.

9) Thermogravimetric (TGA/DTG) Analysis

Figure 3.10 presents the thermogravimetric (TG) and differential thermal degradation (DTG) curves of BC samples, obtained through thermogravimetric analysis (TGA). The thermal degradation of all BC samples occurred in two distinct stages. The first stage (28–240°C) involved weight loss ranging from 2.25% to 7.52%, primarily due to moisture evaporation and the loss of low-molecular-weight compounds. The second stage (240–600°C) showed a significant weight loss between 67.69% and 73.61%, corresponding to cellulose decomposition. At 600°C, the residue weight varied from 23.07% to 27.36%, as detailed in **Table 3.10.**

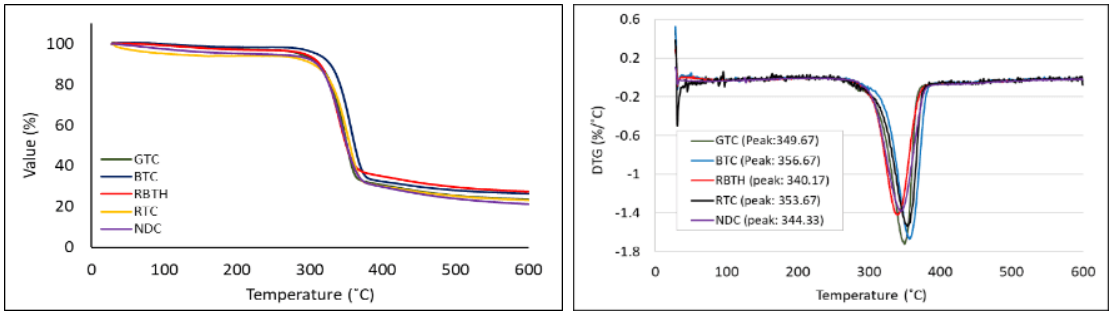

Figure 3.10 TGA (left) and DTG (right) thermographs of BC samples produced from kombucha fermentation using different types of tea

In the first stage, weight loss ranged from 2.25% (BTC) to 7.52% (NDC), with RTC showing a relatively high loss (6.03%), likely due to differences in residual moisture or volatile content. The second stage exhibited the most substantial degradation, with weight loss ranging from 67.69% (NDC) to 73.61% (GTC). At 600°C, the residual weight varied between 23.01% (RTC) and 27.36% (RBTH), indicating differences in thermal stability and carbonization potential among samples.

DTG curves provide further insight into the degradation behavior, with peak degradation temperatures (T_{max}) occurring between 340.17°C (RBTH) and 356.67°C (BTC). BTC exhibited the highest DTG T_{Max}, suggesting superior thermal

stability, while RBTH had the lowest T_{max}, indicating decomposition at a slightly lower temperature. RTC recorded a DTG T_{Max} of 353.67°C, closely resembling BTC, further confirming its thermal resistance. These variations in DTG T_{Max} can be attributed to differences in cellulose crystallinity, molecular structure, and residual compounds from the fermentation process.

Table 3.8 The details of data decomposition during the TGA process of BC samples from kombucha fermentation with different types of tea

Samples	First stage weight loss (%)	Second stage weight loss (%)	Residue (%)	DTG Peak range (°C)	DTG T_{Max} (°C)
GTC	3.45	73.61	23.51	255 – 379	349.67
BTC	2.25	71.99	26.37	255 – 382	356.67
RBTH	3.06	69.55	27.36	252 – 386	340.17
RTC	6.03	71.01	23.01	265 – 381	353.67
NDC	7.52	67.69	24.76	255 – 387	344.33

The findings align with previous research. BC produced by *G. xylinus* AGR 60 showed a first-stage mass loss of 6.2%, a second-stage loss of 64.0%, and a residue of 22.8% at 600°C, with DTG a T_{Max} of 339.6°C (Jenkhongkarn and Phisalaphong 2023). Similarly, BC from *A. xylinum* AGR60 exhibited a first-stage loss of about 6%, a second-stage loss of 74%, and a residue weight of approximately 20% at 700°C, with major decomposition occurring between 300 and 360°C (Potivara and Phisalaphong 2019). Our results are consistent with these studies, where the initial weight loss is attributed to dehydration and volatilization of low-molecular-weight components or residual water in the BC matrix (Teixeira et al. 2019; Mohamad et al. 2022a). The significant weight loss in the second stage corresponds to the decomposition of β-glucan chains and oxidation of cellulosic materials into carbonaceous residue (Mohammadkazemi et al. 2015; Mohamad et al. 2022a). Additionally, the minor weight

loss between 400°C and 600°C is associated with the degradation of carbonaceous residues (De Araújo Júnior et al. 2016; Teixeira et al. 2019).

The TGA results confirm that BC derived from kombucha fermentation exhibits good thermal stability, making it suitable for applications requiring heat resistance, such as food packaging and biomedical materials. BTC and RTC demonstrated the highest thermal stability, with RTC emerging as a promising alternative due to its comparable performance and lower production cost.

10) Mechanical Properties Analysis Using Nanoindentation

Nanoindentation analysis was conducted to assess the nanoscale mechanical properties of BC samples. This highly precise and sensitive technique enables the measurement of local mechanical responses—such as hardness and elastic modulus—at both the micro- and nanoscale. Such detailed evaluation is essential for applications that require materials with excellent mechanical strength, flexibility, and structural integrity, including advanced food packaging, biomedical devices, and nanocomposites.

The BC samples used in this analysis were obtained from kombucha fermentation using Thai Red Tea (RTC) and Thai Black Tea (BTC), selected for their potential as cost-effective and efficient sources of BC. These tea types also offer distinct chemical profiles, providing a meaningful basis for comparing the resulting BC properties. The full results of the nano-indentation analysis are presented in **Table 3.9.**

The data show no significant differences ($P > 0.05$) in the mechanical properties of BC from BTC and RTC. This indicates that both types of tea produce BC with similar properties at the nanoscale. The similarity may be due to the comparable composition of the fermentation medium, suggesting that the type of tea does not greatly affect the mechanical characteristics of the BC. The microbial activity during kombucha fermentation seems to create a uniform cellulose network, leading

to similar properties in both BTC and RTC samples. In contrast, Nata de Coco (NDC) shows significant differences ($P < 0.05$) in some properties compared to BTC and RTC. For example, the reduced modulus is lower in NDC (4.14 GPa) than in BTC and RTC (around 4.94 GPa), and the Young's modulus for NDC is also lower (3.78 GPa) compared to BTC (4.52 GPa) and RTC (4.51 GPa). Since the drying process is the same for all samples, these differences may be due to variations in the fermentation medium, the bacterial strain used, or the purification process. These factors can affect the density and arrangement of the cellulose in the final BC product.

Table 3.9 Mechanical properties data analysis using nano-indenter of BC from kombucha fermentation of BTC, RTC, and commercial product (NDC)

Sample	MD (nm)	Pl (nm)	ML (mN)	H (GPa)	RM (GPa)	ERP	CC (nm/mN)	PW (nJ)	EW (nJ)	YM (GPa)
BTC	3440.51 ±289.23^{a}	3011.45 ±270.30^{a}	50.10 ±0.00^{a}	0.22 ±0.04^{b}	4.94 ±0.70^{b}	0.14 ±0.01^{b}	11.42 ±0.63^{b}	56.11 ±6.39^{a}	20.48 ±1.16^{a}	4.52 ±0.64^{b}
RTC	3412.25 ±259.56^{a}	2980.18 ±253.91^{a}	50.10 ±0.00^{a}	0.22 ±0.05^{b}	4.94 ±0.56^{b}	0.15 ±0.01^{b}	11.50 ±0.22^{b}	54.41 ±4.64^{a}	20.80 ±0.47^{a}	4.51 ±0.51^{b}
NDC	3612.65 ±162.08^{a}	3123.34 ±148.57^{a}	50.10 ±0.00^{a}	0.20 ±0.02^{a}	4.14 ±0.31^{a}	0.16 ±0.00^{a}	13.02 ±0.41^{a}	59.92 ±4.09^{b}	22.90 ±0.80^{b}	3.78 ±0.28^{a}

MD: maximum depth, Pl: plastic, ML: maximum load, H: hardness, RM: reduced modulus, ERP: elastic recovery parameters, CC: contact compliance, PW: plastic work, EW: elastic work, and YM: Young's Modulus. The different lowercase letters within the same column indicate statistically significant differences ($P < 0.05$).

Several factors can influence BC's mechanical properties, including cultivation methods (Krystynowicz et al. 2002), bacterial strains (Zeng et al. 2014; Chen et al. 2018a), NaOH concentration during purification (Suryanto et al. 2019; Chen et al. 2021), carbon sources (Chibrikov et al. 2023), nutrient composition (Betlej et al. 2020), and drying methods (Zeng et al. 2014). The mechanical properties of BC are closely related to its network structure, such as porosity, including intrafibrillar and interfibrillar spaces (Wang et al. 2023b). The Young's modulus values for BTC (4.52 GPa) and RTC

(4.51 GPa) are consistent with previous studies. For example, BC produced from different *Komagataeibacter* strains shows a range of 1.10 to 5.56 GPa (Chen et al. 2018a), and BC from *A. xylinum* AGR60 in coconut water reaches 9.14 GPa (Potivara and Phisalaphong 2019). Our results for BTC, RTC, and NDC fall within these ranges, suggesting that different fermentation conditions can still produce high-quality BC. However, other studies, like Zeng et al. (2014), report different ranges, with Young's modulus between 198 to 659 MPa and hardness between 19 and 39 MPa for BC from different strains and drying methods (Zeng et al. 2014). Research using nano-indentation for BC is limited, with Zeng et al. (2014) being one of the few studies found. Most other studies use conventional methods like tensile strength tests, making it difficult to directly compare our results. Still, our study adds valuable new data by using nano-indentation to measure BC's properties. This method could be very useful for BC research, but more studies are needed to confirm our findings.

3.4.2 Effect of Different Types of Additives on Bacterial Cellulose Yield and Characteristics

1) The Change of pH and Total Soluble Solid (TSS)

The study examined changes in pH and TSS throughout the fermentation process. Initially, before inoculation, the pH of the medium ranged from 3.33 to 5.90. After adding the starter culture, the pH dropped slightly, ranging from 3.18 to 4.42. By the end of the 15-day fermentation, the pH further decreased, ranging from 2.34 to 3.37. Among the additives, the medium with vitamin C (VC) showed the lowest pH, while the soy protein isolate (SPI) maintained the highest pH. The changes in pH over time are detailed in **Table 3.10** and shown in **Figure 3.11** (left).

The initial pH decrease following inoculation is primarily due to the starter culture's naturally lower pH. Organic acids like acetic and gluconic acid, produced as fermentation progresses, contribute to a further reduction in pH (Aswini et al. 2020; Lee et al. 2021). Additional organic acids such as glucuronic, lactic, malic, tartaric, citric, and succinic acids may also be formed during this process (Neffe-

Skocińska et al. 2017). Neffe-Skocińska et al. (2017) observed a similar pH shift, noting a decrease from 3.04 to 2.63 after 10 days of kombucha fermentation. In a study using HS medium supplemented with vitamin C, the pH decreased from 6.0 to a range of 3.9 to 4.9 after one week of fermentation with six different *G. xylinus* strains (Keshk 2014). This result highlights the typical pattern of acid production during kombucha fermentation.

In addition of pH observation, we also monitored the total soluble solids (TSS) of the fermentation broth. Initially, before adding the inoculum, TSS values ranged from 9.97 to 10.90 °Brix. After inoculation, TSS levels varied from 9.50 to 10.70 °Brix. Following fermentation, TSS values declined to a range of 8.57 to 9.60 °Brix, as shown in **Figure 3.11** (right) and **Table 3.10** TSS is an important measure that reflects the sugar concentration in a solution (Muzaifa et al. 2022). A decrease in TSS during fermentation is common. A study conducted by Zubaidah et al. (2019) reported a reduction in TSS for various snake fruit kombucha from 13.30–14.08 °Brix to 12.43–12.97 °Brix (Zubaidah et al. 2019). Similarly, a study reported a drop in TSS for cascara kombucha from 10.97 °Brix on the second day to 9.97 °Brix by the eighth day (Muzaifa et al. 2022). This decline in sugar levels is attributed to the activity of microorganisms, which convert sugars into glucose and other compounds that are then utilized for their growth and metabolic processes (Sinamo et al. 2022).

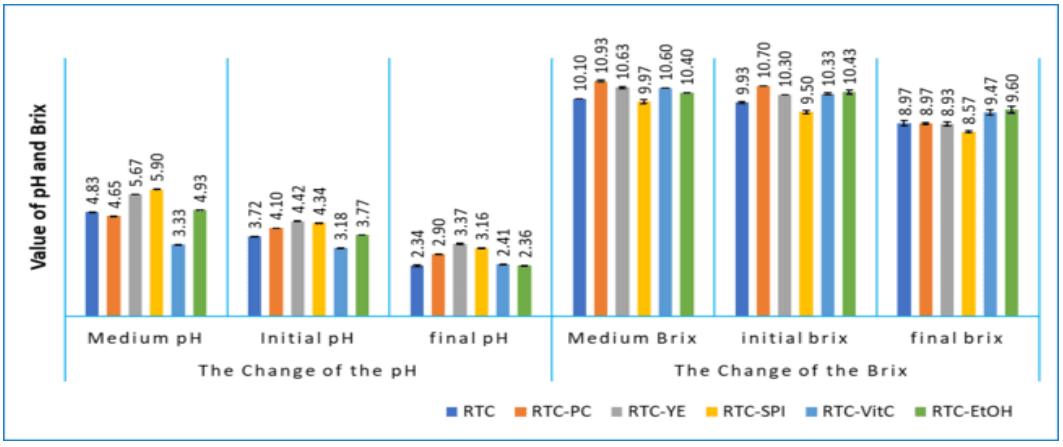

Figure 3.11 Changes in pH and °Brix before and after RTC kombucha fermentation with different type of additives

Table 3.10 Changes in pH and °Brix before and after RTC kombucha fermentation with different type of additives

Samples	The Change of the pH			The Change of the °Brix		
	Medium	Before	after	Medium	Before	after
RTC	4.83±0.01^{c}	3.72±0.00^{b}	2.34±0.04^{a}	10.10±0.00^{b}	9.93±0.05^{b}	8.97±0.13^{b}
RTC-PC	4.65±0.02^{b}	4.10±0.00^{d}	2.90±0.01^{c}	10.93±0.05^{e}	10.70±0.00^{e}	8.97±0.00^{b}
RTC-YE	5.67±0.00^{e}	4.42±0.00^{f}	3.37±0.02^{e}	10.63±0.05^{d}	10.30±0.00^{c}	8.93±0.10^{b}
RTC-SPI	5.89±0.01^{f}	4.34±0.00^{e}	3.16±0.02^{d}	9.97±0.09^{a}	9.50±0.08^{a}	8.57±0.05^{a}
RTC-VC	3.33±0.01^{a}	3.18±0.01^{a}	2.41±0.01^{b}	10.60±0.00^{d}	10.33±0.05^{c}	9.47±0.13^{c}
RTC EtOH	4.93±0.00^{d}	3.77±0.00^{c}	2.36±0.01^{a}	10.40±0.00^{c}	10.43±0.09^{cd}	9.60±0.15^{d}

Different lowercase letters within a column indicate significant differences among the five tea samples (LSD test: P < 0.05).

2) The Change of Sugar Composition

Sugar composition, especially sucrose, glucose, and fructose, was evaluated using HPLC. The result showed that there were changes in the concentration of the sugar components before and after fermentation, as is demonstrated in **Figure 3.12** and **Table 3.11**. The SCOBY used the sucrose in the kombucha as a source of carbon. The SCOBY utilized sucrose in the kombucha as a carbon source, essential for microbial growth and product formation (Shu 2007). It contains various yeasts and bacteria, including *Saccharomyces cerevisiae, Zygosaccharomyces rouxii, Schizosaccharomyces, Torulaspora delbrueckii, A. xylinum, and Gluconobacter* (Greenwalt et al. 2000). Before fermentation, the concentration of sucrose, glucose, and fructose was 9.03 to 9.58%, 0.21 to 2.53%, and 0.05 to 1.19%, respectively. The presence of glucose and fructose prior to fermentation may be attributed to both the use of kombucha culture and the hydrolysis of sucrose during the autoclaving process. Ball (1953) reported that autoclaving a 3% sucrose solution resulted in partial hydrolysis, yielding approximately 0.7–0.9% glucose. Similarly, de Lange (1989) demonstrated that autoclaving sucrose solutions at pH 2 could lead to complete hydrolysis into glucose and fructose, as confirmed by semi-quantitative analysis.

Notably, sucrose hydrolysis was also observed at pH values ranging from 5 to 7, albeit to a lesser extent.

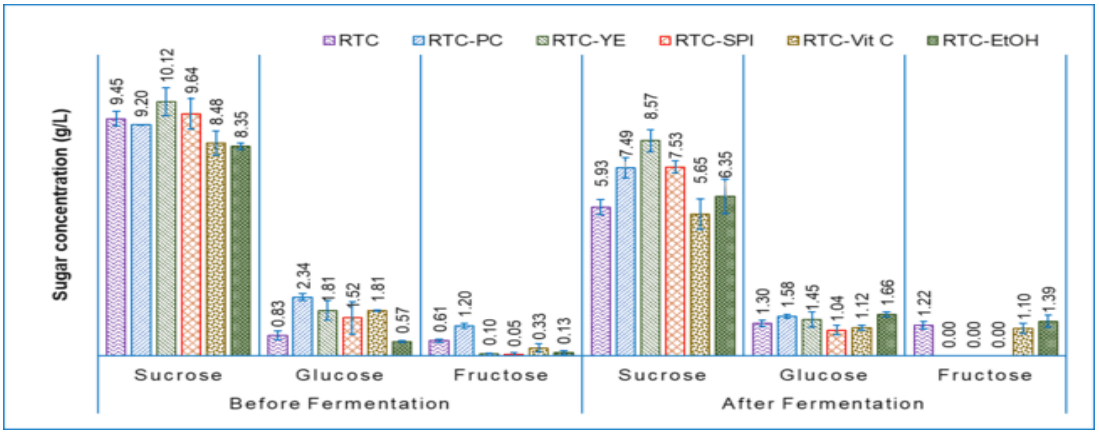

Figure 3.12 Changes in sugar composition (sucrose, glucose, and fructose) in RTC kombucha broth before and after fermentation with different types of additives.

In the early stage of kombucha fermentation, microorganisms hydrolyze sucrose into glucose and fructose, which are metabolized into carbon dioxide and ethanol (Wang et al. 2022a). In BC production, bacteria utilize these sugars for cellulose synthesis. At the end of the fermentation, the concentration of sucrose decreases to the range of 5.65 to 8.57%. For all the different additives, there are significant differences in sucrose concentration before and after fermentation. Before fermentation, the concentration of sucrose in all the samples was not significantly different ($P > 0.05$). However, after fermentation, the concentrations of sucrose in the samples are different. **Table 3.11** provides details about the differences in concentrations of sucrose, glucose and fructose before and after fermentation. Research by Neffe-Skocińska et al. (2017) revealed that over 10 days of Kombucha fermentation at 30°C, the glucose concentration rose from 0.09% to 0.1%, and fructose levels increased from 0.07% to 0.87%. Meanwhile, the sucrose concentration significantly dropped from 9.97% to 0.74%.

Table 3.11 Changes in sugar composition in RTC kombucha broth with different types of additives before and after fermentation

Samples	Before fermentation			After fermentation		
	Sucrose	Glucose	Fructose	Sucrose	Glucose	Fructose
RTC	$9.45\pm0.29^{b,B}$	$0.83\pm0.08^{a,A}$	$0.61\pm0.07^{c,A}$	$5.93\pm0.30^{a,A}$	$1.89\pm0.12^{b,B}$	$1.22\pm0.16^{bc,B}$
RTC-PC	$9.20\pm0.02^{b,B}$	$2.34\pm0.14^{c,B}$	$1.20\pm0.10^{d,B}$	$7.49\pm0.41^{c,A}$	$1.02\pm0.07^{c,A}$	$0.00\pm0.00^{a,A}$
RTC-YE	$10.12\pm0.56^{c,B}$	$1.81\pm0.39^{b,A}$	$0.10\pm0.01^{a,B}$	$8.57\pm0.45^{d,A}$	$2.36\pm0.30^{bc,B}$	$0.00\pm0.00^{a,A}$
RTC-SPI	$9.64\pm0.61^{b,B}$	$1.52\pm0.64^{b,A}$	$0.05\pm0.08^{a,A}$	$7.53\pm0.23^{c,A}$	$2.22\pm0.20^{a,B}$	$0.00\pm0.00^{a,B}$
RTC-VC	$8.48\pm0.07^{a,B}$	$1.81\pm0.03^{b,B}$	$0.33\pm0.17^{b,A}$	$5.65\pm0.60^{a,A}$	$0.92\pm0.10^{ab,A}$	$1.10\pm0.21^{b,A}$
RTC-EtOH	$8.35\pm0.08^{a,B}$	$0.57\pm0.04^{a,A}$	$0.13\pm0.09^{a,A}$	$6.35\pm0.68^{ab,A}$	$1.92\pm0.10^{c,B}$	$1.39\pm0.23^{c,B}$

Different lowercase letters within a column indicate significant differences among the five tea samples (LSD test: $P < 0.05$); different uppercase letters in the same row indicate the significant differences between the same sugar before and after fermentation (LSD test: $P < 0.05$).

3) The Appearance of Bacterial Cellulose

The appearance of BC produced from Thai red tea kombucha fermentation with different uses of additives are presented in **Figure 3.13.** The appearance of BC before purification exhibited distinct color variations depending on the additive used (**Figure 3.13(a)** and **3.13(b))**. As previously reported, BC from the Thai red tea kombucha showed a characteristic red-orange color. RTC-EtOH exhibited a similar red-orange hue to the control. RTC-VC resulted in a noticeably lighter orange shade. In contrast, BC from RTC-SPI, RTC-PC, and RTC-YE displayed significantly lighter colors, ranging from pale white to white-orange, indicating a reduced uptake or masking of natural tea pigments and artificial colorant.

The color variations observed in BC are influenced by the interaction of natural pigments from tea, artificial colorants, and fermentation additives. Thai red tea, in particular, is made from black tea and contains added artificial flavors and colorants. Tea leaves, rich in catechin polyphenols, undergo chemical transformations during black tea processing (Deka et al. 2021; Ito and Yanase 2022). Oxidase enzymes convert catechins into reddish-orange theaflavins and brown

thearubigins, the key pigments in black tea (Izawa et al. 2010; Deka et al. 2021; Ito and Yanase 2022). These water-soluble pigments easily incorporated into the BC matrix during fermentation. Additionally, FD&C Yellow No. 6 (INS 110), an artificial orange-red colorant in Thai red tea, enhances the coloration. The combination of natural and synthetic pigments gives the control BC its distinctive red-orange hue.

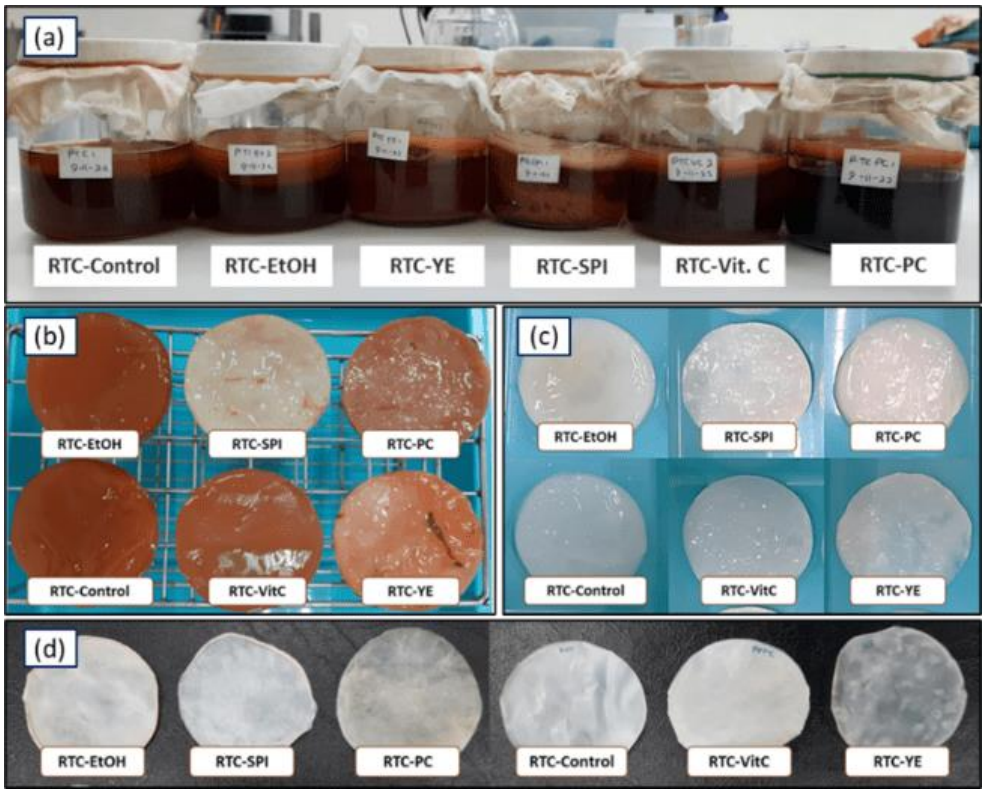

Figure 3.13 The appearance of BC sample from RTC kombucha fermentation with different type of additives: In fermentation process (a), before purification (b), after purification with sodium hydroxide (c), and after oven drying (d).

RTC-EtOH results suggest that ethanol had minimal impact on pigment absorption in BC. Color differences likely stem from interactions between tea pigments, additives, and microbial activity. In control and ethanol-treated samples, pigments remained more available, giving BC a red-orange hue. In contrast, SPI, YE, and PC-treated samples appeared lighter, possibly due to these additives affecting pigment solubility or binding. Interactions between tea polyphenols and artificial colorants may further reduce pigment absorption, as polyphenols form complexes with these

additives through hydrophobic, electrostatic, and hydrogen bonding (Shahidi and Dissanayaka 2023). Covalent interactions, which can occur during processes like heating and enzymatic reactions, may also contribute to reduced pigment incorporation in these additives-treated samples (Zhang et al. 2024).

After purification with 2% sodium hydroxide and drying in the oven at 40°C, the BC exhibits a consistent white, opaque color (**Figure 3.13(c)** and **3.13(d)**). This post-purification color aligns with the findings reported in most BC studies. Sodium hydroxide plays a vital role in BC purification by effectively removing tannins, polyphenols, residual bacteria, yeast cells, and proteins present in trace amounts within the kombucha pellicle (Amarasekara et al. 2020). It also facilitates the elimination of residual organic compounds, nucleic acids, and proteins produced by microbes during the fermentation process (Kamal et al. 2020).

4) BC Productivity and Water Holding Capacity

BC generated through kombucha fermentation exhibited distinct variations in wet yields, dry yields, and WHC based on the type of additives used, as depicted in **Figure 3.14**. The wet yields ranged from 61.73 ± 9.58 g/L for RTC-YE to 218.36 ± 12.85 g/L for RTC-EtOH. In a similar vein, the dry yields varied from 1.06 ± 0.10 g/L for RTC-YE to 2.18 ± 0.22 g/L for RTC-EtOH. The WHC of the samples varied between 57.49 ± 3.96 g water/g cellulose for RTC-YE and 109.31 ± 8.08 g water/g cellulose for RTC. Notably, the addition of certain additives, such as vitamin C and ethanol, significantly increased the wet productivity of BC compared to the RTC-C, with RTC-VC and RTC-EtOH showing significantly different results ($P < 0.05$). Conversely, the use of PC, SPI, and YE led to significantly lower wet yields compared to the control.

The dry yield of BC generally improved with the incorporation of most additives, except for YE, which produced the lowest dry yield among all samples. The highest dry yields were recorded for RTC-VC and RTC-EtOH, which did not differ significantly from each other ($P > 0.05$). Furthermore, WHC was highest in the RTC control, followed by RTC-EtOH, RTC-VC, RTC-SPI, RTC-PC, and RTC-YE, respectively. The

RTC-PC and RTC-SPI samples displayed similar outcomes across all measured parameters, with no significant differences observed ($P > 0.05$).

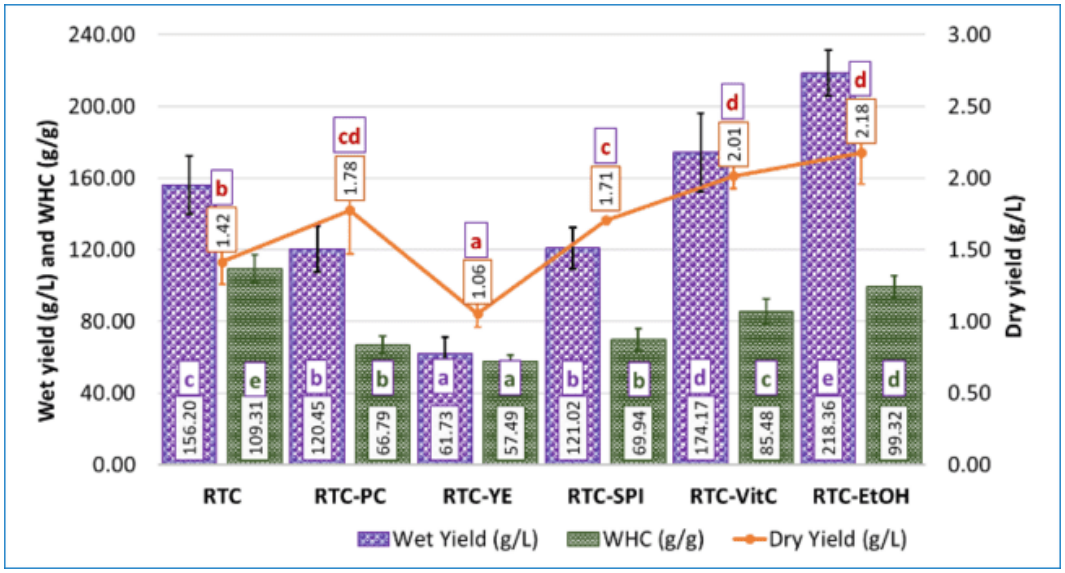

Figure 3.14 Wet yield (g/L), dry yield (g/L), and WHC (g water/g cellulose) from BC produced from RTC kombucha with different types additives.

Previous studies have reported varying effects of additives, including coffee grounds, yeast extract, vitamin C, and ethanol, on BC production. Some studies indicate that vitamin C can both enhance and reduce BC productivity. For instance, Keshk (2014) found that adding 0.5% (w/w) vitamin C increased BC production from 0.25 g/30 mL to 0.47 g/30 mL. Similarly, tropical fruits rich in vitamin C, such as mango, guava, and creole cherry, were shown to enhance BC production (Perna Manrique et al. 2018). Another study reported that a medium containing molasses with 0.5% ascorbic acid produced BC approximately three times higher than a control HS medium using *G. sucrofermentans* (Atykyan et al. 2020). In contrast, the addition of vitamin C to the medium of BC production using *K. hansenii* SI1 and *K. xylinus* PTCC 1734 resulted in lower BC productivity (Raiszadeh-Jahromi et al. 2020; Cielecka et al. 2021). In contrast, ethanol supplementation has consistently shown a significant increase in BC production. For example, the addition of 1% ethanol to the growth medium increased BC production by 57.7% using *G. xylinus* PTCC (Kazemi et

al. 2015). Similarly, a 1% ethanol supplementation in HS medium led to a 279% increase in BC production by *K. medellinensis* (Molina-Ramírez et al. 2018b). Moreover, in another study using *K. nataicola*, the addition of 1% ethanol increased BC yield by 48 ± 3% compared to the control (Fei et al. 2023).

The addition of 0.5% vitamin C and 1% ethanol in this study resulted in a notable increase in BC production. Compared to the control, the wet yield increased by 11.50% with vitamin C and 39.79% with ethanol, while the dry yield rose by 42.23% and 53.72%, respectively. These results align with previous studies suggesting that ethanol and vitamin C can enhance BC synthesis through different metabolic and regulatory mechanisms.

Ethanol has been shown to serve as an alternative energy source, reducing the reliance on glucose for ATP production and allowing more glucose to be diverted toward cellulose biosynthesis. Ethanol is metabolized via pyrroloquinoline quinone-dependent alcohol dehydrogenase (PQQ-ADH), which is linked to the electron transport chain and leads to increased ATP generation. Elevated ATP levels inhibit glucose-6-phosphate dehydrogenase, thereby decreasing flux through the pentose phosphate pathway and promoting the conversion of glucose into UDP-glucose, a direct precursor for cellulose synthesis (Montenegro-Silva et al. 2024). In addition, ethanol has been reported to upregulate genes involved in glucokinase activity, UDP-glucose biosynthesis, and BC production, while also enhancing cellular stress tolerance by promoting the expression of genes related to protein synthesis, iron uptake, and general metabolic stability (Ryngajłło et al. 2019).

In contrast, the stimulatory effect of vitamin C appears to be primarily associated with its role in reducing gluconic acid accumulation in the culture medium. By limiting gluconic acid production, vitamin C creates a more favorable pH environment and supports better bacterial growth and metabolic activity, which ultimately contributes to increased BC yield (Keshk 2014).

The WHC of BC resulted from RTC-C, RTC-PC, RTC-YE, RTC-SPI, RTC-VC, and RTC-EtOH was found to be 109.31±8.08, 66.79±4.74, 57.49±3.96, 69.94±6.11, 85.48±7.19, and 99.32±5.98 g water/g cellulose, respectively. The addition of various additives significantly reduced WHC values compared to the control sample, RTC-C ($P < 0.05$). Among the samples, those supplemented with nitrogen sources (RTC-YE and RTC-SPI) and RTC-PC exhibited the lowest WHC values, with RTC-YE showing the minimum WHC. The variation in the WHC of BC samples with different additives can be attributed to the structural and compositional changes induced during fermentation. A study reported that the addition of a higher concentration single sugar-linked glucuronic acid-based oligosaccharide (SSGO) to the synthetic medium resulted in a lower WHC value of BC (Ul-Islam et al. 2012).

The addition of SPI, YE, and PC are known to affect the metabolic activity of cellulose-producing bacteria, leading to a denser BC matrix with reduced porosity. This structural compactness limits the availability of hydrophilic sites for water retention, thereby decreasing WHC. In contrast, samples containing vitamin C and ethanol retained relatively higher WHC. BC from media containing vitamin C and ethanol holds more water likely because these additives make the BC structure more hydrophilic and better at forming hydrogen bonds with water. In addition, BC with Vitamin C, has smaller BC fiber among others thus increase the surface area. The higher surface area the higher the three-dimensional nanofibril structure the more water molecules trapped on the matrix (Ul-Islam et al. 2012). Ethanol, on the other hand, reduces the crystallinity of BC, making the cellulose network looser and exposing more hydrophilic sites.

These findings align with previous studies. For instance, Gayathry (2015) reported a WHC of approximately 87.14 g/g for BC produced from fermented coconut water (NDC) (Gayathry 2015). WHC values for NDC varied between 38.7±0.6 and 88.1±2.7 g/g when different pH levels, sucrose concentrations, and ammonium sulfate were used during production (Jagannath et al. 2008). Similarly, BC synthesized

using distillery wastewater achieved a WHC of 98.5 g/g (Wu and Liu 2013). WHC values ranging from 102 to 138 g/g were observed for BC produced in fermentation media derived from biodiesel and confectionery industry waste (Tsouko et al. 2015). Higher WHC values have also been documented, such as 114.01 g/g for BC produced via kombucha fermentation using black tea as the substrate (Avcioglu et al. 2021). BC synthesized from co-cultures of *K. hansenii* and *Rhizobium sp.* showed WHC values of 115 to 130 g/g (Almihyawi et al. 2024), higher compare to this study. These studies collectively highlight the variability of WHC based on fermentation conditions, bacterial strains, and additive use.

5) Morphology analysis

The morphology of BC samples produced from RTC kombucha fermentation with various types of additives was examined using scanning electron microscopy (SEM). Each sample was magnified 10,000 and 30,000 times (**Figures 3.15 (a.1 - f.2)**). The distribution size of the diameter of dried BC fiber was observed using ImageJ application and the results is depicted in **Figure 3.16**.

Based on the visual image, while there are similarities in the basic fiber form, differences in the finer details of structure suggest that the fiber morphology is not identical across all the samples. Overall, the BC samples exhibit a consistent fiber pattern, consistent with the findings of the previous studies (Illa et al. 2019; Brandes et al. 2020; Nguyen and Nguyen 2022). The BC sample of RTC-SPI (**Figure 3.15(b.1 an b.2)**) showed residues or insoluble materials persisting after alkali purification, likely due to the attachment of protein molecules to the fiber. This attachment of residual materials to BC fibers was also reported by Amorim et al. (2023) (Amorim et al. 2023).

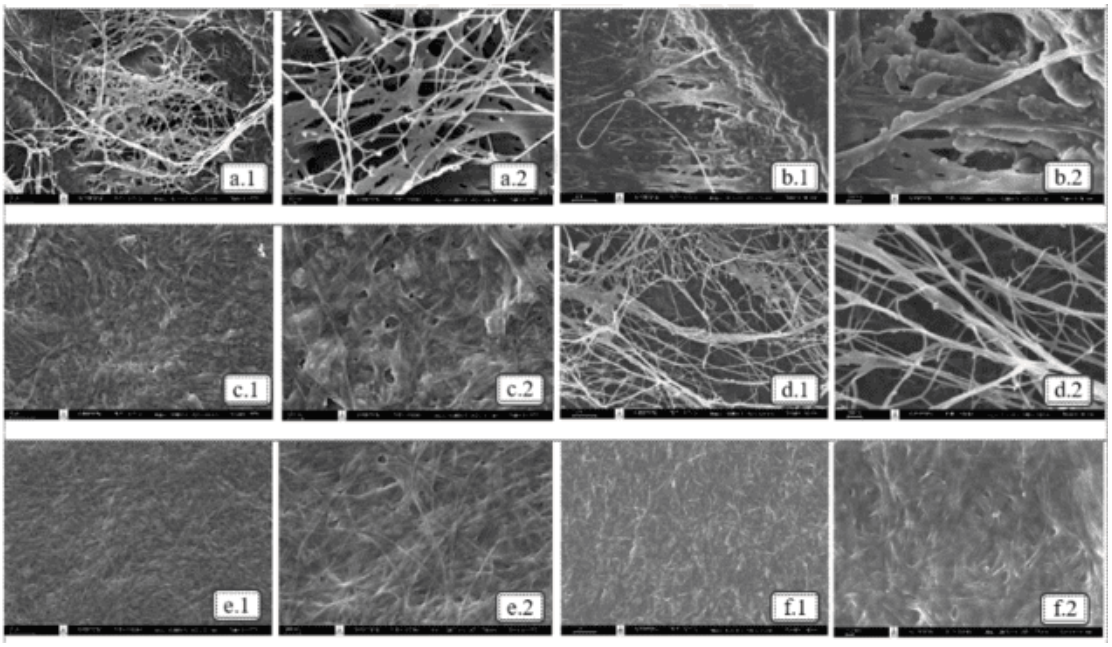

Figure 3.15 SEM image of BC (a) RTC-control; (b) RTC-SPI; (c) RTC-YE; (d) RTC-PC; (e) RTC-VC; (f) RTC-EtOH: (1) magnification of 10000 x; (2) magnification of 30,000x.

The polydispersity graphs of BC fiber diameters (**Figure 3.16**) indicate that the fiber sizes range from 13.74 nm to 68.44 nm, with average diameters varying between 25.49 ± 6.92 nm and 45.98 ± 9.38 nm. The average diameters of RTC-EtOH, RTC-SPI, RTC-YE, RTC-VC, RTC-PC, and RTC-C are 45.98 ± 9.38 nm, 40.92 ± 10.90 nm, 33.85 ± 4.91 nm, 25.50 ± 4.92 nm, and 29.70 ± 5.17 nm, respectively. Among the additives, VC produced BC with the smallest fiber diameters, while ethanol resulted in the largest. Sample with SPI, YE, and PC produced BC fibers with diameters larger than the RTC control but smaller than those in the RTC-EtOH sample. These findings demonstrate the significant role of additives in influencing BC fiber morphology.

The mechanisms by which additives affect BC fiber diameter remain unexplored. Among all the treatments, ethanol had the most significant impact on BC fiber morphology by markedly increasing fiber diameters. This observation supports previous findings by Fatima et al. (2023) who reported that ethanol concentrations of 1.5% and 3% led to increased fiber diameters ranging from 64.1–82.3 nm and 71.6–

88.6 nm, respectively. The underlying mechanism is thought to involve ethanol's disruption of hydrogen bonding during cellulose assembly, which interferes with the orderly formation of microfibrils and promotes the development of thicker fibers.

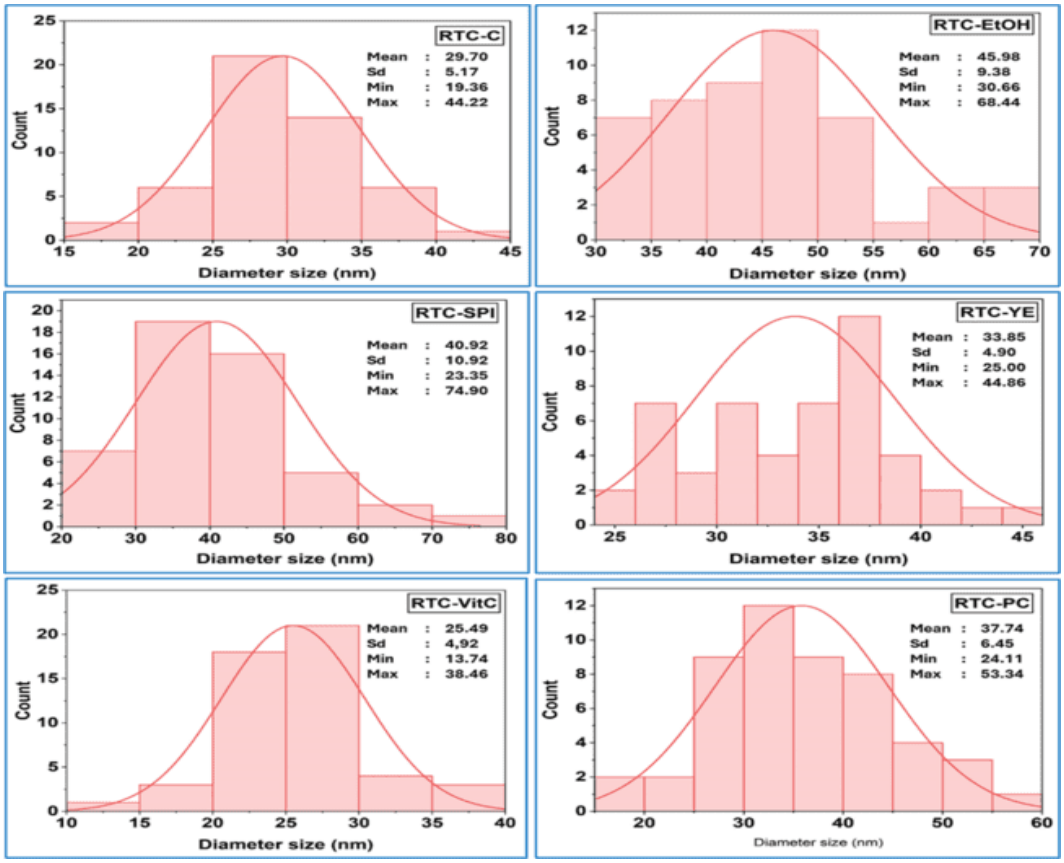

Figure 3.16 Graph of poly distribution size of BC samples diameter from RTC kombucha fermentation with various types of additives.

In contrast, the addition of VC resulted in the production of considerably thinner fibers. This effect may be linked to vitamin C's function as an antioxidant, which helps create a more favorable oxidative environment for bacterial metabolism during fermentation. By minimizing oxidative stress, VC can support enzymatic activity and stabilize the cellulose biosynthesis process. Moreover, it may enhance glucose metabolism and influence the crystallization and polymerization behavior of cellulose chains. Keshk (2014) reported that VC supplementation not only boosted BC yield but also altered its crystalline structure, suggesting that it plays a role in fine-tuning fiber assembly and promoting the formation of finer nanofibrils.

In comparison, samples containing YE, SPI, and PC exhibited moderately increased fiber diameters. This may be attributed to the nutritional contributions of nitrogen sources, peptides, and polyphenols present in these additives. Nitrogen-rich compounds such as YE and SPI are known to support microbial growth and biosynthetic activity, which can indirectly affect fiber thickness and structure (Said Azmi et al. 2023). Additionally, bioactive compounds in PC may interact with microbial cells or enzymes, subtly modifying the organization and bundling of cellulose fibrils.

Consistent with these observations, Illa et al. (2019) reported BC fiber diameters ranging from 10 to 60 nm, produced by *K. hansenii* 23769 (ATCC) and a cellulose-producing strain isolated from grape juice, with average diameters of 28.9 ± 5.6 nm and 28.6 ± 6.7 nm, respectively (Illa et al. 2019). The study highlighted the influence of microbial strain and cultivation medium on fiber dimensions. Similarly, Abol-Fotouh et al. (2020) showed that BC fibers produced by *K. saccharivorans* MD1 cultivated in HS medium with palm date supplementation ranged from 10 to 90 nm, illustrating how nutrient supplementation can modulate bacterial activity and BC properties (Abol-Fotouh et al. 2020).

Yilmaz and Goksungur (2024) further demonstrated that BC nanofibers derived from HS medium exhibited fiber diameters between 18 and 69 nm, averaging 36 nm. BC fibers from a waste fig medium had larger diameters, ranging from 23 to 90 nm, with an average of 44 nm. The larger fiber diameters in the waste fig medium may result from its complex composition, which could enhance nutrient availability and alter the cellulose biosynthesis pathway. In summary, the BC fiber diameters obtained from Thai red tea kombucha with different additives are consistent with those reported in earlier studies. These results confirm that the type and concentration of additives play a significant role in shaping BC fiber morphology.

6) Fourier Transform Infrared Spectroscopy Analysis

Figure 3.17 presents the FTIR spectra of BC samples produced from RTC kombucha fermentation with various additives, alongside the spectra of a BC sample from NDC for comparison. Overall, all BC samples exhibit similar spectral bands, but the intensity of these bands varies among the samples.

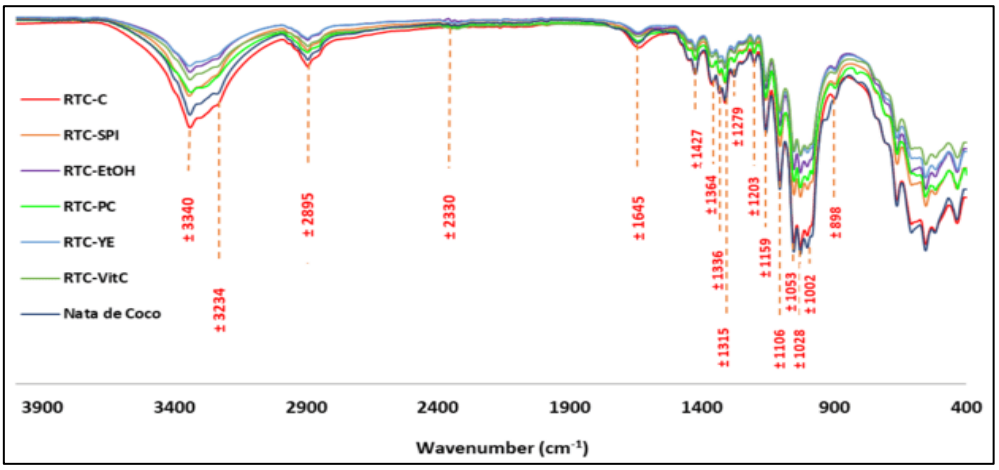

Figure 3.17 FTIR spectra of BCs from RTC kombucha fermentation with various types of additives

The FTIR spectra analysis of BC samples are divided into two main regions: the feature region and the fingerprint region. The feature region encompasses high-frequency wavenumbers between 4000 and 1330 cm^{-1}, while the fingerprint region spans 1330 to 500 cm^{-1} (Liu et al. 2023). In the feature region, key peaks were observed at wavenumbers around 3340 cm^{-1}, 3234 cm^{-1}, and 2895 cm^{-1}. The broad, intense bands at 3340 cm^{-1} and 3234 cm^{-1} indicate O-H stretching vibrations, while the peak near 2895 cm^{-1} corresponds to C-H stretching (Amorim et al. 2023). Additionally, a weak peak around 2330 cm^{-1} suggests the presence of triple-bond functional groups, such as C≡C and C≡N (Srivastava and Mathur 2022).

Another significant region, between 1350 and 2000 cm^{-1}, revealed absorption peaks at 1364 cm^{-1}, 1427 cm^{-1}, and 1644 cm^{-1}. The band at 1364 cm^{-1} corresponds to C-H symmetric bending, while the peak at 1427 cm^{-1} represents CH_2 symmetric bending. The 1644 cm^{-1} peak is associated with C=O stretching vibrations

from the glucose carbonyl group (Liu et al. 2023). In the fingerprint region, several distinct peaks were detected at 1336 cm^{-1}, 1315 cm^{-1}, 1279 cm^{-1}, 1203 cm^{-1}, 1159 cm^{-1}, 1106 cm^{-1}, 1053 cm^{-1}, 1028 cm^{-1}, 1002 cm^{-1}, and 898 cm^{-1}. The peak at 1336 cm^{-1} corresponds to OH in-plane bending, and the one at 1315 cm^{-1} is linked to CH_2 shifting at the C-6 position. The band at 1159 cm^{-1} is attributed to C-O-C antisymmetric bridge stretching, while the peak at 1106 cm^{-1} corresponds to ring asymmetric stretching. Peaks at 1053 cm^{-1} and 1028 cm^{-1} are associated with C-O-C and C-O-H stretching vibrations in the sugar ring, as well as C-O stretching, respectively (Liu et al. 2023). The peak between 898 and 894 cm^{-1} is linked to C-O-C stretching in β-1,4-glycosidic linkages, indicating the presence of an amorphous absorption band (Ciolacu et al. 2011).

The impact of additives on the FTIR spectra of BC is primarily reflected in variations in band intensity, rather than shifts in peak positions. Additives such as phenolic compounds (PC, e.g., caffeine), ethanol (EtOH), yeast extract (YE), vitamin C (VC), and soy protein isolate (SPI) can disrupt the hydrogen-bonding network within the BC matrix, as evidenced by the reduced intensity of the O–H stretching region (~3300–3400 cm^{-1}) (Moura et al. 2019; Feng et al. 2021; Wang et al. 2023, 2024; Liu et al. 2025). This suggests diminished hydroxyl group interactions and potentially increased hydrophobicity. As reported by Fornaro et al. (2015), hydrogen bonding significantly influences IR spectra by modifying both the frequency and intensity of bands associated with vibrational modes of directly involved functional groups. The observed spectral changes, particularly with ethanol treatment, support its role in weakening hydrogen bonding in the cellulose matrix.

A distinct peak at approximately 1645 cm^{-1}, observed across all samples, is attributed to the H–O–H bending vibration of water adsorbed by the hydroxyl-rich cellulose network (Zheng et al. 2019). Its consistent presence indicates that moisture remains associated with the BC structure regardless of the additive. However, variations in its intensity among different treatments reflect differences in

water retention capacity or the interaction of functional groups introduced by each additive, affecting the hydration behavior of the BC matrix.

7) X-Ray Diffraction (XRD) Analysis

Figure 3.18 illustrates the X-ray diffraction (XRD) patterns of different BC samples, highlighting three prominent peaks consistently observed at 2θ values of approximately 14.78°, 16.89°, and 22.90°. These peaks confirm the crystalline structure characteristic of BC (Said Azmi et al. 2023). The XRD profiles align closely with those previously reported for BC (Revin et al. 2018; Jittaut et al. 2023; Said Azmi et al. 2023). Despite the uniformity in chemical structure indicated by the XRD patterns, variations in diffraction peak intensities are evident among the samples. The most intense peak near 23°, is associated with cellulose type I (Said Azmi et al. 2023; Hossen et al. 2024). According to Gaspar et al. (2014), the peaks at 2θ values of 14.7°, 16.8°, and 22.7° correspond to the 100, 110, and 200 crystallographic planes, typical of monolithic cellulose type I found in native cellulose (Gaspar et al. 2014). The peak appeared at around 22.90° (2θ) indicate that the celluloses are crystalline in nature (Samuel and Adefusika 2019). Differences in relative peak intensity among the samples likely reflect subtle variations in cellulose chain orientation (Said Azmi et al. 2023).

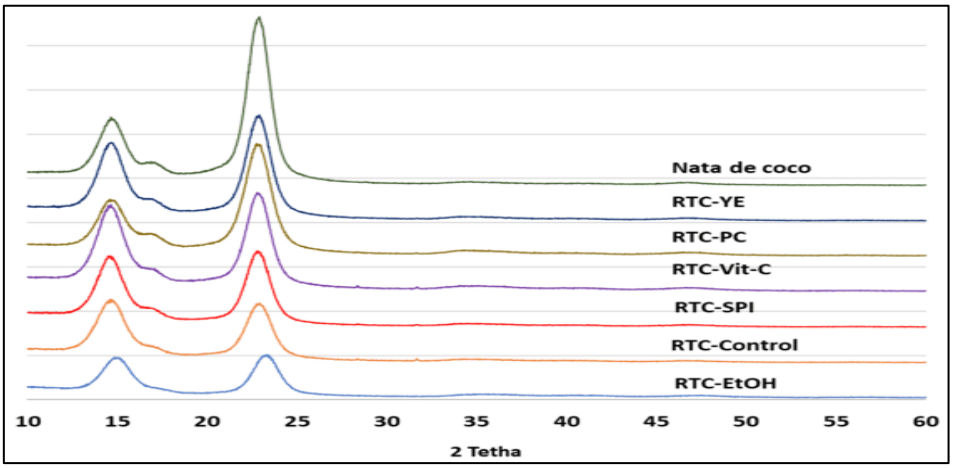

Figure 3.18 XRD spectra of BC from Thai red tea kombucha with different type of additives

The XRD data was used to calculate the crystallinity index (CI) and crystallite size of the BC samples, with the CI values presented in **Table 3.12**. The CI was determined using the Segal peak height method, yielding values ranging from 80.22% to 87.65%. All BC samples, except for RTC-EtOH, closely resembled the CI of NDC, which was 86.66%. The RTC-EtOH sample exhibited the lowest CI, likely due to the absence of, or a very subtle, peak around 16.89° (2θ). Several factors are known to influence the crystallinity of BC. These include the type of carbon and nitrogen sources, the use of various additives, the bacterial strain, fermentation conditions (such as temperature and duration), and post-production treatments (Zeng et al. 2011; Thielemans et al. 2023). Some previous studies reported that the effect of ethanol lead to decrease of crystallinity index of BC (Zeng et al. 2011; Cielecka et al. 2021; Wang et al. 2021). This reduction in crystallinity suggests that the cellulose structure becomes more disordered and less compact, possibly as a result of hydrogen bond disruption caused by ethanol treatment (Wang et al. 2021).

The CI results of BC in this study are consistent with findings from various other studies. For example, BC produced from pineapple peel waste fermentation achieved a CI of 87% (Sardjono et al. 2019), while BC fermented from pineapple waste solution had a CI of 82.2% (Pham and Tran 2023). BC derived from citrus processing waste or discarded fruits exhibited a CI of 86.9% (Andritsou et al. 2018), and BC produced in a HS-medium with different carbon sources showed a crystallinity ranging from 57% to 85% (Heydorn et al. 2023). Other studies have reported slightly lower CI values, such as BC produced using crude distillery effluent, which had a CI of 80.2% (Gayathri and Srinikethan 2019), and BC derived from wastewater of Arenga starch production, which had a CI of approximately 79.6% (Rahmayetty and Sulaiman 2023).

Table 3.12 Crystallinity index and average crystallite size of dried BC from Thai red tea kombucha fermentation with different type of additives.

Sample	Crystallinity Index (%)	Average Crystallite Size (nm)
RTC-C	85.36	3.512
RTC-PC	86.48	3.162
RTC-YE	87.65	3.356
RTC-SPI	85.30	3.302
RTC VC	85.71	3.286
RTC-EtOH	80.22	3.165
NDC	86.66	3.544

XRD analysis was performed once; therefore, variance data are not available

Further analysis is the average of the crystallite size of BC samples as shown in **Table 3.12**. The size of the crystallite ranging from 3.162 to 3.512 nm, slightly lower than crystallite size of NDC, 3.544 nm. This results in accordance with some of previous studies. BC produced by *G. xylinus* InaCC B404 in HS medium has a crystallite size of 3.06 nm (Agustin et al. 2021). In comparison, BC produced from black tea kombucha after 3 and 5 days of fermentation has crystallite sizes of 3.29 nm and 4.80 nm, respectively (Balistreri et al. 2024). However many studies reported the higher of crystallite size such as 4.9 and 4.76 nm (Sardjono et al. 2019), 5.6 nm (Jia et al. 2017), and 8.36 nm (Gayathri and Srinikethan 2019).

8) Thermogravimetric Analysis (TGA/DTG)

Figure 3.19 presents the thermogravimetric (TG) and derivative thermogravimetric (DTG) curves of the BC samples, analyzed using thermogravimetric analysis (TGA). **Table 3.13** shows the data of the decomposition change during analysis process. The data reveal the thermal stability and decomposition behavior of BC samples, including RTC-C, RTC-PC, RTC-YE, RTC-SPI, RTC-VC, and RTC-EtOH. The data from NDC was included for comparison. TGA and DTG analyses are crucial for studying BC applications. They help assess the purity, composition, drying behavior, and ignition

temperatures of materials. Additionally, these analyses provide insights into the thermal stability of BC, which is important for evaluating the effectiveness of chemical treatments that enhance bonding between natural fibers and polymer or synthetic fiber matrices (Nurazzi et al. 2021).

The first-stage weight loss, ranging from 1.42% to 7.52%, corresponds to the dehydration and volatilization of low-molecular-weight components or residual water in the BC matrix (Teixeira et al. 2019; Mohamad et al. 2022a). RTC-PC showed the lowest first-stage weight loss (1.42%), likely due to reduced moisture retention from the additive. This result relatively close result to previous result i.e. 1-2% (Gismatulina and Budaeva 2024) and 5-9% (Mohamad et al. 2022a).

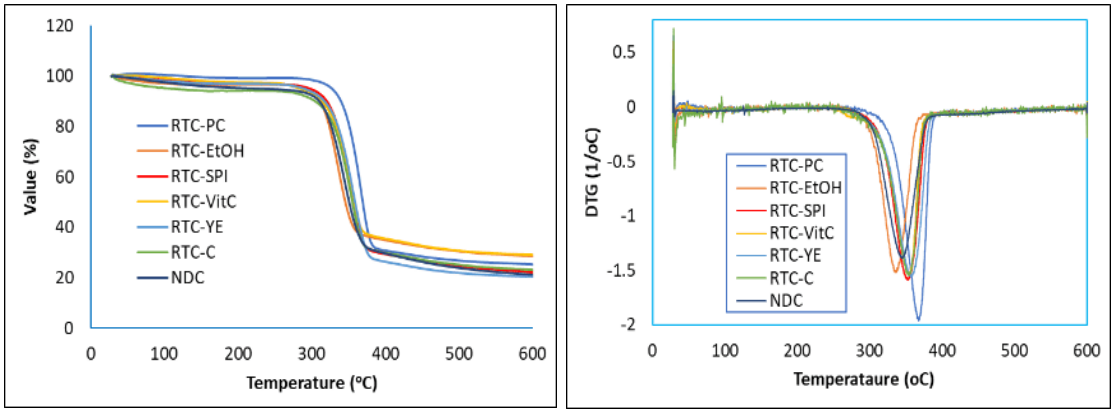

Figure 3.19 TGA (left) and DTG (right) thermographs of BC samples from RTC kombucha fermentation with different types of additives.

The second-stage weight loss, corresponding to the thermal decomposition of cellulose, ranged from 68.13% (RTC-EtOH) to 76.48% (RTC-YE), reflecting variations in thermal stability influenced by the additives. Nitrogen-based additives (RTC-PC, RTC-YE, RTC-SPI) generally showed higher second-stage losses, indicating enhanced cellulose decomposition under thermal stress. Residual weights at 600°C varied between 20.37% (RTC-YE) and 29.08% (RTC-VC), suggesting differences in the formation of thermally stable by-products. This stage represents the most significant weight loss, primarily driven by the breakdown of β-glucan chains and the

oxidation of cellulosic materials into carbonaceous residues (Mohammadkazemi et al. 2015; Mohamad et al. 2022a).

Table 3.13 The details of data decomposition during the TGA process of BC samples from RTC kombucha fermentation with different types of additives

Samples	First stage weight loss (%)	Second stage weight loss (%)	Residue (%)	DTG Peak range (°C)	DTG T_{Max} (°C)
RTC-C	6.03	71.06	23.07	255 – 379	353.67
RTC-PC	1.42	73.90	25.30	285 – 396	347.50
RTC-YE	3.09	76.48	20.37	270 – 389	356.67
RTC-SPI	2.94	74.81	22.21	271 – 384	352.67
RTC VC	2.60	68.27	29.08	258 – 378	354.17
RTC-EtOH	3.25	68.13	28.52	270 – 380	347.50
NDC	7.52	67.69	24.76	255 – 387	343.67

The findings of this study are consistent with previous research. For instance, BC produced by *G. xylinus* AGR 60 exhibited a first-stage mass loss of 6.2%, a second-stage mass loss of approximately 64.0%, and a residue of around 22.8% at 600°C, with a DTG T_{Max} of 339.6°C (Jenkhongkarn and Phisalaphong 2023). Similarly, BC from *A. xylinum* AGR 60 showed a first-stage mass loss of about 6%, a second-stage loss of approximately 74%, and a residue weight of around 20% at 700°C, with major thermal decomposition occurring between 300°C and 360°C (Potivara and Phisalaphong 2019).

The DTG peak temperature range (255–396°C) and maximum degradation temperatures (DTG T_{Max}: 343.67–356.67°C) show slight variations in the thermal degradation profiles, with RTC-YE exhibiting the highest DTG T_{Max} (356.67°C). These differences highlight the influence of additives on the thermal behavior of BC. The results align with previous studies, which report DTG peak ranges of 186–363°C and 199–347°C for BC treated by freeze-drying and hot-press drying, respectively, with

DTG T_{Max} values of 343.6°C and 313.4°C (Mohamad et al. 2022a). Additionally, BC produced by *G. xylinus* shows a DTG T_{Max} at 328.36°C (Jia et al. 2017).

9) Mechanical Properties Analysis Using Nanoindentation

Nanoindentation analysis was utilized to evaluate the nanoscale mechanical properties of BC samples. This highly precise technique measures local mechanical responses at micro- and nanoscale levels, making it essential for applications requiring durability and flexibility. BC samples selected for this analysis included RTC-EtOH and RTC-VC, chosen for their higher productivity, alongside control (RTC-C) and NDC samples for comparison. Detailed results are presented in **Table 3.14**.

The data show that in general, mechanical properties of RTC-EtOH and RTC-VC are quite different in many parameters such as maximum depth, plastic, reduced modulus, elastic recovery parameter, elastic work, and young's modulus. This indicates that both types of additives produce BC with quite different mechanical properties at the nanoscale. The differences in the mechanical properties of both could be attributed to the effects of the additives used during the fermentation process. Ethanol (EtOH) and vitamin C influence BC structure differently, impacting its mechanical behavior. Compare to RTC-C and NDC, some parameters show significantly different value, while others parameters are not significantly different.

The mechanical properties of BC are influenced by various factors, including cultivation methods, bacterial strains, purification processes, carbon sources, nutrient composition, and drying methods. Different cultivation techniques and bacterial strains affect the structure and quality of BC, impacting its strength and crystallinity (Krystynowicz et al. 2002; Zeng et al. 2014; Chen et al. 2018a). The purification process, particularly the concentration of NaOH used, determines the removal of impurities, influencing fiber quality (Suryanto et al. 2019; Chen et al. 2021). Additionally, the type of carbon source and nutrients, such as nitrogen, used during fermentation can affect BC's yield and mechanical properties (Betlej et al. 2020; Chibrikov et al. 2023). Drying methods also play a crucial role, in altering porosity and

density, which directly impact BC's flexibility, strength, and network structure, including intrafibrillar and interfibrillar spaces (Zeng et al. 2014; Wang et al. 2023b). These combined factors determine the unique mechanical characteristics of BC.

Another important factor to consider, complementing the earlier discussion, is the CI which plays a crucial role in determining the mechanical properties of BC. Research has shown that a higher CI generally results in increased stiffness and hardness while reducing ductility (Dusunceli and Colak 2008). Additionally, an increase in crystallinity has been linked to a higher Young's modulus (Adekoya et al. 2022). In this study, RTC-EtOH, with a CI of 80.22%, exhibited lower stiffness and hardness compared to RTC-VC, which had a CI of 85.71%. The Young's modulus (YM) of RTC-EtOH was 4.03 GPa, whereas RTC-VC displayed a higher YM of 4.47 GPa. Although the difference in hardness (H) was not statistically significant, RTC-EtOH showed a lower hardness value (0.20 GPa) compared to RTC-VC (0.23 GPa). Furthermore, the reduced CI in RTC-EtOH contributed to greater plasticity, as evidenced by its higher contact compliance (CC: 12.24 nm/mN) compared to RTC-VC (11.66 nm/mN). The plastic work (PW: 55.32 nJ) and elastic work (EW: 22.00 nJ) of RTC-EtOH were also higher than those of RTC-VC (PW: 52.73 nJ, EW: 20.90 nJ), indicating an increased energy absorption capability. Further supporting the notion that higher crystallinity contributes to enhanced stiffness and mechanical strength (Dusunceli and Colak 2008).

Young’s modulus values for RTC-EtOH were lower than those of RTC-VC and RTC-C but comparable to the NDC sample. Generally, these values align with previous studies. For instance, BC produced from various *Komagataeibacter* strains exhibits a Young's modulus range of 1.10 to 5.56 GPa (Chen et al. 2018a), while BC derived from *A. xylinum* AGR60 grown in coconut water reaches 9.14 GPa ((Potivara and Phisalaphong 2019).. The values observed for RTC-EtOH, RTC-VC, and RTC-C are within these ranges, indicating that different fermentation conditions can still yield high-quality BC. However, other studies, such as Zeng et al. (2014), report lower values,

with Young's modulus ranging from 198 to 659 MPa and hardness between 19 and 39 MPa, depending on the strain and drying methods used (Zeng et al. 2014).

Table 3.14 Mechanical properties data analysis using nano-indenter of BC from kombucha fermentation of RTC-C, RTC-EtOH, RTC-VC, and NDC.

Sample	MD (nm)	Pl (nm)	ML (mN)	H (GPa)	RM (GPa)	ERP	CC (nm/mN)	PW (nJ)	EW (nJ)	YM (GPa)
RTC-EtOH	3570.13 ±50.11^{b}	3110.31 ±48.59^{b}	50.10 ±0.00^{a}	0.20 ±0.01^{a}	4.41 ±0.09^{a}	0.15 ±0.00^{a}	12.24 ±0.09^{b}	55.32 ±1.14^{b}	22.00 ±0.16^{b}	4.03 ±0.08^{a}
RTC-VC	3308.46^{a} ±145.22	2870.18 ±121.85^{a}	50.10 ±0.00^{a}	0.23 ±0.02^{a}	5.04 ±0.51^{c}	0.15 ±0.01^{a}	11.66 ±0.82^{a}	52.73 ±3.34^{ab}	20.90 ±1.30^{a}	4.61 ±0.47^{b}
RTC-C	3412.25 ±259.56^{ab}	2980.18 ±253.91^{b}	50.10 ±0.00^{a}	0.22 ±0.05^{a}	4.94 ±0.56^{b}	0.15 ±0.01^{a}	11.50 ±0.22^{a}	54.41 ±4.64^{a}	20.80 ±0.47^{a}	4.51 ±0.51^{b}
NDC	3612.65 ±162.08^{bc}	3123.34 ±148.57^{b}	50.10 ±0.00^{a}	0.20 ±0.02^{a}	4.14 ±0.31^{a}	0.16 ±0.00^{a}	13.02 ±0.41^{c}	59.92 ±4.09^{bc}	22.90 ±0.80^{c}	3.78 ±0.28^{a}

MD: maximum depth, Pl: plastic, ML: maximum load, H: hardness, RM: reduced modulus, ERP: elastic recovery parameters, CC: contact compliance, PW: plastic work, EW: elastic work, and YM: Young's Modulus. The different lowercase letters within the same column indicate statistically significant differences ($P < 0.05$).

3.4.3 Effect of Carbon Source Combinations on Bacterial Cellulose Yield and Characteristics

1) The Change of pH and Total Soluble Solid (TSS)

This study investigated how various carbon sources influenced pH changes during a 15-day kombucha fermentation. The initial pH values of the media before inoculation ranged from 4.57 to 4.84, showing some statistically significant differences among groups. After inoculation with the kombucha culture, the pH dropped immediately to a range of 3.61 to 3.66, which can be attributed to the naturally acidic nature of the starter itself. Over the course of fermentation, the pH continued to decrease significantly, with final values ranging from 2.17 to 2.66 by day 15.

The reduction in pH is primarily due to microbial metabolism, particularly the activity of acetic acid bacteria (AAB) and yeasts that convert sugars into organic acids. As fermentation progresses, these microorganisms produce compounds such as acetic acid and gluconic acid, both of which contribute to the acidification of the medium (Aswini et al. 2020; Lee et al. 2021). Other minor acids like glucuronic, lactic, malic, citric, tartaric, and succinic acids may also be formed, further lowering the pH (Neffe-Skocińska et al. 2017).

The choice of carbon source significantly influenced the final pH levels, reflecting distinct metabolic behaviors during fermentation. RTC-SGlu (sucrose-glucose) and RTC-SD (sucrose-dextrose) yielded the lowest final pH values (2.17 ± 0.01 and 2.21 ± 0.01, respectively; $P > 0.05$), indicating pronounced acid production. This aligns with the rapid fermentability of glucose and dextrose, which are readily metabolized by microbial communities to support efficient growth and acid generation. In contrast, RTC-SGly (sucrose-glycerol) exhibited the highest final pH (2.66 ± 0.00), suggesting limited acidification due to the slower assimilation of glycerol by acetic acid bacteria (AAB) and yeasts. RTC-SF (sucrose-fructose) demonstrated intermediate acidification (pH 2.46 ± 0.01), likely attributable to fructose's preferential uptake over

sucrose, which requires prior hydrolysis. The control (RTC-C, pH 2.52 ± 0.04) displayed a typical fermentation profile but with marginally lower acid production compared to glucose- or dextrose-amended groups, underscoring the metabolic advantage of monosaccharide supplementation.

These findings are consistent with previous research showing that pH consistently declines during kombucha fermentation due to the production of organic acids. For example, Neffe-Skociń ska et al. (2017) observed a pH drop from 3.04 to 2.63 after 10 days of fermentation. Yilmaz and Goksungur (2024) also reported final pH values between 3.51 and 4.54 when using *K. xylinus* with different initial pH levels (4.0–7.0), emphasizing the influence of starting conditions. Other studies have reported similar final pH ranges after 14 days of kombucha fermentation, such as 3.36 to 3.82 (Vohra et al. 2019) and 2.91 to 3.74 (Zhao et al. 2018). Chong et al. (2024) documented a pH decrease from 3.19–3.27 to 2.72–2.79 within 10 days when using black, green, and oolong teas. These comparisons highlight a consistent trend of acid production in kombucha systems.

In this study, **Table 3.** summarizes pH values before and after inoculation, as well as at the end of fermentation, showing statistically significant differences across treatments. **Figure 5.1** (left side) illustrates the progression of acidification over 15 days. The sharp pH decline observed in RTC-SGlu compared to the more gradual decrease in RTC-SGly clearly demonstrates how different carbon sources affect the rate and extent of acid production during fermentation.

For the TSS observation, initial values ranged from 9.70±0.00 to 10.70±0.00 °Brix before inoculation. After adding the inoculum, the TSS remained relatively stable, ranging from 9.70±0.00 to 10.60±0.00 °Brix. However, by the end of the fermentation process, TSS values decreased significantly, reaching a range of 7.87±0.05 to 8.60±0.00 °Brix, as presented in **Table 3.15** and illustrated in **Figure 3.20** (right).

Table 3.15 Changes in pH and °Brix degree during RTC kombucha fermentation with different carbon source combinations.

Samples	The Change of the pH			The Change of the °Brix		
	Medium	Before	after	Medium	Before	after
RTC-C	4.84±0.00^{d}	3.65±0.00^{c}	2.52±0.04^{c}	10.70±0.00^{d}	10.60±0.00^{c}	8.57±0.05^{c}
RTC-SD	4.76±0.00^{b}	3.62±0.00^{b}	2.21±0.01^{a}	10.10±0.00^{b}	10.10±0.00^{b}	8.33±0.09^{a}
RTC-SF	4.57±0.00^{a}	3.61±0.00^{a}	2.46±0.01^{b}	10.50±0.00^{c}	10.40±0.00^{a}	7.87±0.12^{b}
RTC-SGlu	4.76±0.00^{b}	3.62±0.00^{a}	2.17±0.01^{a}	10.70±0.00^{d}	10.40±0.00^{b}	8.40±0.08^{a}
RTC-Sgly	4.78±0.00^{c}	3.66±0.00^{c}	2.66±0.00^{d}	9.70±0.00^{a}	9.70±0.00^{c}	8.60±0.00^{d}

Different lowercase letters within a column indicate significant differences among the five tea samples (LSD test: P < 0.05)

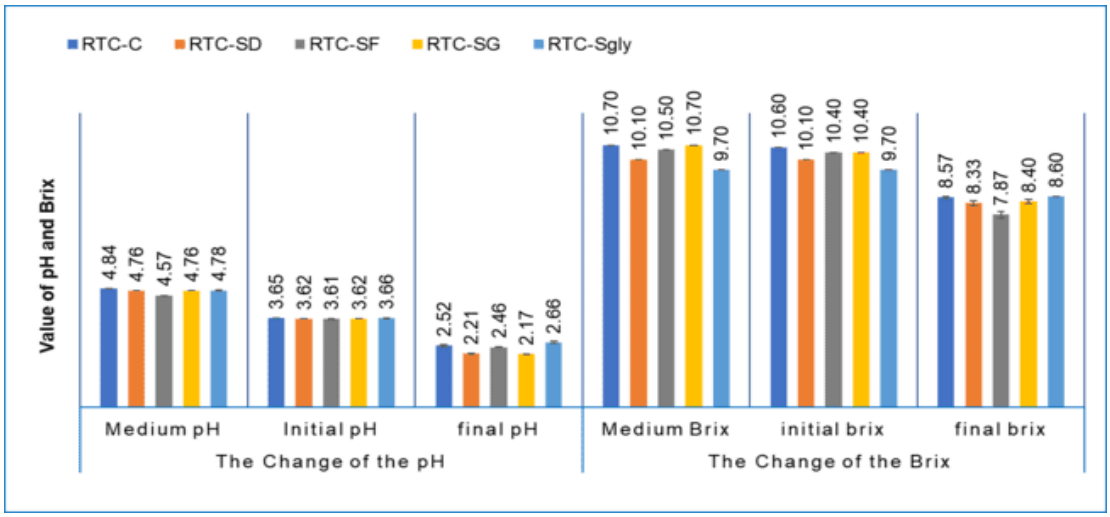

Figure 3.20 Changes in pH and °Brix degree during RTC kombucha fermentation with different carbon source combinations.

The reduction in TSS during fermentation is mainly driven by microbial activity. In kombucha, yeasts break down complex sugars into simpler ones like glucose and fructose. These are then further metabolized by acetic acid bacteria into organic acids and other by-products (Muzaifa et al. 2022), resulting in a decrease in soluble sugar concentration and, consequently, °Brix values.

The extent of TSS reduction varied depending on the carbon source, reflecting differences in sugar utilization efficiency. RTC-SF showed the greatest decline, from 10.40±0.00 to 7.87±0.12 °Brix, indicating a strong microbial preference and rapid metabolism. RTC-SD (dextrose) and RTC-SGlu had similar final values—8.33±0.09 and 8.40±0.08 °Brix, respectively—suggesting that both monosaccharides were efficiently utilized. The RTC-C dropped from 10.60±0.00 to 8.57±0.05 °Brix, reflecting normal microbial activity without added sugars. Meanwhile, RTC-SGly showed the smallest reduction, ending at 8.60±0.00 °Brix, possibly due to slower or more selective microbial metabolism of glycerol.

The structural similarity between dextrose and glucose likely accounts for their comparable fermentation behavior. In contrast, the more complex structure or lower fermentability of glycerol may have limited its consumption. These results are consistent with earlier studies (e.g., Zubaidah et al. 2019; Muzaifa et al. 2022), which highlight the influence of carbon source composition on microbial activity and sugar conversion during kombucha fermentation (Sinamo et al. 2022).

These findings are consistent with previous kombucha studies. For example, (Zubaidah et al. 2019) reported a TSS decrease from 13.30–14.08 °Brix to 12.43–12.97 °Brix in snake fruit kombucha, while (Muzaifa et al. 2022). observed a reduction in cascara kombucha from 10.97 °Brix on day two to 9.97 °Brix on day eight. Such comparisons reinforce the role of microbial metabolism in altering sugar profiles and show that the degree of TSS reduction varies by both fermentation duration and substrate type (Sinamo et al. 2022).

2) The Change of Sugar Composition

The sugar profile, including sucrose, glucose, fructose, and glycerol, was analyzed before and after fermentation using high-performance liquid chromatography (HPLC). Significant changes in sugar concentrations were observed following fermentation, as illustrated in **Figure 3.21** and detailed in **Table 3.16**.

Sucrose served as the primary carbon source for the SCOBY, promoting microbial growth and the synthesis of various metabolites, including BC (Shu 2007).

Before fermentation, the sucrose content in the control sample was 9.05 ± 0.18%, whereas in the sugar combination samples it ranged from 4.41% to 4.75%. Glucose levels ranged from 0.82% to 5.16%, and fructose from 0.00% to 4.92%. Glycerol was detected only in the RTC-SGly sample, at 5.40 ± 0.23%.

The presence of glucose and fructose in samples without added glucose or dextrose likely results from sucrose hydrolysis during autoclaving, as well as from enzymatic activity by the kombucha culture. Similar findings were reported by Ball (1953), who observed that autoclaving a 3% sucrose solution produced 0.7–0.9% glucose. Additionally, de Lange (1989) showed that sucrose can be completely hydrolyzed into glucose and fructose at pH 2 during autoclaving, with partial hydrolysis occurring at pH 5–7. These results align with observations discussed in the previous experiments of this study.

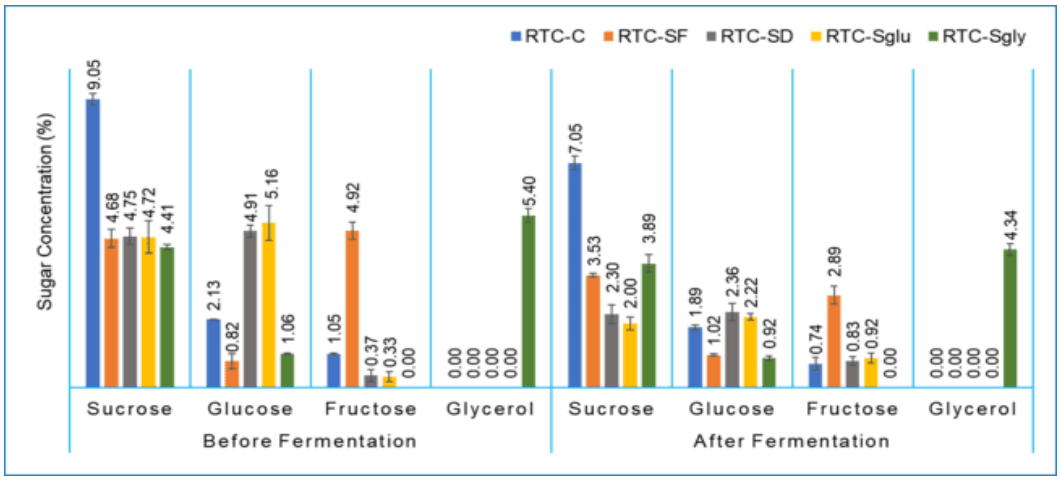

Figure 3.21 Change of sugar composition of RTC kombucha broth with different types of carbon sources combinations before and after fermentation

During kombucha fermentation, normally, sucrose serves as the primary carbon source. It is enzymatically hydrolyzed by yeasts into glucose and fructose through the action of invertase (Gao et al. 2019; Lee 2023). These simpler

sugars especially glucose are metabolized preferentially, providing energy and substrates for microbial activity (Gao et al. 2019). Under anaerobic conditions, yeasts convert glucose and fructose into ethanol and carbon dioxide (Wang et al. 2022a). Subsequently, acetic acid bacteria oxidize ethanol into acetic acid in the presence of oxygen, contributing to the characteristic tartness of kombucha (Wang et al. 2022a). If glucose, dextrose, and fructose are already present in the fermentation medium, microorganisms prioritize these simpler carbon sources over sucrose because they can be directly metabolized without enzymatic hydrolysis. This metabolic preference is demonstrated by the higher consumption of dextrose, glucose, and fructose compared to sucrose in various carbon source combinations. These results underline the efficiency of microbial metabolism in utilizing readily available simple sugars when presented in the fermentation medium.

All kombucha samples showed a significant reduction in sucrose levels post-fermentation, primarily due to invertase-mediated hydrolysis and microbial uptake. The largest decrease occurred in the control (RTC-C), where sucrose dropped from 9.05% to 7.05%. Despite overall sucrose consumption, the relatively high residual level in RTC-C suggests slower fermentation in the absence of added monosaccharides. Since sucrose requires hydrolysis before utilization, the lack of readily available simple sugars likely delayed microbial activity. In contrast, RTC-SGlu and RTC-SD exhibited similar and more efficient sugar consumption, with glucose levels falling from 5.16% to 2.22% in RTC-SGlu and from 4.91% to 2.36% in RTC-SD. The absence of a significant difference ($P > 0.05$) supports their metabolic equivalence and highlights the microbial preference for readily assimilable monosaccharides over disaccharides like sucrose.

In the RTC-SF sample, a substantial reduction in fructose concentration was observed—from 4.92% to 2.89%—indicating its active involvement in microbial metabolism. However, the remaining fructose suggests a relatively slower utilization rate compared to glucose, aligning with previous findings that yeasts tend to metabolize glucose more efficiently than fructose (Wang et al. 2022a). The RTC-SGly

sample exhibited a modest decrease in glycerol levels, from 5.40% to 4.34%, implying partial microbial usage. Glycerol is generally considered a secondary carbon source in kombucha fermentation, as it enters metabolic pathways differently and is not a primary substrate for most SCOBY microbes. The persistence of elevated glycerol levels post-fermentation suggests limited microbial affinity under the given conditions, potentially due to its lower energy yield and the availability of more favorable sugars.

These findings are consistent with those of Neffe-Skocińska et al. (2017), who reported a substantial decrease in sucrose concentration—from 9.97% to 0.74%—over a 10-day kombucha fermentation, highlighting the active hydrolysis of sucrose. Although the reduction observed in our study was less pronounced, the overall trend of sucrose consumption aligns with their results. However, due to the limited number of studies directly examining the effect of added monosaccharides on sucrose reduction in kombucha fermentation, direct comparisons remain challenging. Nonetheless, available evidence supports the idea that the presence of readily fermentable monosaccharides can accelerate fermentation by providing immediate energy sources, whereas reliance solely on sucrose may lead to slower sugar utilization.

Table 3.16 The change of sugar composition during RTC kombucha fermentation with different types of carbon source combinations

Samples	Before fermentation				After fermentation			
	Sucrose	Glucose	Fructose	Glycerol	Sucrose	Glucose	Fructose	Glycerol
RTC-C	9.05±0.18 (b, B)	2.13±0.02 (b, B)	1.05±0.03 (c, A)	ND	7.05±0.21 (d, A)	1.89±0.08 (b, A)	0.74±0.20 (b, A)	ND
RTC-SF	4.68±0.29 (a, B)	0.82±0.23 (a, A)	4.92±0.28 (d, B)	ND	3.53±0.06 (b, A)	1.02±0.03 (a, A)	2.89±0.28 (c, A)	ND
RTC-SD	4.75±0.26 (a, B)	4.91±0.20 (c, B)	0.37±0.20 (b, A)	ND	2.30±0.29 (a, A)	2.36±0.27 (bc, A)	0.83±0.13 (b, B)	ND
RTC-SG	4.72±0.51 (a, B)	5.16±0.54 (c, B)	0.33±0.16 (b, A)	ND	2.00±0.20 (a, A)	2.22±0.10 (b, A)	0.92±0.16 (b, B)	ND
RTC-SGly	4.41±0.07 (a, B)	1.06±0.03 (a, A)	0.00±0.00 (a, A)	5.40±0.23 (B)	3.89±0.29 (c, A)	0.92±0.08 (a, A)	0.00±0.00 (a, A)	4.34±0.18 (A)

Different lowercase letters within a column indicate significant differences among the five tea samples (LSD test: $P < 0.05$); different uppercase letters in the same row indicate the significant differences between the same sugar before and after fermentation (LSD test: $P < 0.05$). ND = not detected.

3) The appearance of Bacterial cellulose

The appearance of BC produced from Thai red tea kombucha fermentation with different uses of carbon sources combinations are presented in **Figure 3.22.**

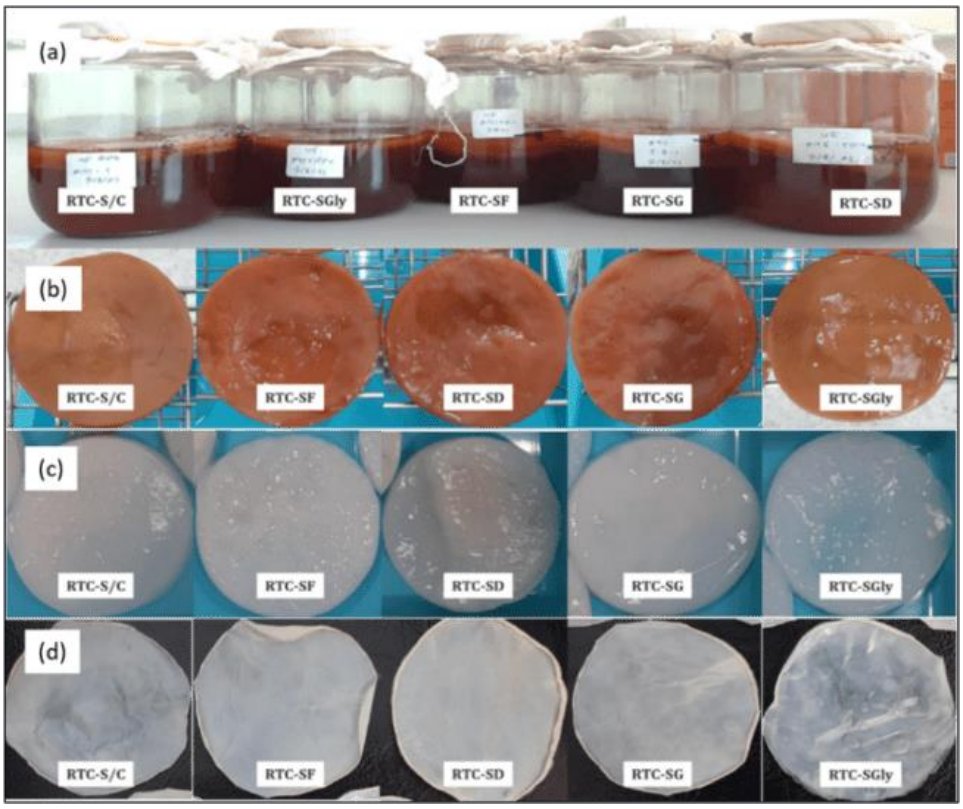

Figure 3.22 BC appearance at different stages of RTC kombucha fermentation with various carbon source combinations: (a) during fermentation, (b) before purification, (c) after purification with sodium hydroxide, and (d) after oven drying.

The appearance of BC before purification shows red-orange colors with the BC from RTC-SD, RTC-SGlu, and RTC SF show slightly darker compare to RTC-C and RTC-Gly (**Figure 3.22(a) and (b)**). The red-orange color of the BC samples produced during Thai red tea kombucha fermentation can be attributed likely to the combined effect of natural tea pigments, artificial colorants. Thai red tea, made from black tea with added artificial flavor and FD&C Yellow No. 6 (INS 110), contributes to the color. Black tea leaves contain catechins, which, through oxidation, are converted

into theaflavins (reddish-orange pigments) and thearubigins (brown pigments) during processing (Deka et al. 2021; Ito and Yanase 2022). These pigments are water-soluble and can be absorbed into the BC matrix during fermentation. Additionally, the presence of FD&C Yellow No. 6 enhances the orange-red hue of the BC samples (Izawa et al. 2010; Deka et al. 2021; Ito and Yanase 2022). The same results were also reported in the previous chapter of this thesis.

In the next steps, after purification using sodium hydroxide solution (2% w/v) the BC exhibits a similar white color (**Figure 3.22(c)**) and after drying in the oven at 40°C showed consistent white, opaque color (**Figure 3.22(d)**). This post-purification color aligns with findings reported in most BC studies. Sodium hydroxide plays a vital role in BC purification by effectively removing tannins, polyphenols, residual bacteria, yeast cells, and proteins present in trace amounts within the kombucha pellicle (Amarasekara et al. 2020). It also facilitates the elimination of residual organic compounds, nucleic acids, and proteins produced by microbes during the fermentation process (Kamal et al. 2020).

4) BC Productivity and Water Holding Capacity

Figure 3.23 presents the wet yield, dry yield, and WHC of BC produced from Thai red tea kombucha (RTC) using various carbon source combinations: RTC-C, RTC-SF, RTC-SD, RTC-SGlu, and RTC-SGly. The wet yields of BC for these treatments were 167.44 ± 24.00, 193.87 ± 36.68, 234.87 ± 39.10, 259.54 ± 8.92, and 74.53 ± 8.95 g/L, respectively, while the corresponding dry yields were 1.72 ± 0.19, 1.88 ± 0.23, 2.20 ± 0.54, 2.59 ± 0.16, and 0.66 ± 0.03 g/L. The WHC values were 109.31 ± 4.65, 101.92 ± 9.12, 105.79 ± 25.13, 99.07 ± 2.85, and 112.44 ± 17.49 g water/g cellulose, respectively.

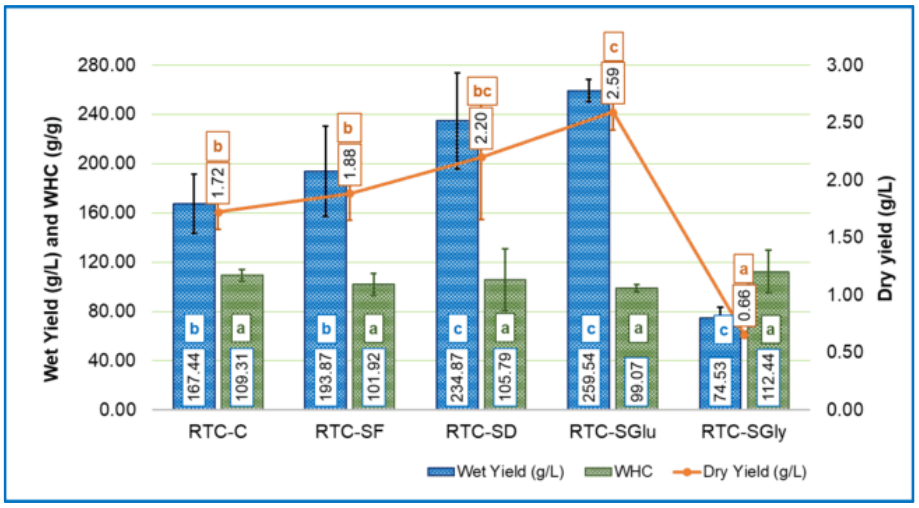

Figure 3.23 Wet yield (g/L), dry yield (g/L), and WHC (g water/g cellulose) of BC produced from RTC kombucha using different combinations of carbon sources.

Among the treatments, RTC-SGlu resulted in the highest wet and dry BC yields, significantly exceeding those of RTC-C, RTC-SF, and RTC-SGly ($P < 0.05$), though not significantly different from RTC-SD ($P > 0.05$). This enhancement can be attributed to the efficient microbial metabolism of glucose, which serves as a direct substrate for the biosynthesis of cellulose. As reported by Gao et al. (2019), simple sugars such as glucose and fructose are metabolized more efficiently than disaccharides like sucrose, accelerating the formation of cellulose precursors like UDP-glucose. In treatments such as RTC-SD and RTC-SGlu, sucrose likely underwent enzymatic hydrolysis by invertase into glucose and fructose, with glucose being preferentially utilized by the microbial consortium for cellulose biosynthesis (Wang et al. 2022a). As shown in **Table 3.16**, the higher consumption of carbon sources, particularly sucrose and glucose, in RTC-SD and RTC-SGlu likely contributed to the enhanced cellulose production observed in these treatments.

RTC-SF showed moderate increases in yield compared to the control, although the difference was not statistically significant. The use of fructose in combination with sucrose may have supported BC formation, as fructose is also metabolizable, though generally less efficiently than glucose (Gao et al. 2019). The

control group (RTC-C), containing sucrose alone, had lower yields, suggesting that additional monosaccharides improve sugar utilization and enhance BC biosynthesis.

In contrast, RTC-SGly showed the lowest wet and dry yields. This suggests that glycerol is a less favorable carbon source under the tested conditions, possibly due to slower metabolic conversion into cellulose precursors or inhibitory effects at the concentration used. While previous studies have reported high BC production with glycerol under optimized conditions (Keshk and Sameshima 2005; Tabaii and Emtiazi 2016; Agustin et al. 2018; Thorat and Dastager 2018; Amorim et al. 2019; Ho Jin et al. 2019), differences in bacterial strains, pH, and medium composition may explain the lower performance in this study.

These results align with those from Treviño-Garza et al. (2020), who found that glucose yielded the highest BC production, followed by dextrose, fructose, and sucrose in kombucha systems. Specifically, wet and dry yields reached 301.81 g/L and 11.19 g/L with glucose and 300.74 g/L and 12.12 g/L with dextrose. Similarly, (Amorim et al. (2024) reported that glucose supported higher BC yields than other carbon sources such as raffinose and glycerol. Thorat and Dastager (2018) also observed that *K. rhaeticus* produced maximum BC (~8.7 g/L) at 3% glycerol, but yields dropped at concentrations above 4%. In addition, Adnan et al. (2015) reported that the highest BC yield was obtained at a glycerol concentration of 2%, while yields decreased at concentrations of 3% and above.

Regarding WHC, no statistically significant differences were observed among the treatments, indicating that carbon source type primarily affects BC yield but not its water-holding functionality. WHC is influenced more by the nanofiber structure, porosity, and surface area of the dried BC, which remained comparable under similar culture conditions. The WHC values in this study (99.07–112.44 g water/g cellulose) are consistent with literature reports. Wu and Liu (2013) observed a WHC of 98.5 g/g in BC from distillery wastewater, while Avcioglu et al. (2021) reported values of ~114 g/g in kombucha using black tea. Other studies noted WHC ranges from 90 to

200 g/g depending on the bacterial strain, fermentation time, and drying method (Tsouko et al. 2015; Treviño-Garza et al. 2020; Almihyawi et al. 2024; U˘gurel and Ö˘güt 2024).

In summary, this study demonstrates that the choice of sugar significantly affects BC yield, with glucose and dextrose promoting the highest productivity. Fructose and sucrose supported moderate yields, while glycerol was least effective under the tested conditions. However, WHC was not significantly impacted, suggesting that yield improvements can be achieved without compromising the BC's functional properties.

5) Morphology Analysis Using SEM

Figure 3.24 presents SEM images showing the surface morphology of BC produced using different carbon sources. These images were captured at magnifications of 10,000x and 30,000x for all samples. Additionally, magnification at 50,000x was applied to RTC-C and RTC-SGlu to provide a more detailed view of their fiber structures. Overall, the BC samples exhibit a consistent fiber pattern, consistent with the findings of the previous studies (Illa et al. 2019; Brandes et al. 2020; Nguyen and Nguyen 2022).

The RTC-C sample exhibits a dense and compact fibril network at 10,000x, with higher magnifications (30,000x and 50,000) revealing tightly packed and uniform cellulose fibrils. For RTC-SF, the structure is less dense at 10,000x, with more visible voids and irregular fibril arrangements at 30,000x. RTC-SD displays a highly interconnected and dense network at 10,000x, while the fibrils are smooth and regularly arranged at higher magnifications, indicating uniform cellulose synthesis. The RTC-SGlu sample shows a tightly interwoven fibril network at 10,000x, with well-organized and continuous fibrils visible at higher magnifications, suggesting high-quality BC formation. In contrast, RTC-SGly demonstrates a disrupted network with larger gaps between fibrils at 10,000x, and irregular shapes and uneven fibril distributions are observed at 30,000, indicating less effective cellulose production. Overall, the images

highlight the significant influence of the carbon source on BC morphology, with RTC-SG and RTC-SD producing denser and more organized fibril networks, while RTC-SGly results in a looser and less uniform structure. The denser fibril networks observed in RTC-SD and RTC-SGlu are likely due to the thicker BC layers formed before drying, while the thinner network in RTC-SGly reflects a less compact structure. This difference aligns with the wet yield results, where BC from RTC-SD and RTC-SGlu had the highest wet yields, whereas RTC-SGly had the lowest. These findings suggest that the initial wet thickness of BC significantly influences its final structure and density. Some impurities are visible in the SEM images especially in RTC-C sample, likely representing residues or insoluble materials remaining after alkali purification.

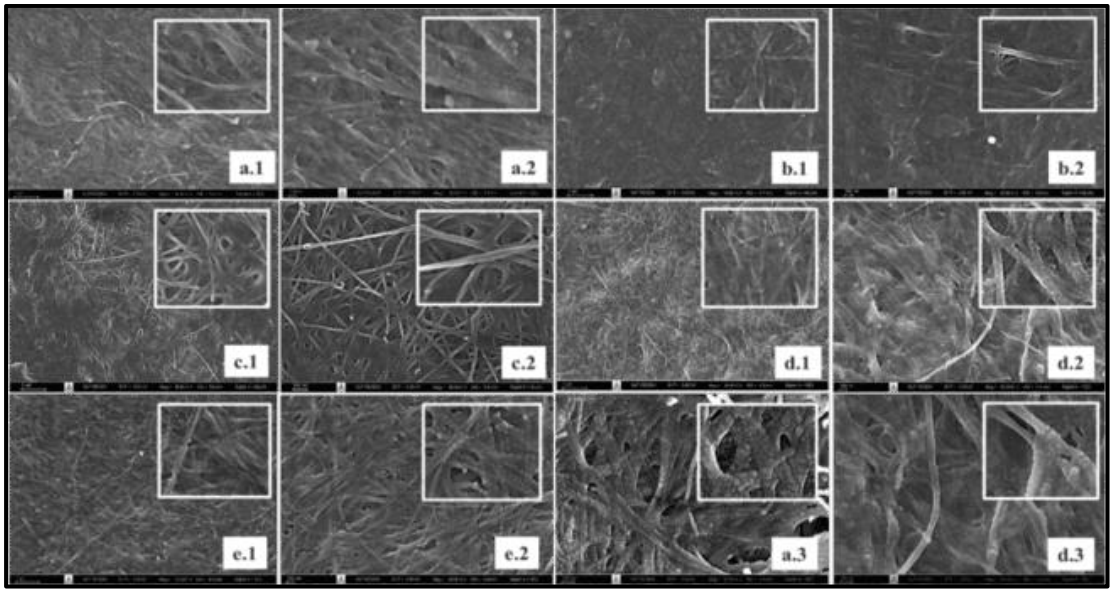

Figure 3.24 SEM image of BC (a) RTC-control; (b) RTC-SF; (c) RTC-SD; (d) RTC-SG; and (e) RTC-SGly; (1) magnification of 10000 x; (2) magnification of 30,000x; (3) magnification 50.000x.

The analysis following SEM imaging focused on the polydispersity of BC fiber diameters, as shown in **Figure 3.25.** The polydispersity graphs reveal that fiber diameters ranged from 19.35 nm (RTC-C) to 63.28 nm (RTC-SD), with average diameters varying between 29.70 ± 5.17 nm (RTC-C) and 40.39 ± 8.65 nm (RTC-SD). Compared to RTC-C, the use of sugar combinations resulted in slightly larger BC fiber

diameters. Among the sugar combination samples, the average diameters ranged from 34.34 ± 7.56 nm (RTC-SG) to 40.39 ± 8.65 nm (RTC-SD). These findings suggest that, although sugar combinations slightly increased fiber size, the effect was not as pronounced as the variations caused by different additives discussed in the previous section. Overall, the use of different carbon source combinations had a relatively minor impact on BC fiber diameter.

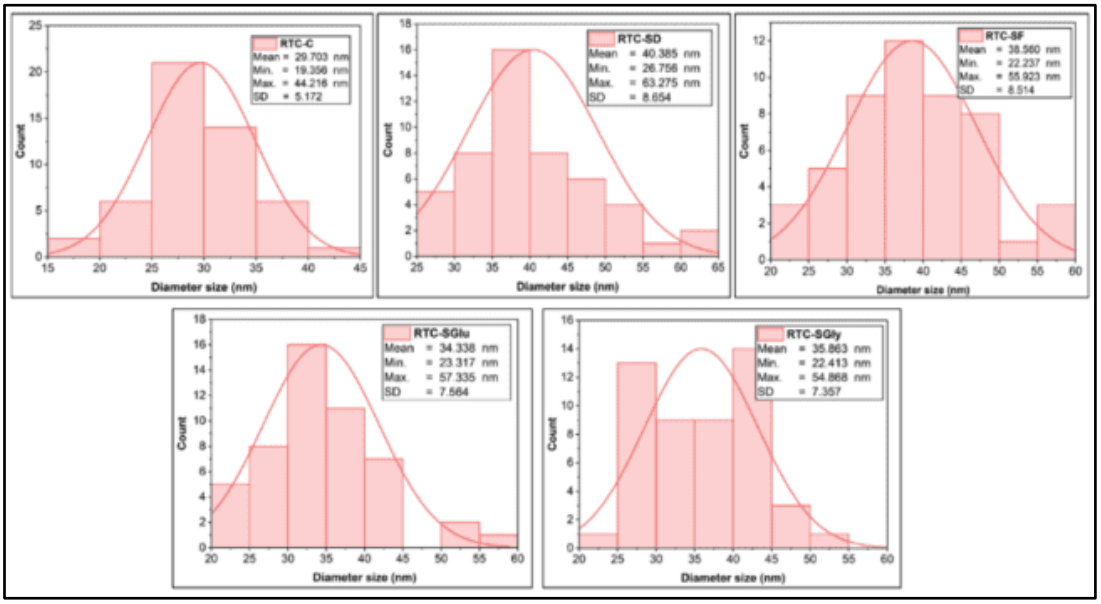

Figure 3.25 Graph of poly distribution size of BC samples diameter from RTC kombucha fermentation with various types of carbon source combinations.

Previous studies support the findings on BC fiber morphology observed in this study. The BC fibers produced by *K. hansenii* 23769 (ATCC) and a cellulose-producing strain isolated from grape juice exhibited diameters ranging from 10 to 60 nm. (Illa et al. 2019). Similarly, BC produced by *K. saccharivorans* MD1 cultivated in HS medium with palm date supplementation exhibited fiber diameters between 10 and 90 nm (Abol-Fotouh et al. 2020). In another study, BC nanofibers synthesized in HS medium had fiber diameters between 18 and 69 nm, with an average diameter of 36 nm, while BC derived from a waste fig medium ranged from 23 to 90 nm, with an average diameter of 44 nm (Yilmaz and Goksungur 2024).

BC fiber produced by *K. rhaeticus* PG2 in HS medium using glucose and glycerol as carbon sources demonstrated a similar diameter range of approximately 30–60 nm (Thorat and Dastager 2018). Additionally, BC synthesized in low-cost media, such as date syrup and cheese whey, by *K. xylinus* exhibited nanofiber diameters averaging 45–55 nm across all samples (Raiszadeh-Jahromi et al. 2020). Wang et al. (2018) reported that BC membranes produced using various carbon sources were composed of nanofibrils with average diameters ranging from 35 to 50 nm (Wang et al. 2018).

In conclusion, the BC fiber diameters obtained from Thai red tea kombucha using different carbon sources align well with the ranges reported in previous studies. This consistency suggests that the BC produced in this study exhibits comparable morphological characteristics to those synthesized using diverse bacterial strains and cultivation conditions in earlier research.

6) Fourier Transform Infrared Spectroscopy Analysis

Figure 3.26 presents the FTIR spectra of BC samples produced from RTC kombucha fermentation with various carbon source combinations (RTC, RTC-SD, RTC-SGlu, RTC-Sgly, and RTC-SF). Overall, all BC samples exhibit similar spectral bands, but the intensity of these bands varies among the samples. The FTIR spectra reveal characteristic absorption bands associated with cellulose, with notable variations in peak intensities and positions such as have been reported in some previous studies (Wang et al. 2018; Adekoya et al. 2022; Razali et al. 2022).

The FTIR spectra of BC samples can be categorized into two primary regions: the feature region and the fingerprint region. The feature region covers the high-frequency range from 4000 to 1330 cm^{-1}, while the fingerprint region extends from 1330 to 500 cm^{-1} (Liu et al. 2023). In the feature region, prominent peaks were identified at approximately 3340 cm^{-1}, 3234 cm^{-1}, and 2895 cm^{-1}. The broad and intense bands around 3340 cm^{-1} and 3234 cm^{-1} are attributed to O-H stretching vibrations, typical of hydroxyl groups. The slight variations in peak intensity indicate differences in the

hydrogen bonding network among the samples. Additionally, the peak near 2895 cm^{-1} is associated with C-H stretching vibrations, which are characteristic of aliphatic groups (CH_2 or CH_3) (Leonarski et al. 2021a; Fatima et al. 2023). The image shows comparable intensities across the spectra, although RTC-SD exhibits slightly reduced absorption, potentially due to altered C-H interactions. Furthermore, a faint peak detected at around 2340 cm^{-1} indicates the possible presence of triple-bond functional groups, such as C≡C or C≡N (Srivastava and Mathur 2022). These functional groups may come from polyphenols and other organic compounds in Thai red tea, fermentation byproducts, or the activity of the kombucha's microbial community, which may contribute to their incorporation into the BC matrix.

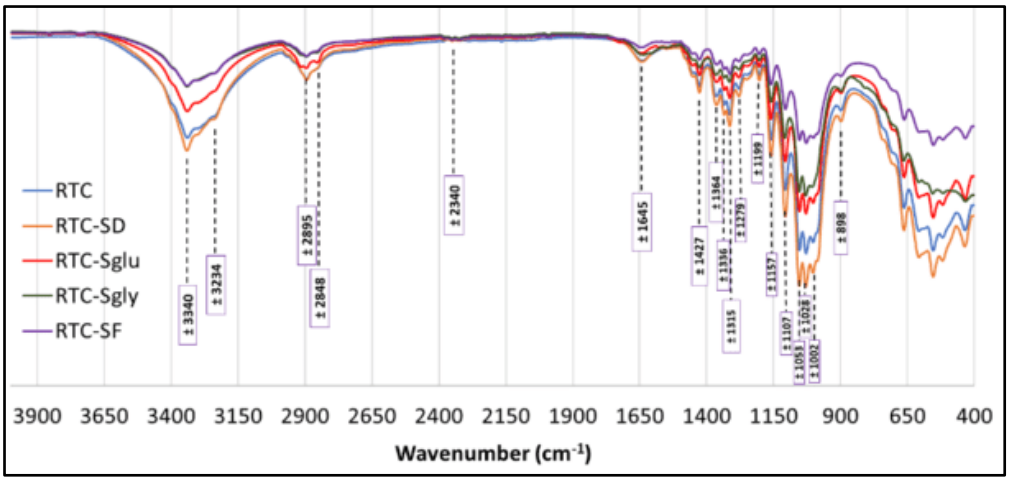

Figure 3.26 FTIR spectra of BCs from RTC kombucha fermentation with various of carbon sources combinations.

A distinct band arose at around between 1350 and 2000 cm^{-1} i.e. 1645, 1427, and 1364 cm^{-1}. The peak at around 1645 cm^{-1} is associated with C=O stretching vibrations from the glucose carbonyl group (Leonarski et al. 2021a; Liu et al. 2023). The peak at 1427 cm^{-1} represents CH_2 symmetric bending, while the peak at 1364 cm^{-1} corresponds to C-H symmetric bending (Fatima et al. 2023; Liu et al. 2023).

In the fingerprint region between 1330 to 500 cm^{-1}, several distinct peaks were detected at 1315 cm^{-1}, 1279 cm^{-1}, 1203 cm^{-1}, 1159 cm^{-1}, 1106 cm^{-1}, 1053 cm^{-1}, 1028 cm^{-1}, 1002 cm^{-1}, and 898 cm^{-1} The peak at 1336 cm^{-1} corresponds to OH in-

plane bending (Liu et al. 2023). The peak at 1315 cm^{-1} is linked to CH_2 wagging at the C-6 position (Liu et al. 2023) or maybe C-OH deformation vibrations (Wu et al. 2014). The peak observed around 1247 cm^{-1} remains unidentified. A similar peak was reported by Wang et al. (2018) in BC samples produced using glucose, fructose, sucrose, and glycerol as carbon sources, appearing at a wavenumber of 1248 cm^{-1}. The band observed at 1159 cm^{-1} is attributed to C-O-C antisymmetric bridge stretching, while the peak at 1106 cm^{-1} represents ring asymmetric stretching. Peaks at 1053 cm^{-1} and 1028 cm^{-1} are associated with C-O-C and C-O-H stretching vibrations within the sugar ring and C-O stretching, respectively (Liu et al. 2023). Additionally, the peak between 898 and 894 cm^{-1} corresponds to C-O-C stretching in **β**-1,4-glycosidic linkages, signifying the presence of an amorphous absorption band (Ciolacu et al. 2011).

7) X-Ray Diffraction (XRD) Analysis

The X-ray diffraction (XRD) patterns of BC samples obtained from Thai red tea kombucha fermentation using different carbon source combinations are illustrated in **Figure 3.27**. Further analysis result of crystallinity index (CI) and crystallite size are presented in **Table 3.17**. The XRD profiles for all samples consistently display three prominent peaks at 2θ values around 14.74°, 17.03°, and 22.90°, indicative of the crystalline structure characteristic of BC (Said Azmi et al. 2023). These peaks correspond to the 100, 110, and 200 crystallographic planes of monolithic cellulose type I, as reported by Gaspar et al. (2014). Notably, the most intense peak, located near 23°, is associated with cellulose type I (Said Azmi et al. 2023; Hossen et al. 2024), confirming its crystalline nature (Samuel and Adefusika 2019). Despite similarities in peak positions, differences in relative intensities and overall crystallinity among the samples suggest variations in cellulose chain orientation and structural properties (Said Azmi et al. 2023).

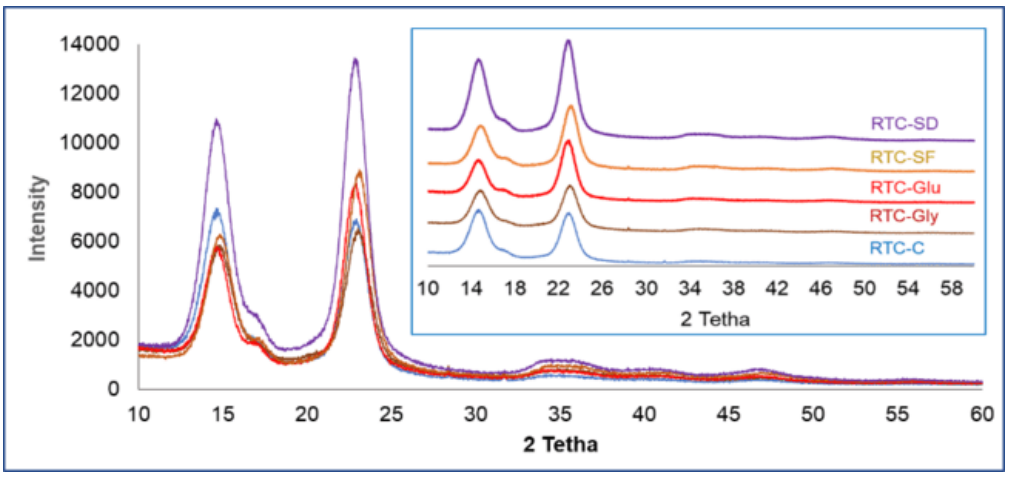

Figure 3.27 XRD spectra of BC from RTC kombucha fermentation with different carbon sources combinations

In the provided XRD spectrum, variations in peak intensities are evident among samples, with RTC-SD exhibiting the highest overall intensities. Such differences likely reflect variations in the degree of crystallinity and cellulose chain orientation, influenced by the type of carbon source used during fermentation (Said Azmi et al. 2023). The peaks at 14.74° and 17.03° exhibit minor shifts in intensity across the samples, further emphasizing these structural differences. Despite these variations, the XRD profiles align closely with previously reported patterns for BC, reinforcing the consistent crystalline structure typical of this material BC (Revin et al. 2018; Jittaut et al. 2023; Said Azmi et al. 2023). The peak at 22.90°, which consistently appears across all samples, highlights the crystalline properties of the cellulose, in agreement with findings by Samuel and Adefusika (2019).

The CI and crystallite size of the BC samples were calculated from the XRD data using the Segal peak height method, which involves subtracting the baseline intensity (**Table 3.17**). The CI values ranged from 84.74% RTC-SGly) to 89.54% (RTC-C). Among the samples, RTC-SD and RTC-SF exhibited relatively similar CI values. Notably, all BC samples produced with carbon source combinations showed relatively lower CI compared to RTC-C, which used sucrose as the sole carbon source. Various factors can affect the crystallinity of BC, including the type of carbon and nitrogen

sources, the addition of specific additives, the bacterial strain used, fermentation conditions (such as temperature and duration), and post-production treatments (Zeng et al. 2011; Thielemans et al. 2023).

Table 3.17 Crystallinity index and average crystallite size of dried BC from RTC kombucha fermentation with different carbon source combinations

Samples	Crystallinity Index (%)	Average Crystallite Size (nm)
RTC-C	89.54	3.194
RTC-SF	88.35	3.112
RTC-SD	88.17	3.181
RTC-SGlu	86.00	3.327
RTC-SGly	84.74	3.069

XRD analysis was performed once; therefore, variance data are not available.

The CI results in this study align with findings from some previous researchs. For instance, the use of glucose, fructose, and sucrose as carbon sources in HS medium for BC production by *K. medellinensis* resulted in CI values of 83%, 90%, and 85%, respectively (Molina-Ramírez et al. 2018b). Similarly, BC produced by *K. hansenii* (ATCC 53582) using glucose and glycerol as carbon sources showed CI values exceeding 80% (Amorim et al. 2024). Furthermore, BC produced by *Komagataeibacter sp.* W1 in HS medium exhibited CI values of 74%, 89%, 86%, and 87% with sucrose, fructose, glucose, and glycerol as carbon sources, respectively (Wang et al. 2018).

The results indicate that while sucrose as the sole carbon source produced BC with the highest crystallinity (89.5%), combinations with glucose or fructose resulted in only slight reductions (86–88%). In contrast, RTC-SGly showed a more noticeable decrease (84.7%), likely due to glycerol's less efficient metabolic conversion. These findings suggest that the choice of carbon source—particularly the inclusion of glycerol—can affect BC's structural properties. Nevertheless, all samples maintained high crystallinity (>84%), highlighting the robust crystalline nature of BC across different carbon sources.

Further analysis is the average of the crystallite size of BC samples as shown in **Table 3.17**. The average crystallite size of BC varies depending on the carbon source and fermentation conditions, as demonstrated in this study and supported by previous research. In this study, BC samples produced using different carbon source combinations exhibited average crystallite sizes ranging from 3.069 to 3.327 nm. Comparatively, BC produced by *G. xylinus* InaCC B404 in HS medium had a crystallite size of 3.06 nm (Agustin et al. 2021). BC derived from *K. xylinus* strains using fructose and glucose as carbon sources showed crystallite sizes between 4.7 and 6.8 nm (Singhsa et al. 2018). BC produced by *Lactobacillus plantarum* in a green tea leaf solution (1% green tea, 10% sucrose) displayed crystallite sizes of 5.36, 5.94, and 5.98 nm after 7, 14, and 30 days of fermentation, respectively (Charoenrak et al. 2023). BC from black tea kombucha exhibited crystallite sizes of 3.29 nm and 4.80 nm after 3 and 5 days of fermentation, respectively (Balistreri et al. 2024). Other average crystallite sizes have been reported in other studies such as with values of 4.9 nm and 4.76 nm (Sardjono et al. 2019), 5.6 nm (Jia et al. 2017), and 8.36 nm (Gayathri and Srinikethan 2019). This comparison highlights the significant influence of carbon source selection on the crystallite size of BC, with variations reflecting differences in substrate composition, microbial activity, and fermentation conditions. The consistent findings reinforce that carbon source plays a crucial role in determining the structural characteristics of BC.

8) Thermogravimetric (TGA/DTG) Analysis

Figure 3.28 illustrates the thermogravimetric (TG) and derivative thermogravimetric (DTG) curves of the BC samples, analyzed through thermogravimetric analysis (TGA). **Table 3.18** summarizes the decomposition data observed during the analysis. The results highlight the thermal stability and decomposition patterns of BC samples, including RTC-C, RTC-SF, RTC-SD, RTC-Glu, and RTC-Gly. TGA and DTG analyses play a vital role in evaluating BC for various applications, as they provide valuable information on the material's purity,

composition, drying behavior, and ignition temperatures. Moreover, these analyses offer insights into the thermal stability of BC, which is crucial for assessing the effectiveness of chemical treatments designed to improve bonding between natural fibers and polymer or synthetic fiber matrices (Nurazzi et al. 2021).

The first-stage weight loss, ranging from 1.34% to 6.03%, corresponds to the dehydration and volatilization of low-molecular-weight components or residual water in the BC matrix (Teixeira et al. 2019; Mohamad et al. 2022a). RTC-SD showed the lowest first-stage weight loss (1.42%), likely due to reduced moisture retention from the sample. This result relatively close result to previous result i.e. 1-2% (Gismatulina and Budaeva 2024) and 5-9% (Mohamad et al. 2022a).

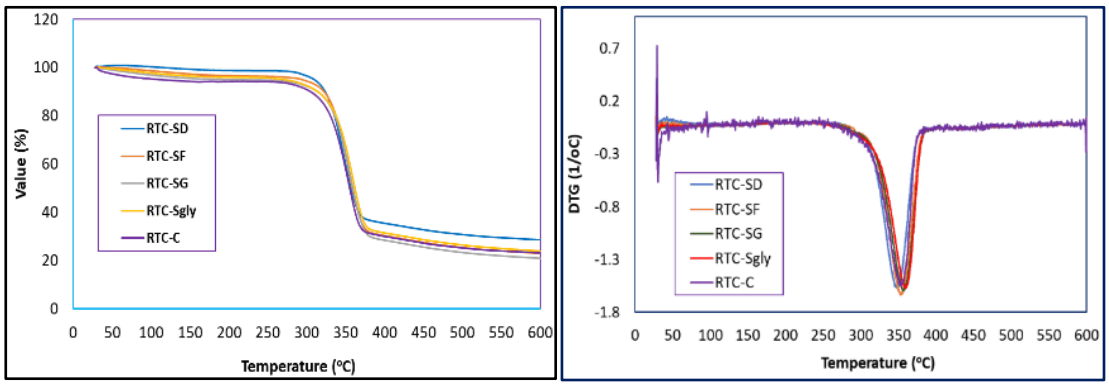

Figure 3.28 TGA (left) and DTG (right) thermographs of BC samples from RTC kombucha fermentation with different combinations of carbon sources.

The second stage of weight loss, attributed to the thermal decomposition of cellulose, ranged from 70.10% in RTC-SD to 73.90% in RTC-SGlu. These values indicate slight variations in thermal stability influenced by the different carbon sources, though the differences are not particularly pronounced. The residual weights at 600°C varied from 20.92% for RTC-SGlu to 28.52% for RTC-SD, reflecting differences in the formation of thermally stable by-products. This stage accounts for the most substantial weight loss, driven primarily by the breakdown of β-glucan chains

and the oxidation of cellulosic materials into carbonaceous residues (Mohammadkazemi et al. 2015; Mohamad et al. 2022a).

Table 3.18 Thermal decomposition of BC produced from RTC kombucha fermentation using different carbon source combinations, as analyzed by thermogravimetric analysis (TGA).

Samples	First stage weight loss (%)	Second stage weight loss (%)	Residue (%)	DTG Peak range (°C)	DTG T_{Max} (°C)
RTC-C	6.03	71.01	23.01	256 – 384	353.67
RTC-SD	1.34	70.10	28.52	260 – 391	349.50
RTC-SF	3.60	73.43	22.94	267 - 390	353.33
RTC-SGlu	5.14	73.90	20.92	268 – 389	356.83
RTC-SGly	4.15	71.92	23.90	258 – 388	359.50

The findings of this study align with previous research. BC from *A. xylinum* AGR 60 showed a first-stage mass loss of about 6%, a second-stage loss of approximately 74%, and a residue weight of around 20% at 700°C, with major thermal decomposition occurring between 300°C and 360°C (Potivara and Phisalaphong 2019). Similarly, BC produced by *G. xylinus* AGR 60 exhibited a first-stage mass loss of 6.2%, a second-stage mass loss of approximately 64.0%, and a residue of around 22.8% at 600°C, with a DTG T_{Max} of 339.6°C (Jenkhongkarn and Phisalaphong 2023). BC produced from different carbon sources, including glucose, fructose, sucrose, and glycerol, showed residual BC at 600°C ranging from 15.2% to 23.1% and exhibited a decomposition pattern similar to that observed in this study (Tureck et al. 2021). Slightly different, BC produced through kombucha fermentation of green tea undergoes three decomposition stages at 152°C, 267°C, and 359°C, with a total weight loss of 74.42% and 25.58% residue remaining, differing from this study, which typically observed only two stages of thermal decomposition (Lima et al. 2023).

The DTG peak temperature range (256–391°C) and maximum degradation temperatures (DTG T_{Max}: 349.50–359.50°C) exhibit slight variations in the thermal degradation profiles, with RTC-SGly showing the highest DTG T_{Max} (359.50°C). These differences underscore the impact of additives on the thermal behavior of BC. BC produced by *G. xylinus* demonstrates a DTG T_{Max} of 328.36°C (Jia et al. 2017). Similarly, BC produced by *G. hansenii* in HS medium shows DTG T_{Max} values of 354.5°C and 355.4°C after freeze-drying and oven-drying, respectively (Vasconcellos and Farinas 2018). The BC produced by *K. medellinensis* from various waste and agricultural by-products exhibits DTG T_{Max} values ranging from 327°C to 368°C (Molina-Ramírez et al. 2018a). Studies report DTG peak ranges of 186–363°C and 199–347°C for BC treated with freeze-drying and hot-press drying methods, yielding DTG T_{Max} values of 343.6°C and 313.4°C, respectively (Mohamad et al. 2022a). Furthermore, BC produced through kombucha fermentation of green tea reaches a DTG T_{Max} of 366°C (Lima et al. 2023). The DTG analysis indicates that different carbon sources have a slight impact on the thermal stability of BC, as evidenced by the small variations in DTG T_{Max} values. While RTC-SGly showed the highest DTG Max, the narrow range of differences suggests that the influence of carbon source on thermal properties is relatively minor.

9) Mechanical Properties Analysis Using Nanoindentation

Nanoindentation analysis was utilized to evaluate the mechanical properties of BC samples at the nanoscale. This precise technique measures localized mechanical responses with high accuracy at micro- and nanoscale resolutions, making it an essential tool for assessing materials designed for applications requiring both strength and flexibility. The analysis focused on BC samples RTC-SD and RTC-SGlu, selected for their higher productivity, with the RTC-C sample included as a control for comparison. The detailed findings are summarized in **Table 3.19.**

The mechanical properties of BC samples, including RTC-SD, RTC-SGlu, and the control (RTC-C), were no significant differences across all parameters, such as maximum depth, plastic indentation depth, hardness, reduced modulus, and

Young's modulus ($P > 0.05$). This indicates that the different carbon sources used, particularly sucrose, combination of sucrose-dextrose (SD), and combinations of sucrose-glucose (SGlu), do not result in distinct variations in the mechanical properties of BC. These findings suggest that the choice of carbon source in these cases has minimal impact on the nanoscale mechanical behavior of BC. Actually, carbon source is one of the factor affect the mechanical properties of BC (Betlej et al. 2020; Chibrikov et al. 2023). However, in this case, the effect is not significantly different.

Various factors can affect the mechanical properties of BC such as bacterial strains, cultivation methods, purification, nutrient composition including carbon and nitrogen sources, and drying techniques. Cultivation methods and bacterial strains significantly affect the structure and crystallinity of BC, which in turn impacts its strength (Krystynowicz et al. 2002; Zeng et al. 2014; Chen et al. 2018a; Betlej et al. 2020; Chibrikov et al. 2023). The NaOH concentration during purification is essential for removing impurities, directly affecting the quality and properties of BC fibers (Suryanto et al. 2019; Chen et al. 2021). Drying methods affect BC's porosity and density, which are crucial for its flexibility, tensile strength, and the organization of intra- and interfibrillar spaces (Zeng et al. 2014; Wang et al. 2023b).

The mechanical properties of BC are closely linked to its crystallinity, which plays a significant role in determining material strength and stiffness. Studies have shown that an increase in the crystallinity index (CI) generally enhances stiffness and hardness while reducing ductility (Dusunceli and Colak 2008). Furthermore, higher crystallinity has been associated with an increase in Young's modulus, reinforcing the connection between CI and mechanical strength (Adekoya et al. 2022).

In this study, the CI values of RTC-C, RTC-SD, and RTC-SGlu samples are relatively similar and show no significant differences in relation to their Young's modulus values. The Young's modulus values of the BC samples vary, with some falling within, below, or above the ranges reported in previous research.

Table 3.19 Mechanical properties of BC from kombucha fermentation of RTC-SD, RTC-SGlu, and RTC-C analyzed using a nano-indenter

Sample	MD (nm)	Pl (nm)	ML (mN)	H (GPa)	RM (GPa)	ERP	CC (nm/mN)	PW (nJ)	EW (nJ)	YM (GPa)
RTC-SD	3402.68 ±388.52	2950.54 ±366.31	50.10 ±0.00	0.23 ±0.07	4.844 ±1.02	0.16 ±0.02	12.03 ±0.82	49.29 ±5.30	21.67 ±1.40	4.43 ±0.94
RTC-SGlu	3206.75 ±250.54	2754.19 ±240.80	50.10 ±0.00	0.26 ±0.05	5.106 ±0.64	0.17 ±0.01	12.04 ±0.65	51.22 ±4.42	21.08 ±1.08	4.67 ±0.59
RTC-C	3412.25 ±259.56	2980.18 ±253.91	50.10 ±0.00	0.22 ±0.05	4.94 ±0.56	0.15 ±0.01	11.50 ±0.22	54.41 ±4.64	20.80 ±0.47	4.51 ±0.51

MD: maximum depth, Pl: plastic, ML: maximum load, H: hardness, RM: reduced modulus, ERP: elastic recovery parameters, CC: contact compliance, PW: plastic work, EW: elastic work, and YM: Young's Modulus. Based on the statistical analysis, there were no significant differences among the samples across all parameters ($P < 0.05$).

For instance, Chen et al. (2018a) reported Young's modulus values ranging from 1.10 to 5.56 GPa for BC produced from various Komagataeibacter strains. Zeng et al. (2014) observed lower values, between 198 and 659 MPa, depending on the bacterial strains and drying methods used. Krystynowicz et al. (2002) found that BC produced by *A. xylinum* E25 under static and rotating conditions exhibited Young's modulus values of 2.7 and 0.3 GPa, respectively. At the higher end, *A. xylinum* AGR60 cultured in coconut water reached 9.14 GPa (Potivara and Phisalaphong 2019), while kombucha-derived BC was reported to have a Young's modulus of 8.0 ± 1.9 GPa (Oliver-Ortega et al. 2021).

3.4.4 Effect of Process Parameters: pH, Harvesting Time, Tea Concentration, and Cultivation Method on Bacterial Cellulose yield and Water Holding Capacity

1) Effect of Initial pH on the Yield and WHC of BC

- **Profile of Fermentation Broth**

The pH and °Brix of the kombucha fermentation broth were measured at the beginning and after 15 days of fermentation. The initial pH of the medium was adjusted to 5, 6, 7, and a control value of 5.20 for the respective treatments. After inoculation with a kombucha starter, the pH dropped significantly to acidic levels of 3.40, 3.55, 3.61, and 3.41, respectively. After 15 days of fermentation, the pH further decreased to 2.48, 2.46, 2.53, and 2.39. These changes, along with the °Brix data, are presented in **Table 3.20.**

A similar pH trend has been observed in previous studies on kombucha fermentation, where the pH typically drops to around 3.5 shortly after inoculation and reaches approximately 2.8 within five days (Petrosian 2021). In black tea kombucha fermentation, the pH was reported to decrease from 4.6 ± 0.1 to 3.6 following the addition of a kombucha starter and further to 2.8 after 30 days (Charoenrak et al. 2023). The continued decline in pH during fermentation is attributed to the production of organic acids, including acetic and gluconic acids, by

microorganisms in the SCOBY acid (Aswini et al. 2020; Lee et al. 2021). These microorganisms thrive in acidic conditions, typically within a pH range of 2–4 (Goh et al. 2012), which protects the fermentation medium from contamination by undesirable microbes (Petrosian 2021; Wang et al. 2023a). Additionally, the presence of polyphenols in the medium supports the growth of the SCOBY while inhibiting the proliferation of other microorganisms (Jayabalan et al. 2014).

Table 3.20 The change of pH and °Brix during RTC kombucha fermentation with different initial pH condition

Sample	The change of the pH		The change of the °Brix	
	initial pH	final pH	initial °Brix	final °Brix
RTC-Control* (pH-5.20)	3.43±0.03^{a}	2.39±0.04^{a}	10.30±0.00^{a}	9.33±0.35^{ab}
RTC-pH-5	3.41±0.01^{a}	2.48±0.01^{b}	10.40±0.00^{b}	9.17±0.13^{a}
RTC-pH-6	3.55±0.02^{b}	2.46±0.03^{b}	10.70±0.00^{d}	9.60±0.17^{b}
RTC-pH-7	3.61±0.03^{c}	2.53±0.03^{c}	10.50±0.00^{c}	9.57±0.22^{ab}

**The control sample was prepared without pH adjustment. Different lowercase letters within a column indicate significant differences among the four treatments, as determined by the LSD test ($P < 0.05$).*

Despite the initial adjustments of pH using HCl (acid) and NaOH (base), the pH of the medium after inoculation dropped to a similar range (3.40–3.61) across all treatments. This suggests a buffering effect likely caused by organic acids in the kombucha starter, as reported in other studies (Hruška et al. 1999; Dartiguenave et al. 2000; Zheng et al. 2023). Kombucha cultures are known to stabilize the pH around this acidic range regardless of initial pH adjustments, driven by microbial metabolic pathways that favor acid production (Teoh et al. 2004; Jayabalan et al. 2007).

The initial pH values recorded in this study align with prior research, which reported ranges such as 3.19–3.27 (Chong et al. 2024), 3.85–4.99 (Phung et al. 2023), and 3.24–3.34 (Leonarski et al. 2021b). However, the final pH values in this study—2.48, 2.46, 2.53, and 2.39—are lower than those in some studies, such as black,

green, and oolong tea fermentations (2.72–2.79) (Chong et al. 2024), black tea fermentation after 30 days (2.8) (Charoenrak et al. 2023), and beverages made from black tea and pineapple (2.95–3.30) (Phung et al. 2023). Similar final pH values have been reported in acerola byproduct-based fermentations (2.49–2.58) (Leonarski et al. 2021b), while others have documented even lower values, such as 1.88 after 21 days of fermentation (Chakravorty et al. 2016).

These findings emphasize the critical role of pH control in BC production. Kombucha fermentation media typically maintain pH levels between 3 and 4, which is conducive to BC synthesis. This observation is consistent with previous studies, such as those by Oliver-Ortega et al. (2021), which identified similar pH conditions as optimal for BC production (Oliver-Ortega et al. 2021).

In addition to pH, we also measured the total soluble solids (TSS) of the broth before and after fermentation (**Table 3.20**). Initially, TSS ranged from 10.30 to 10.70 °Brix, but after fermentation, it dropped to 9.17 to 9.60 °Brix. TSS indicates sugar concentration in the solution (Muzaifa et al. 2022). Similar reductions in TSS during fermentation have been reported in other studies, such as snake fruit kombucha, where TSS decreased from 13.30–14.08 °Brix to 12.43–12.97 °Brix (Zubaidah et al. 2019), and cascara kombucha, which dropped from 10.97 °Brix to 9.97 °Brix over eight days (Muzaifa et al. 2022). This decrease is due to microbial activity, which converts sugar into glucose for microbial growth and development (Sinamo et al. 2022). Although the TSS values remain relatively high, they no longer accurately reflect the original sugar content, as the broth volume has significantly decreased during fermentation, resulting in an actual reduction in total sugar.

- **The Yield and WHC of BC**

This study examined the impact of pH on the yield and water-holding capacity (WHC) of BC by adjusting the medium's initial pH using HCl for pH 5 and NaOH for pH 6 and 7. **Figure 3.29** shows the effect of different pre-inoculation medium pH on the yield and water-holding capacity of BC.

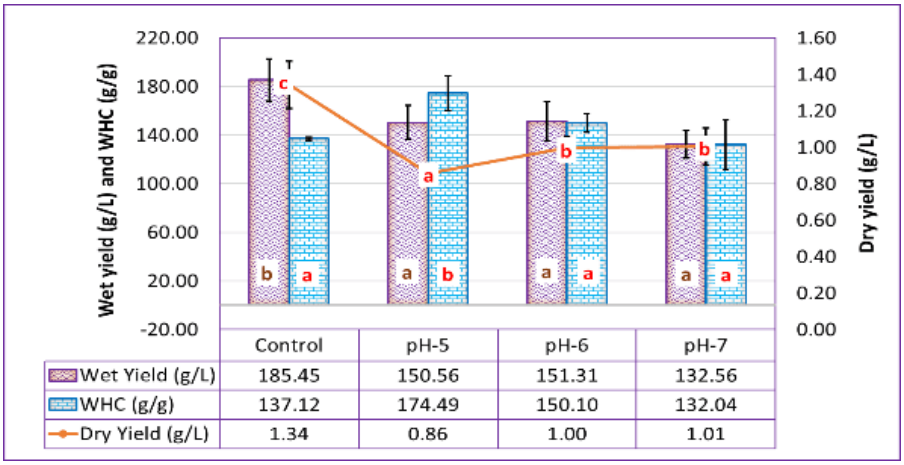

Figure 3.29 Wet yield (g/L), dry yield (g/L), and WHC of BC samples from RTC kombucha fermentation with different pH conditions.

The control sample (pH = 5.20), with the lowest final pH of 2.39, produced the highest wet yield at 185±17.28 g/L and a dry yield of 1.34±0.13 g/L. In contrast, the pH 5, 6, and 7 samples had lower wet yields of 150±13.73, 151±16.17, and 132±11.51 g/L, and dry yields of 0.86±0.01, 1.01±0.06, and 1.01±0.10 g/L, respectively. Despite these variations, the wet yields of the pH 5, 6, and 7 samples were not significantly different from each other ($P > 0.05$), suggesting that adjusting the initial pH with HCl and NaOH had minimal impact on overall yield. The fermentation process caused the pH to drop to similar levels, which normalized microbial activity across all samples (**Table 3.20**). The result of this study show that the pH of around 3.40 is ideal for BC production in kombucha fermentation, as the microorganisms in the SCOBY thrive in pH conditions of 2 to 4 (Goh et al. 2012). This range is typical for BC production using kombucha. However, different bacterial strains and media can require higher pH levels. For example, *K. xylinus* produced BC optimally at a pH of 6.05 using fig waste as the medium (Yilmaz and Goksungur 2024). Other research indicates that a pH range of 4 to 6 is optimal for BC fermentation (Lahiri et al. 2021). Strains like *A. xylinum* thrive at pH levels between 5.5 and 7.5 (Son et al. 2001; Junaidi and Azlan 2012), while *A. senegalensis* MA1 and *K. rhaeticus* K23 require pH levels of 4.5 and 5.5, respectively, for optimal production (Aswini et al. 2020; U˘gurel and Ö˘güt 2024).

The dry yield followed a similar pattern to the wet yield. The control had the highest dry yield (1.34±0.13 g/L), while the pH 5, 6, and 7 samples had lower yields (0.86±0.01, 1.01±0.06, and 1.01±0.10 g/L). There was no significant difference between the pH 6 and 7 samples ($P > 0.05$), but the pH 5 sample had the lowest dry yield ($P < 0.05$). For WHC, the pH 5 sample had the highest value at 174±14.29 g water/g cellulose, while the pH 6, 7, and control samples had lower WHC values (150±7.58, 132±20.42, and 137±1.23 g water/g cellulose) with no significant differences ($P > 0.05$). The low dry yield and high WHC of the pH 5 sample maybe due to the addition of HCl, which could increase WHC by promoting structural changes, enhancing hydrophilic properties, and affecting microbial activity, leading to a BC network better suited for water retention. These findings provide insights into how pH, chemical additions, and fermentation dynamics influence BC production in terms of wet yield, dry yield, and WHC.

2) Effect of Harvesting Period on the Yield and WHC of BC

The objective of this study was to have information about the effect of the harvesting period on the yield of BC from Thai red tea kombucha fermentation. Many previous studies conducted BC fermentation through kombucha fermentation for around one to four weeks (AL-Kalifawi and Hassan 2014; Ramírez Tapias et al. 2022; Charoenrak et al. 2023). After being harvested at a certain time, usually, the fermentation broth is still left over and can be continued to the next fermentation to produce more BC. This study conducted the experiment on various harvesting times during four weeks.

- **Profile of fermentation broth**

Table 3.21 presents the analysis of pH and °Brix changes during the fermentation process. The results indicate a consistent decrease in both pH and °Brix values over time. It is important to note that the final °Brix value does not necessarily reflect the total residual sugar content, as sugars are metabolized by microbial activity and water content may also decrease during fermentation.

The initial pH prior to fermentation was 3.58 ± 0.01, which gradually declined to 2.84 ± 0.06 in the week 1–4 sample, 2.59 ± 0.02 in the week 2–4 sample, 2.45 ± 0.01 in the week 3–4 sample, and 2.33 ± 0.06 in the week 4–4 sample. These reductions were statistically significant across all sampling intervals. After 28 days of fermentation (week 4), all samples exhibited a relatively similar pH range (2.26–2.33), with no statistically significant differences among treatments. Several previous studies have reported comparable trends in pH reduction during kombucha fermentation. Charoenrak et al. (2023) reported a decrease in pH from approximately 3.6 on day 0, to 3.2 on day 7, 3.0 on day 14, and 2.3 after 30 days of fermentation. Ramírez Tapias et al. (2022) observed final pH values ranging from 2.37 to 2.65 after 21 days of herbal infusion fermentation. Similarly, Chakravorty et al. (2016) reported pH values of 2.28, 1.98, and 1.88 after 7, 14, and 21 days of fermentation, respectively.

In addition to pH, TSS evaluation showed that the initial °Brix value for all samples was 10.70 ± 0.00, indicating uniform sugar concentrations at the start of fermentation. Following the first harvest, a decrease in °Brix was observed, likely due to microbial sugar metabolism. However, °Brix values remained relatively stable from the first to the final harvest. No statistically significant differences were detected among the samples after either the first or final harvest. This stabilization may be explained by a balance between ongoing microbial sugar consumption and water loss through evaporation. As the fermentation progressed under static conditions in open vessels, water evaporation likely contributed to a slight concentration of the fermentation broth, partially offsetting further reductions in °Brix. This effect could have masked continued sugar depletion, resulting in relatively unchanged °Brix readings despite ongoing microbial activity.

Table 3.21 The change of pH and °Brix during RTC kombucha fermentation time

Samples	The Change of the pH			The Change of the °Brix		
	Initial	1st harvest	final	initial	1st harvest	final
Week 1-4	3.58±0.01[a]	2.84±0.06[d]	2.26±0.04[a]	10.70±0.17[a]	9.93±0.18[a]	9.73±0.11[a]
Week 2-4	3.58±0.01[a]	2.59±0.02[c]	2.29±0.02[a]	10.70±0.17[a]	9.62±0.10[a]	9.90±0.17[a]
Week 3-4	3.58±0.01[a]	2.45±0.01[b]	2.27±0.01[a]	10.70±0.17[a]	9.82±0.17[a]	9.79±0.24[a]
Week 4-4	3.58±0.01[a]	2.33±0.06[a]	2.33±0.06[a]	10.70±0.17[a]	9.83±0.20[a]	9.83±0.20[a]

- **The Yield and WHC of BC**

Figure 3.30 shows the effect of different harvesting times on the yield and water-holding capacity of BC from Thai red tea kombucha fermentation. Samples W1-4, W2-4, and W3-4 were harvested twice: once at their assigned week (week 1, 2, or 3) and again in the fourth week. W4-4 was harvested only once in the fourth week. The results indicate that harvesting time significantly affects BC yield, with higher yields observed for samples harvested later, especially W4-4. This aligns with studies showing increased BC production with extended fermentation, as *Acetobacter* continues producing cellulose with adequate nutrients and sugar.

For both wet and dry yields, samples harvested after longer fermentation time (W3-4 and W4-4) consistently show higher yields than those harvested earlier (W1-4 and W2-4). The W4-4 sample, which was harvested after four weeks without interruption, achieved the highest wet yield (268.39±35.02 g/L) and dry yield (2.35±2.35 g/L). This trend is expected because BC production typically accelerates after the initial microbial adaptation phase. Previous studies have reported similar increases in yield with extended fermentation time, where wet yields rose from 1,162 ± 28 g (7 days) to 3,931 ± 43 g (30 days), while dry yields increased from 120 ± 10 g to 880 ± 27 g (Charoenrak et al. 2023). Comparable growth trends were also documented over 8, 12, and 20 days of fermentation (Petrosian 2021). This consistent

pattern occurs because bacteria continue synthesizing cellulose until nutrient depletion or the accumulation of inhibitory byproducts limits further production.

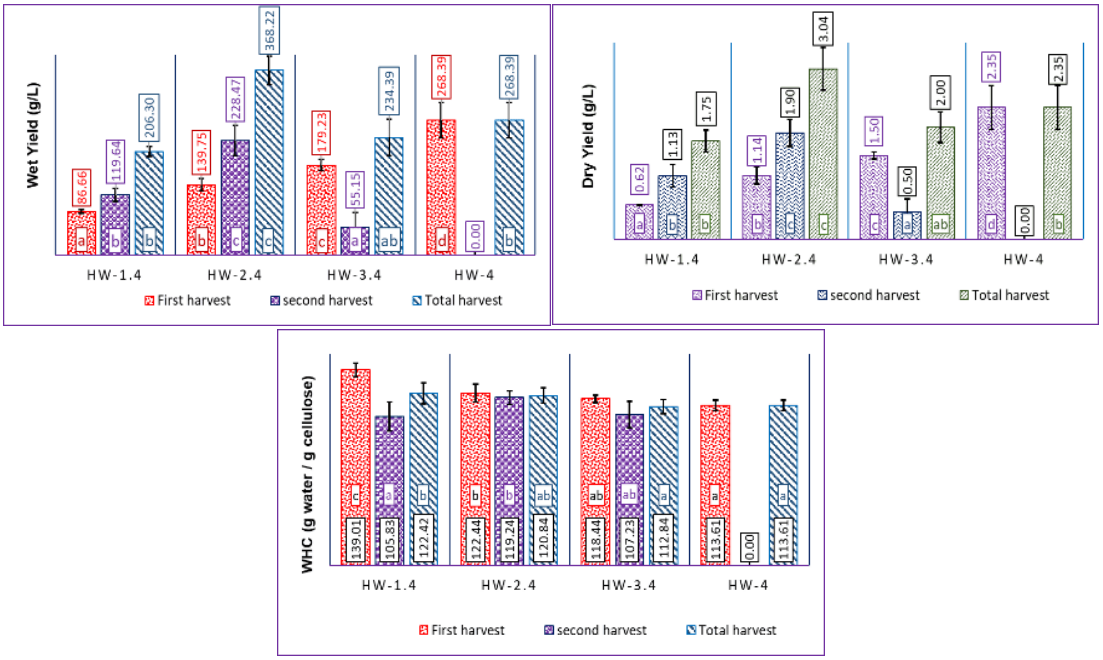

Figure 3.30 Wet yield (g/L), dry yield (g/L), and WHC (g water / g cellulose) of BC samples from RTC kombucha fermentation with different harvesting period

Comparing the total yields across the different samples (W1-4, W2-4, W3-4, and W4-4), W2-4 had the highest overall yield, with a total wet yield of 368.22±28.33 g/L and a total dry yield of 3.04±0.38 g/L. This suggests that harvesting after the second week may strike a balance between maximizing yield and allowing sufficient time for bacterial growth. While W4-4 achieved the highest yields for a single harvest, the cumulative yield from earlier harvesting periods in W2-4 was superior. This finding aligns with some studies where BC production increased until about 15 days of fermentation, and further increases in yield were minor (Yanti et al. 2018; Aswini et al. 2020; Photphisutthiphong and Vatanyoopaisarn 2020).

The WHC trends show a different pattern compared to the yield data (**Figure 3.20**). Initially, the WHC decreases as the fermentation progresses. For example, W1-4 had the highest WHC at the first harvest (139.01±4.77 g water/g

cellulose), while W4-4, which was harvested after the longest period, had the lowest WHC (113.61±3.73 g water/g cellulose). The average WHC values for the samples followed a similar trend, with the earliest sample (W1-4) having the highest average WHC (122.42±7.37) and the later samples (W2-4, W3-4, and W4-4) having lower WHC values (120.84±5.38, 112.84±4.93, and 113.61±3.73 g water/g cellulose, respectively). This finding is align with a previous study (Charoenrak et al. 2023). The reduction in WHC over time could be related to structural changes in the BC matrix. Longer fermentation times allow for more extensive cross-linking of cellulose fibers, leading to a denser structure that holds less water. The reduction of WHC with the age of BC suggests that the nanoribbons arrangement must have significantly varied with incubation time, conditioning the weight of water held per unit weight of cellulose (Corzo Salinas et al. 2021). Previous investigations on sheet BC pellicles have shown that increasing fermentation times, more micro-fibrils were secreted by bacteria, resulted in membranes with a less porous and more compact nanoribbons network structure which in turn affected the water holding capacity (Tang et al. 2010; Cerrutti et al. 2016).

Overall, the results suggest that harvesting time plays a critical role in determining the yield and WHC of BC from kombucha fermentation. Extended fermentation times increase both wet and dry yields but reduce the WHC due to structural changes in the cellulose matrix. Optimal harvesting times depend on whether the goal is to maximize yield or maintain higher WHC properties. Future studies should further investigate the balance between yield and WHC to optimize BC production for specific applications.

3) Effect of Tea Concentration on the Yield and WHC of BC

In kombucha fermentation, tea concentration plays a critical role in BC production. A concentration of 1% (w/v) is most commonly used in previous studies, as it provides essential nutrients—particularly polyphenols—that support the growth of Komagataeibacter species, the primary producers of BC. This level is

generally considered optimal due to its balance between microbial growth support and cost-effectiveness. However, the impact of higher tea concentrations—such as 2% and 3%—on BC production, particularly using Thai red tea, remains largely unexplored. This study aims to investigate the effects of increased tea concentrations on both the yield and WHC of BC. The goal is to determine whether a greater supply of nutrients from higher tea concentrations can enhance BC production or influence its physical characteristics.

- **Profile of Fermentation Broth**

The changes in pH and °Brix before and after fermentation are presented in **Table 3.22**. The observed decrease in °Brix aligns with results reported in previous studies. Regarding pH, the initial values of the tea infusions at 1% (RTC-1%), 2% (RTC-2%), and 3% (RTC-3%) concentrations before inoculation were approximately 5.22, 5.20, and 5.19, respectively. After inoculation, the pH values shifted to 3.72, 3.94, and 4.08, respectively. Notably, higher tea concentrations corresponded with higher pH values after both inoculation and fermentation. This trend may be attributed to the buffering capacity of soluble compounds present in the tea infusions. Previous research has demonstrated that components such as carboxyl and amino groups in green tea extracts contribute to buffering effects—organic acids and carboxylic groups of amino acids buffer around pH 3.7, while catechins, theanine, and amino groups contribute to buffering near pH 9.3 (Yamano and Miyagawa 1997).

In contrast, the °Brix values decreased after fermentation across all samples but remained statistically similar, ranging from approximately 9.8 to 10.0 °Brix. This suggests that sugar consumption during fermentation was relatively consistent despite variations in initial pH and tea concentration.

Table 3.22 The change of pH and °Brix (before and after) RTC kombucha fermentation with different tea concentration

Sample	The Change of the pH		The Change of the Brix	
	Initial pH	final pH	Initial °Brix	°Brix
RTC-1%	3.72±0.00[a]	2.58±0.03[a]	11.00±0.00[a]	9.87±0.13[a]
RTC-2%	3.94±0.01[b]	2.94±0.02[b]	11.10±0.00[b]	9.83±0.10[a]
RTC-3%	4.08±0.00[c]	3.20±0.03[c]	11.40±0.00[c]	10.00±0.07[a]

Overall, these results indicate that while initial pH and tea concentration influence the acidity attained during fermentation, their effect on residual sugar content (as measured by °Brix) is less significant. Microbial activity lowers pH through acid production, but sugar consumption, reflected by the decrease in °Brix, appears to be relatively uniform across treatments.

- **The Yield and WHC of BC**

The effect of varying tea concentrations on the wet yield, dry yield, and WHC of BC from Thai red tea kombucha is presented **in Figure 3.31.** The data reveal distinct trends that align with findings from prior studies on kombucha fermentation and BC production.

The wet yield results indicate that increasing tea concentrations do not necessarily improve BC production. The 2% tea concentration (RTC-2%) yielded the highest wet yield at 195.72±18.53 g/L, although this was not significantly different from the 1% tea sample (177.36±13.72 g/L). Interestingly, the 3% tea concentration (RTC-3%) produced the lowest wet yield (157.60±8.01 g/L), significantly lower than both the 1% and 2% samples ($P < 0.05$). For the dry yield, the RTC-2% sample again showed the highest value at 1.66±0.24 g/L, significantly greater than RTC-1% (1.40±0.03 g/L) and RTC-3% (1.53±0.01 g/L). While RTC-3% had a slightly higher dry yield than RTC-1%, the difference was not statistically significant ($P > 0.05$). These findings suggest

that moderate tea concentrations, between 1% and 2%, provide optimal conditions for cellulose synthesis by balancing nutrient availability and microbial activity.

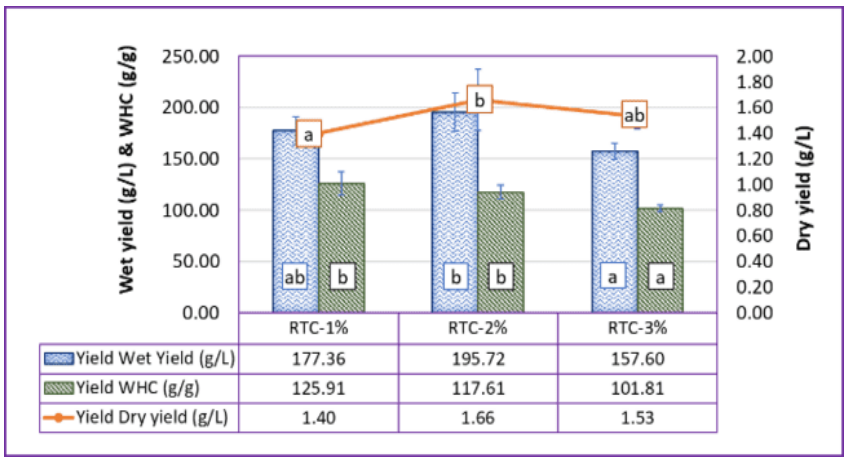

Figure 3.31 Wet yield (g/L), dry yield (g/L), and WHC of BC samples from RTC kombucha fermentation with different tea concentration

This study differs slightly from previous research, where a 1% tea concentration (10 g/L tea infusion) was considered optimal and commonly used for BC production through kombucha fermentation (AL-Kalifawi and Hassan 2014; Kalifawi 2018; Avcioglu et al. 2021; China et al. 2021; Oliver-Ortega et al. 2021). Further investigation is necessary to determine the optimal tea concentration for BC production, particularly using Thai red tea kombucha. Notably, the Thai red tea used in this experiment contains 94% Assam red tea powder, 5% sugar, and 1% other ingredients such as artificial flavoring and coloring agents (as indicated on the packaging). Research findings indicate that higher tea concentrations can reduce the efficiency of cellulose-producing bacteria, possibly due to excess polyphenols and other compounds interfering with fermentation. This inverse relationship between tea concentration and BC yield has been observed in previous studies, where excessive tea inhibited the growth of microbes like *G. xylinus* (Nguyen et al. 2008).

The trend in WHC shows a clear decline with increasing tea concentrations. RTC-1% had the highest WHC (125.91±11.63 g water/g cellulose), though it was not significantly different from RTC-2% (117.6±7.12 g water/g cellulose).

However, the sample from RTC-3% exhibited the lowest WHC (108.81±3.40 g water/g cellulose), with a significant difference from the other samples ($P < 0.05$). The decrease in WHC with higher tea concentrations may be due to the denser and less porous structure of the BC matrix formed in the presence of higher levels of polyphenols. These polyphenols can bind to cellulose, reducing its ability to retain water. Several studies have reported on the interaction between polyphenols and the cellulose matrix, supporting this explanation (Phan et al. 2015; Liu et al. 2017, 2018; Makarewicz et al. 2021). Although NaOH is used to purify BC, some polyphenols may remain bound to the cellulose structure. Stable polyphenols can form strong bonds with cellulose, making them hard to remove completely. Further investigation is necessary to determine whether polyphenols exist in purified BC.

4) Effect of Cultivation Methods on the Yield and WHC Of BC

This study investigated the effects of different cultivation methods—static, agitated, and shaking—on the yield and WHC of BC. The choice of cultivation method is a critical factor in BC production, as it influences not only the yield but also the structural properties and suitability of the material for various applications. Static cultivation is often favored for its simplicity and the high-quality cellulose it produces, though it generally results in lower yields (Wang et al. 2019b; Gao et al. 2020; Lahiri et al. 2021). In contrast, shaking and agitation methods improve oxygen and nutrient availability, which can enhance productivity levels (Lahiri et al. 2021; Akintunde et al. 2022). This study compares the impact of static, agitated, and shaking cultivation methods on the yield and WHC of BC from Thai red tea kombucha fermentations, aiming to understand how different conditions affect production efficiency. The shaking method was performed using an orbital shaker at 150 rpm, while the agitation was carried out with a magnetic stirrer, also set to 150 rpm.

- **Profile of Fermentation Broth**

The changes in pH and °Brix during Thai red tea kombucha fermentation under different cultivation methods (static, shaking, and agitating) are

presented in **Table 3.23**. The results show consistent trends with previous experiments, where the final pH and °Brix values varied depending on the cultivation method. The initial pH for all samples was consistent at 3.43±0.03. After fermentation, the static method resulted in the lowest final pH (2.47±0.03), followed by agitating (2.51±0.15) and shaking (2.53±0.02). However, the differences in pH among the methods were not statistically significant ($P > 0.05$). The slightly lower pH in the static method may be attributed to the accumulation of organic acids produced during fermentation, as static conditions limit oxygen availability, promoting acid production.

Table 3.23 The change of pH and °Brix (before and after) RTC kombucha fermentation with different cultivation methods

Sample	The Change of the pH		The Change of the °Brix	
	Initial pH	final pH	initial °Brix	final °Brix
RTC-static	3.43±0.03[a]	2.47±0.03[a]	10.90±0.00[a]	10.17±0.35[a]
RTC-Shaking	3.43±0.03[a]	2.53±0.02[a]	10.90±0.00[a]	12.37±2.32[b]
RTC-Agitating	3.43±0.03[a]	2.51±0.15[a]	10.90±0.00[a]	12.96±1.33[b]

In terms of °Brix, the initial value for all samples was 10.90±0.00, indicating uniform sugar concentration at the start. However, the final °Brix values varied significantly: static (10.17±0.35), shaking (12.37±2.32), and agitating (12.96±1.33). The static method showed the lowest final °Brix, suggesting greater sugar consumption by microbes due to prolonged fermentation under limited oxygen. In contrast, shaking and agitating methods retained higher °Brix levels, which may be due to water evaporation during fermentation, leading to increased sugar concentration, or improved oxygen and nutrient distribution slowing sugar utilization. These findings align with previous studies, where static conditions promote acid production and sugar consumption, while agitated or shaken methods enhance oxygen availability, potentially altering fermentation dynamics. Further research is needed to fully

understand the impact of cultivation methods on microbial behavior and BC production efficiency.

- **The Yield and WHC of BC**

Figure 3.32 visualized the effect of different cultivation methods on the yields and WHC of BC from Thai red tea kombucha fermentations. In this study, static and shaking cultivations resulted in comparable wet and dry yields, with no significant difference between them ($P > 0.05$). Static cultivation produced a wet yield of 185.45 g/L and a dry yield of 1.34 g/L, while shaking and agitated cultivation yielded of 182.99 g/L and 37.37 g/L for wet yield, respectively and 1.07 g/L and 0.45 g/L for dry yield, respectively. These results contrast with several previous studies, which generally report that shaking provides the highest productivity due to enhanced oxygenation and nutrient dispersion (Ullah et al. 2019; Barja 2021a). However, our findings indicate that under specific conditions, such as optimized inoculum concentration or nutrient availability, static cultivation can match shaking in yield.

Despite the similarity in yields, the WHC results showed significant differences among the cultivation methods. Shaking produced the highest WHC at 171 g/g, which is significantly greater than that of static (137 g/g) and agitated (81.09 g/g) cultivations ($P < 0.05$). This higher WHC under shaking conditions aligns with previous research indicating that shaking promotes a more porous BC structure, enhancing its water holding capacity (Krystynowicz et al. 2002). Conversely, the agitated method, using a magnetic stirrer, had the lowest yield and WHC, likely due to the shear forces and limited oxygenation disrupting BC fibril formation. Many previous studies also emphasize that agitation often leads to lower BC yields compared to both static and shaking methods, due to the excessive shear forces that can inhibit proper cellulose formations (Zhang et al. 2022a). Agitated cultivation presents a challenge in BC production due to the potential for cellulose-producing cells (*Cel+* cells) to mutate into non-producing mutant cells (*Cel-* mutants)) (Moon et al. 2006; Jacek et al. 2019). This genetic instability often results in reduced yields of BC (Martirani-VonAbercron and

Pacheco-Sánchez 2023). Additionally, Furthermore, not all bacterial strains are suitable for cultivation using agitation methods (Barja 2021a), which limits their application in certain cases. Our study supports this trend, with the agitated samples showing significantly lower yields (wet yield of 37.37 g/L and dry yield of 0.45 g/L) and the lowest WHC.

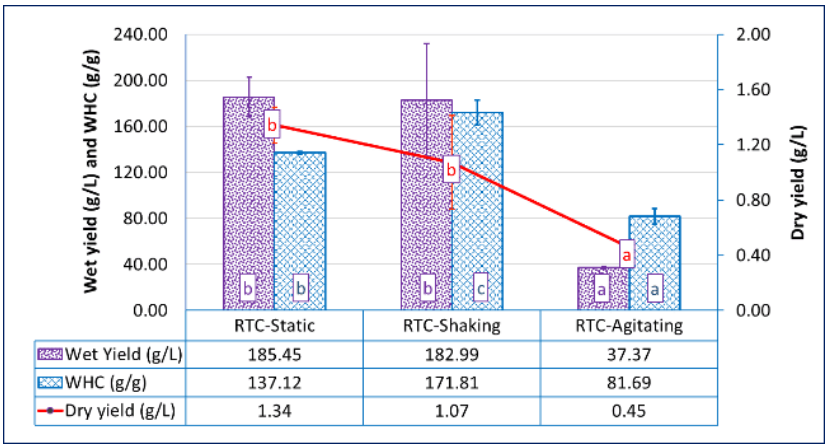

Figure 3.32 Wet yield (g/L), dry yield (g/L), and WHC of BC samples from RTC kombucha fermentation with different cultivation method

3.5 Conclusion

This study has demonstrated that Thai red tea kombucha constitutes a promising and economically viable medium for bacterial cellulose production. Among the four tea varieties evaluated—Chinese Black Tea, *Assamica* Black Tea, Thai Green Tea, and Thai Red Tea—the latter yielded the highest BC production of 168.00 ± 2.93 g/L, which was further enhanced by supplementation with ethanol and specific carbon source combinations, achieving a maximum yield of 259.54 g/L. Optimization of critical fermentation parameters, including maintaining the unadjusted initial pH (~5.20), tea concentrations of 1–2%, cultivation duration, and bi-weekly harvesting over four weeks, significantly increased the cumulative BC yield to 368.22 ± 28.33 g/L under static cultivation at 30 °C. Comprehensive characterization of the produced BC confirmed its favorable physicochemical properties, including a well-defined fiber morphology, high crystallinity, thermal stability, and satisfactory mechanical strength. These results

validate the suitability of Thai red tea kombucha as a culturally relevant and cost-effective substrate for BC biosynthesis. The present study provides essential baseline data to guide subsequent statistical optimization and scale-up efforts aimed at improving BC production efficiency for diverse industrial applications.

3.6 References

Abol-Fotouh D, Hassan MA, Shokry H, et al (2020) Bacterial nanocellulose from agro-industrial wastes: low-cost and enhanced production by Komagataeibacter saccharivorans MD1. Sci Rep 10:1–14. https://doi.org/10.1038/s41598-020-60315-9

Adekoya MA, Liu S, Oluyamo SS, et al (2022) Influence of size classifications on the crystallinity index of Albizia gummifera cellulose. Heliyon 8:. https://doi.org/10.1016/j.heliyon.2022.e12019

Adnan A, Nair GR, Lay MC, et al (2015) Glycerol as a Cheaper Carbon Source in Bacterial Cellulose (BC) Production by Gluconacetobacter Xylinus Dsm46604 in Batch Fermentation System

Agustin S, Wahyuni ET, Suparmo, et al (2021) Production and characterization of bacterial cellulose-alginate biocomposites as food packaging material. Food Res 5:204–210. https://doi.org/10.26656/fr.2017.5(6).733

Agustin YE, Padmawijaya KS (2018) Effect of acetic acid and ethanol as additives on bacterial cellulose production by acetobacter xylinum. IOP Conf Ser Earth Environ Sci 209:. https://doi.org/10.1088/1755-1315/209/1/012045

Agustin YE, Padmawijaya KS, Rixwari HF, Yuniharto VAS (2018) Glycerol as an additional carbon source for bacterial cellulose synthesis. IOP Conf Ser Earth Environ Sci 141:. https://doi.org/10.1088/1755-1315/141/1/012001

Akintunde MO, Adebayo-Tayo BC, Ishola MM, et al (2022) Bacterial Cellulose Production from agricultural Residues by two Komagataeibacter sp. Strains. Bioengineered 13:10010–10025. https://doi.org/10.1080/21655979.2022.2062970

Al-Kalifawi EJ, Hassan IA (2014) Factors Influence on the yield of Bacterial Cellulose of Kombucha (Khubdat Humza). Baghdad Sci J 11:1420–1428. https://doi.org/10.21123/bsj.11.3.1420-1428

AL-Kalifawi EJ, Hassan IA (2014) Factors Influence on the yield of Bacterial Cellulose of Kombucha (Khubdat Humza). Baghdad Sci J 11:1420–1428. https://doi.org/10.21123/bsj.11.3.1420-1428

Al-Kalifawi EJ (2018) Produce bacterial cellulose of kombucha (Khubdat Humza) from honey. J Genet Environ Resour Conserv 2:39–45

Almihyawi RAH, Musazade E, Alhussany N, et al (2024) Production and characterization of bacterial cellulose by Rhizobium sp. isolated from bean root. Sci Rep 14:1–17. https://doi.org/10.1038/s41598-024-61619-w

Amarasekara AS, Wang D, Grady TL (2020) A comparison of kombucha SCOBY bacterial cellulose purification methods. SN Appl Sci 2:1–7. https://doi.org/10.1007/s42452-020-1982-2

Amorim J, Liao K, Mandal A, et al (2024) Impact of Carbon Source on Bacterial Cellulose Network Architecture and Prolonged Lidocaine Release. Polymers (Basel) 16:. https://doi.org/10.3390/polym16213021

Amorim JDP, Costa AFS, Galdino CJS, et al (2019) Bacterial cellulose production using fruit residues as substract to industrial application. Chem Eng Trans 74:1165–1170. https://doi.org/10.3303/CET1974195

Amorim LFA, Fangueiro R, Gouveia IC (2022) Characterization of Bioactive Colored Materials Produced from Bacterial Cellulose and Bacterial Pigments. Materials (Basel) 15:. https://doi.org/10.3390/ma15062069

Amorim LFA, Li L, Gomes AP, et al (2023) Sustainable bacterial cellulose production by low cost feedstock: evaluation of apple and tea by-products as alternative sources of nutrients. Cellulose 30:5589–5606. https://doi.org/10.1007/s10570-023-05238-0

Andritsou V, De Melo EM, Tsouko E, et al (2018) Synthesis and Characterization of

Bacterial Cellulose from Citrus-Based Sustainable Resources. ACS Omega 3:10365–10373. https://doi.org/10.1021/acsomega.8b01315

Aswini K, Gopal NO, Uthandi S (2020) Optimized culture conditions for bacterial cellulose production by Acetobacter senegalensis MA1. BMC Biotechnol 20:1–16. https://doi.org/10.1186/s12896-020-00639-6

Atykyan N, Revin V, Shutova V (2020) Raman and FT-IR Spectroscopy investigation the cellulose structural differences from bacteria Gluconacetobacter sucrofermentans during the different regimes of cultivation on a molasses media. AMB Express 10:. https://doi.org/10.1186/s13568-020-01020-8

Avcioglu NH, Birben M, Seyis Bilkay I (2021) Optimization and physicochemical characterization of enhanced microbial cellulose production with a new Kombucha consortium. Process Biochem 108:60–68. https://doi.org/10.1016/j.procbio.2021.06.005

Azeredo HMC, Barud H, Farinas CS, et al (2019) Bacterial Cellulose as a Raw Material for Food and Food Packaging Applications. Front. Sustain. Food Syst. 3:1–14

Balistreri GN, Campbell IR, Li X, et al (2024) Bacterial cellulose nanoparticles as a sustainable drug delivery platform for protein-based therapeutics. RSC Appl Polym 2:172–183. https://doi.org/10.1039/d3lp00184a

Ball E (1953) Hydrolysis of Sucrose by Autoclaving Media, a Neglected Aspect in the Technique of Culture of Plant Tissues. Bull Torrey Bot Club 80:409–411

Barja F (2021) Bacterial nanocellulose production and biomedical applications. J Biomed Res 35:310–317. https://doi.org/https://doi.org/10.7555/JBR.35.20210036

Betlej I, Salerno-Kochan R, Krajewski KJ, et al (2020) The influence of culture medium components on the physical and mechanical properties of cellulose synthesized by kombucha microorganisms. BioResources 15:3125–3135. https://doi.org/10.15376/biores.15.2.3125-3135

Brandes R, De Souza L, Carminatti C, Recouvreux D (2020) Production with a High Yield of Bacterial Cellulose Nanocrystals by Enzymatic Hydrolysis. Int J Nanosci

19:1–8. https://doi.org/10.1142/S0219581X19500157

Cazón P, Vázquez M (2021) Improving bacterial cellulose films by ex-situ and in-situ modifications: A review. Food Hydrocoll 113:1–9. https://doi.org/10.1016/j.foodhyd.2020.106514

Cerrutti P, Roldán P, García RM, et al (2016) Production of bacterial nanocellulose from wine industry residues: Importance of fermentation time on pellicle characteristics. J Appl Polym Sci 133:1–9. https://doi.org/10.1002/app.43109

Chakravorty S, Bhattacharya S, Chatzinotas A, et al (2016) Kombucha tea fermentation: Microbial and biochemical dynamics. Int J Food Microbiol 220:63–72. https://doi.org/10.1016/j.ijfoodmicro.2015.12.015

Charoenrak S, Charumanee S, Sirisa-ard P, et al (2023) Nanobacterial Cellulose from Kombucha Fermentation as a Potential Protective Carrier of Lactobacillus plantarum under Simulated Gastrointestinal Tract Conditions. Polymers (Basel) 15:. https://doi.org/10.3390/polym15061356

Chen S-Q, Lopez-Sanchez P, Wang D, et al (2018) Mechanical properties of bacterial cellulose synthesised by diverse strains of the genus Komagataeibacter. Food Hydrocoll 1–25. https://doi.org/10.1016/j.foodhyd.2018.02.031.This

Chen SQ, Meldrum OW, Liao Q, et al (2021) The influence of alkaline treatment on the mechanical and structural properties of bacterial cellulose. Carbohydr Polym 271:118431. https://doi.org/10.1016/j.carbpol.2021.118431

Chibrikov V, Pieczywek PM, Cybulska J, Zdunek A (2023) Evaluation of elasto-plastic properties of bacterial cellulose-hemicellulose composite films. Ind Crops Prod 205:117578. https://doi.org/10.1016/j.indcrop.2023.117578

China S La, De Vero L, Anguluri K, et al (2021) Kombucha tea as a reservoir of cellulose producing bacteria: Assessing diversity among komagataeibacter isolates. Appl Sci 11:1–18. https://doi.org/10.3390/app11041595

Chong AQ, Chin NL, Talib RA, Basha RK (2024) Modelling pH Dynamics, SCOBY Biomass Formation, and Acetic Acid Production of Kombucha Fermentation

Using Black, Green, and Oolong Teas. Processes 12:1301. https://doi.org/10.3390/pr12071301

Cielecka I, Ryngajłło M, Maniukiewicz W, Bielecki S (2021a) Highly Stretchable Bacterial Cellulose Produced by. Polymers (Basel) 4455:1–23. https://doi.org/https://doi.org/10.3390/polym13244455

Cielecka I, Ryngajłło M, Maniukiewicz W, Bielecki S (2021b) Response surface methodology-based improvement of the yield and differentiation of properties of bacterial cellulose by metabolic enhancers. Int J Biol Macromol 187:584–593. https://doi.org/10.1016/j.ijbiomac.2021.07.147

Ciolacu D, Ciolacu F, Popa VI (2011) Amorphous cellulose - Structure and characterization. Cellul Chem Technol 45:13–21

Corzo Salinas DR, Sordelli A, Martínez LA, et al (2021) Production of bacterial cellulose tubes for biomedical applications: Analysis of the effect of fermentation time on selected properties. Int J Biol Macromol 189:1–10. https://doi.org/10.1016/j.ijbiomac.2021.08.011

Czernicka M, Zaguła G, Bajcar M, et al (2017) Study of nutritional value of dried tea leaves and infusions of black, green and white teas from Chinese plantations. Rocz Panstw Zakl Hig 68:237–245

Dartiguenave C, Jeandet P, Maujean A (2000) Study of the contribution of the major organic acids of wine to the buffering capacity of wine in model solutions. Am J Enol Vitic 51:352–356. https://doi.org/10.5344/ajev.2000.51.4.352

De Araújo Júnior AM, Braido G, Saska S, et al (2016) Regenerated cellulose scaffolds: Preparation, characterization and toxicological evaluation. Carbohydr Polym 136:892–898. https://doi.org/10.1016/j.carbpol.2015.09.066

de Lange JH (1989) Significance of autoclaving-induced toxicity from and hydrolysis of carbohydrates in in vitro studies of pollen germination and tube growth. South African J Bot 55:1–5. https://doi.org/10.1016/s0254-6299(16)31225-x

De Souza KC, Trindade NM, De Amorim JDP, et al (2021) Kinetic study of a bacterial

cellulose production by komagataeibacter rhaeticus using coffee grounds and sugarcane molasses. Mater Res 24:. https://doi.org/10.1590/1980-5373-MR-2020-0454

Deka H, Sarmah PP, Chowdhury P, et al (2023) Impact of the Season on Total Polyphenol and Antioxidant Properties of Tea Cultivars of Industrial Importance in Northeast India. Foods 12:. https://doi.org/10.3390/foods12173196

Deka H, Sarmah PP, Devi A, et al (2021) Changes in major catechins, caffeine, and antioxidant activity during CTC processing of black tea from North East India. RSC Adv 11:11457–11467. https://doi.org/10.1039/d0ra09529j

Devje S (2022) What Is Thai Tea? Everything You Need to Know About This Sweet, Spiced Delight. https://www.healthline.com/nutrition/thai-tea#basics. Accessed 6 Feb 2023

Dhali K, Ghasemlou M, Daver F, et al (2021) Science of the Total Environment A review of nanocellulose as a new material towards environmental sustainability. Sci Total Environ 775:145871. https://doi.org/10.1016/j.scitotenv.2021.145871

Dusunceli N, Colak OU (2008) Modelling effects of degree of crystallinity on mechanical behavior of semicrystalline polymers. Int J Plast 24:1224–1242. https://doi.org/10.1016/j.ijplas.2007.09.003

El-Gendi H, Taha TH, Ray JB, Saleh AK (2022) Recent advances in bacterial cellulose: a low-cost effective production media, optimization strategies and applications. Cellulose 29:7495–7533

Fahim N, Montazer M (2020) Effect of Althaea officinalis and Green Tea Extracts on the Bacterial Cellulose Production. In: 14 th International Seminar on Polymer Science and Technology (ISPST 2020). Tarbiat Modares University, Tehran - Iran, pp 7–9

Fatima A, Ortiz-Albo P, Neves LA, et al (2023) Biosynthesis and characterization of bacterial cellulose membranes presenting relevant characteristics for air/gas filtration. J Memb Sci 674:. https://doi.org/10.1016/j.memsci.2023.121509

Fei S, Yang X, Xu W, et al (2023) Insights into Proteomics Reveal Mechanisms of Ethanol-Enhanced Bacterial Cellulose Biosynthesis by Komagataeibacter nataicola. Fermentation 9:1–14. https://doi.org/10.3390/fermentation9060575

Feng Y, Ma X, Kong B, et al (2021) Ethanol induced changes in structural, morphological, and functional properties of whey proteins isolates: Influence of ethanol concentration. Food Hydrocoll 111:106379. https://doi.org/10.1016/j.foodhyd.2020.106379

Fontana JD, Franco VC, De Souza SJ, et al (1991) Nature of plant stimulators in the production of Acetobacter xylinum (“tea fungus”) biofilm used in skin therapy. Appl Biochem Biotechnol 28–29:341–351. https://doi.org/10.1007/BF02922613

Fornaro T, Burini D, Biczysko M, Barone V (2015) Hydrogen-bonding effects on infrared spectra from anharmonic computations: Uracil-water complexes and uracil dimers. J Phys Chem A 119:4224–4236. https://doi.org/10.1021/acs.jpca.5b01561

Gao H, Sun Q, Han Z, et al (2020) Comparison of bacterial nanocellulose produced by different strains under static and agitated culture conditions. Carbohydr Polym 227:115323. https://doi.org/10.1016/j.carbpol.2019.115323

Gao M, Ploessl D, Shao Z (2019) Enhancing the co-utilization of biomass-derived mixed sugars by yeasts. Front Microbiol 10:1–21. https://doi.org/10.3389/fmicb.2018.03264

Gaspar D, Fernandes SN, De Oliveira AG, et al (2014) Nanocrystalline cellulose applied simultaneously as the gate dielectric and the substrate in flexible field effect transistors. Nanotechnology 25:. https://doi.org/10.1088/0957-4484/25/9/094008

Gayathri G, Srinikethan G (2019) Bacterial Cellulose production by K. saccharivorans BC1 strain using crude distillery effluent as cheap and cost effective nutrient medium. Int J Biol Macromol 138:950–957. https://doi.org/10.1016/j.ijbiomac.2019.07.159

Gayathry G (2015) Production of Nata de Coco - a Natural Dietary Fibre Product from Mature Coconut Water using Gluconacetobacter xylinum (sju-1). Int J Food

Ferment Technol 5:231. https://doi.org/10.5958/2277-9396.2016.00006.4

Gismatulina YA, Budaeva V V. (2024) Cellulose Nitrates-Blended Composites from Bacterial and Plant-Based Celluloses. Polymers (Basel) 16:. https://doi.org/10.3390/polym16091183

Goh WN, Rosma A, Kaur B, et al (2012) Fermentation of black tea broth (kombucha): I. effects of sucrose concentration and fermentation time on the yield of microbial cellulose. Int Food Res J 19:109–117

Gorgieva S, Trček J (2019) Bacterial cellulose: Production, modification and perspectives in biomedical applications. Nanomaterials 9:1–20. https://doi.org/10.3390/nano9101352

Greenwalt CJ, Steinkraus KH, Ledford RA (2000) Kombucha, the fermented tea: microbiology, composition, and claimed health effects. J Food Prot 7:976–981. https://doi.org/doi: 10.4315/0362-028x-63.7.976

Hamed DA, Maghrawy HH, Abdel Kareem H (2023) Biosynthesis of bacterial cellulose nanofibrils in black tea media by a symbiotic culture of bacteria and yeast isolated from commercial kombucha beverage. World J Microbiol Biotechnol 39:1–16. https://doi.org/10.1007/s11274-022-03485-0

Heydorn RL, Lammers D, Gottschling M, Dohnt K (2023) Effect of food industry by-products on bacterial cellulose production and its structural properties. Cellulose 30:4159–4179. https://doi.org/10.1007/s10570-023-05097-9

Ho Jin Y, Lee T, Kim JR, et al (2019) Improved production of bacterial cellulose from waste glycerol through investigation of inhibitory effects of crude glycerol-derived compounds by Gluconacetobacter xylinus. J Ind Eng Chem 75:158–163. https://doi.org/10.1016/j.jiec.2019.03.017

Hossen MT, Kundu CK, Pranto BRR, et al (2024) Synthesis, characterization, and cytotoxicity studies of nanocellulose extracted from okra (Abelmoschus Esculentus) fiber. Heliyon 10:e25270. https://doi.org/10.1016/j.heliyon.2024.e25270

Hruška J, Köhler S, Bishop K (1999) Buffering processes in a boreal dissolved organic carbon-rich stream during experimental acidification. Environ Pollut 106:55–65. https://doi.org/10.1016/S0269-7491(99)00061-5

Illa MP, Khandelwal M, Sharma CS (2019) Modulated Dehydration for Enhanced Anodic Performance of Bacterial Cellulose derived Carbon Nanofibers. ChemistrySelect 4:6642–6650. https://doi.org/10.1002/slct.201901359

Ito A, Yanase E (2022) Study into the chemical changes of tea leaf polyphenols during japanese black tea processing. Food Res Int 160:. https://doi.org/10.1016/j.foodres.2022.111731

Izawa K, Amino Y, Kohmura M, et al (2010) Human-environment interactions - taste. In: Comprehensive Natural Products II: Chemistry and Biology. pp 631–671

Jacek P, Dourado F, Gama M, Bielecki S (2019) Molecular aspects of bacterial nanocellulose biosynthesis. Microb Biotechnol 12:633–649. https://doi.org/10.1111/1751-7915.13386

Jagannath A, Kalaiselvan A, Manjunatha SS, et al (2008) The effect of pH, sucrose and ammonium sulphate concentrations on the production of bacterial cellulose (Nata-de-coco) by Acetobacter xylinum. World J Microbiol Biotechnol 24:2593–2599. https://doi.org/10.1007/s11274-008-9781-8

Jayabalan R, Malbaša R V., Lončar ES, et al (2014) A review on kombucha tea-microbiology, composition, fermentation, beneficial effects, toxicity, and tea fungus. Compr Rev Food Sci Food Saf 13:538–550. https://doi.org/10.1111/1541-4337.12073

Jayabalan R, Marimuthu S, Swaminathan K (2007) Changes in content of organic acids and tea polyphenols during kombucha tea fermentation. Food Chem 102:392–398. https://doi.org/10.1016/j.foodchem.2006.05.032

Jenkhongkarn R, Phisalaphong M (2023) Effect of Reduction Methods on the Properties of Composite Films of Bacterial Cellulose-Silver Nanoparticles. Polymers (Basel) 15:. https://doi.org/10.3390/polym15142996

Jia Y, Wang X, Huo M, et al (2017) Preparation and characterization of a novel bacterial cellulose/chitosan bio-hydrogel. Nanomater Nanotechnol 7:1–8. https://doi.org/10.1177/1847980417707172

Jiménez-Sánchez A, Hernández-Gil L, Jiménez-Sánchez Y, et al (2024) Production of bacterial cellulose from kombucha tea and coffee husk infusion. Nativa 12:567–573. https://doi.org/10.31413/nat.v12i3.17720

Jittaut P, Hongsachart P, Audtarat S, Dasri T (2023) Production and characterization of bacterial cellulose produced by Gluconacetobacter xylinus BNKC 19 using agricultural waste products as nutrient source. Arab J Basic Appl Sci 30:221–230. https://doi.org/10.1080/25765299.2023.2172844

Junaidi Z, Azlan NM (2012) Optimization of Bacterial Cellulose Production from Pineapple Waste: Effect of Temperature, pH and Concentration. In: 5th Engineering Conference, “Engineering Towards Change - Empowering Green Solutions.” Kuching Sarawak, pp 1–7

Kamal ASM, Misnon MI, Fadil F (2020) The effect of sodium hydroxide concentration on yield and properties of Bacterial Cellulose membranes. IOP Conf Ser Mater Sci Eng 732:. https://doi.org/10.1088/1757-899X/732/1/012064

Kamal T, Ul-Islam M, Fatima A, et al (2022) Cost-Effective Synthesis of Bacterial Cellulose and Its Applications in the Food and Environmental Sectors. Gels 8:552

Kazemi M, Faranak, Doosthoseini K, Azin M (2015) Effect of Ethanol and Medium on Bacterial Cellulose (Bc) Production By Gluconacetobacter Xylinus (Ptcc 1734). Cellul Chem Technol 49:455–462

Keshk SMAS (2014) Vitamin C enhances bacterial cellulose production in Gluconacetobacter xylinus. Carbohydr Polym 99:98–100. https://doi.org/10.1016/j.carbpol.2013.08.060

Keshk SMAS, Sameshima K (2005) Evaluation of different carbon sources for bacterial cellulose production. African J Biotechnol 4:478–482

Khan A, Wen Y, Huq T, Ni Y (2018) Cellulosic Nanomaterials in Food and Nutraceutical Applications: A Review. J Agric Food Chem 66:8–19. https://doi.org/10.1021/acs.jafc.7b04204

Klepacka J, Tonska E, Rafałowski R, et al (2021) Tea as a Source of Biologically Active Compounds in the Human Diet. Molecules 26:1–14. https://doi.org/https://doi.org/10.3390/molecules26051487

Krystynowicz A, Czaja W, Wiktorowska-Jezierska A, et al (2002) Factors affecting the yield and properties of bacterial cellulose. J Ind Microbiol Biotechnol 29:189–195. https://doi.org/10.1038/sj.jim.7000303

Lahiri D, Nag M, Dutta B, et al (2021) Bacterial cellulose: Production, characterization and application as antimicrobial agent. Int. J. Mol. Sci. 22:1–18

Lee J (2023) Exploring Sucrose Fermentation : Microorganisms , Biochemical Pathways , and Applications. Ferment Technol 12:1000166. https://doi.org/10.4172/2167-7972.23.12.166

Lee KR, Jo K, Ra KS, et al (2021) Kombucha fermentation using commercial kombucha pellicle and culture broth as starter. 2061:1–7

Leonarski E, Cesca K, Zanella E, et al (2021a) Production of kombucha-like beverage and bacterial cellulose by acerola byproduct as raw material. Lwt 135:1–8. https://doi.org/10.1016/j.lwt.2020.110075

Leonarski E, Cesca K, Zanella E, et al (2021b) Production of kombucha-like beverage and bacterial cellulose by acerola byproduct as raw material. Lwt 135:1–8. https://doi.org/10.1016/j.lwt.2020.110075

Li Q, Wu Y, Fang R, et al (2021) Application of Nanocellulose as particle stabilizer in food Pickering emulsion: Scope, Merits and challenges. Trends Food Sci Technol 110:573–583. https://doi.org/10.1016/j.tifs.2021.02.027

Lima NF, Maciel GM, Fernandes I de AA, Haminiuk CWI (2023) Optimising the Production Process of Bacterial Nanocellulose: Impact on Growth and Bioactive Compounds. Food Technol Biotechnol 61:494–504.

https://doi.org/10.17113/ftb.61.04.23.8182

Lin D, Liu Z, Shen R, et al (2020) Bacterial cellulose in food industry: Current research and future prospects. Int J Biol Macromol 158:1007–1019. https://doi.org/10.1016/j.ijbiomac.2020.04.230

Lin SP, Loira Calvar I, Catchmark JM, et al (2013) Biosynthesis, production and applications of bacterial cellulose. Cellulose 20:2191–2219. https://doi.org/10.1007/s10570-013-9994-3

Liu D, Martinez-Sanz M, Lopez-Sanchez P, et al (2017) Adsorption behaviour of polyphenols on cellulose is affected by processing history. Food Hydrocoll 63:496–507. https://doi.org/10.1016/j.foodhyd.2016.09.012

Liu X, Cao L, Wang S, et al (2023) Isolation and characterization of bacterial cellulose produced from soybean whey and soybean hydrolyzate. Sci Rep 13:1–10. https://doi.org/10.1038/s41598-023-42304-w

Liu X, Pan L, Cheng Y, et al (2025) Effect of high hydrostatic pressure on Alcalase-assisted hydrolysis of soy protein isolate and the anti-aging activity of the hydrolysates. Process Biochem 156:191–201. https://doi.org/10.1016/j.procbio.2025.05.020

Liu Y, Ying D, Sanguansri L, et al (2018) Adsorption of catechin onto cellulose and its mechanism study: Kinetic models, characterization and molecular simulation. Food Res Int 112:225–232. https://doi.org/10.1016/j.foodres.2018.06.044

Makarewicz M, Drożdż I, Tarko T, Duda-Chodak A (2021) The interactions between polyphenols and microorganisms, especially gut microbiota. Antioxidants 10:1–70. https://doi.org/10.3390/antiox10020188

Mann FM, Dickmann M, Schneider R, et al (2017) Analysis of the role of acidity and tea substrate on the inhibition of α-amylase by Kombucha. J Nutr Food Res Technol 0:1–5. https://doi.org/10.30881/jnfrt.00001

Martirani-VonAbercron SM, Pacheco-Sánchez D (2023) Bacterial cellulose: A highly

versatile nanomaterial. Microb Biotechnol 16:1174–1178. https://doi.org/10.1111/1751-7915.14243

Mehrotra R, Sharma S, Shree N, Kaur K (2023) Bacterial Cellulose: An Ecological Alternative as A Biotextile. Biosci Biotechnol Res Asia 20:449–463. https://doi.org/10.13005/bbra/3101

Minaker SA, Mason RH, Chow DR (2021) Optimizing Color Performance of the Ngenuity 3-Dimensional Visualization System. Ophthalmol Sci 1:100054. https://doi.org/10.1016/j.xops.2021.100054

Miranda B, Lawton NM, Tachibana SR, et al (2016) Titration and HPLC Characterization of Kombucha Fermentation: A Laboratory Experiment in Food Analysis. J Chem Educ 93:1770–1775. https://doi.org/10.1021/acs.jchemed.6b00329

Mohamad S, Abdullah LC, Jamari SS, et al (2022) Production and Characterization of Bacterial Cellulose Nanofiber by Acetobacter Xylinum 0416 Using Only Oil Palm Frond Juice as Fermentation Medium. J Nat Fibers 19:16005–16016. https://doi.org/10.1080/15440478.2022.2140243

Mohammadkazemi F, Azin M, Ashori A (2015) Production of bacterial cellulose using different carbon sources and culture media. Carbohydr Polym 117:518–523. https://doi.org/10.1016/j.carbpol.2014.10.008

Molina-Ramírez C, Castro C, Zuluaga R, Gañán P (2018a) Physical Characterization of Bacterial Cellulose Produced by Komagataeibacter medellinensis Using Food Supply Chain Waste and Agricultural By-Products as Alternative Low-Cost Feedstocks. J Polym Environ 26:830–837. https://doi.org/10.1007/s10924-017-0993-6

Molina-Ramírez C, Enciso C, Torres-Taborda M, et al (2018b) Effects of alternative energy sources on bacterial cellulose characteristics produced by Komagataeibacter medellinensis. Int J Biol Macromol 117:735–741. https://doi.org/10.1016/j.ijbiomac.2018.05.195

Montenegro-Silva P, Ellis T, Dourado F, et al (2024) Enhanced bacterial cellulose

production in Komagataeibacter sucrofermentans: impact of different PQQ-dependent dehydrogenase knockouts and ethanol supplementation. Biotechnol Biofuels Bioprod 17:1–16. https://doi.org/10.1186/s13068-024-02482-9

Moon S-H, Park J-M, Chun H-Y, Kim S-J (2006) Comparisons of physical properties of bacterial celluloses produced in different culture conditions using saccharified food wastes. Biotechnol Bioprocess Eng 11:

Moura TA, Oliveira L, Rocha MS (2019) Effects of caffeine on the structure and conformation of DNA: A force spectroscopy study. Int J Biol Macromol 130:1018–1024. https://doi.org/10.1016/j.ijbiomac.2019.02.125

Muzaifa M, Rohaya S, Nilda C, Harahap KR (2022) Kombucha Fermentation from Cascara with Addition of Red Dragon Fruit (Hylocereus polyrhizus): Analysis of Alcohol Content and Total Soluble Solid. Proc Int Conf Trop Agrifood, Feed Fuel (ICTAFF 2021) 17:125–129. https://doi.org/10.2991/absr.k.220102.020

Naveed M, BiBi J, Kamboh AA, et al (2018) Pharmacological values and therapeutic properties of black tea (Camellia sinensis): A comprehensive overview. Biomed Pharmacother 100:521–531. https://doi.org/10.1016/j.biopha.2018.02.048

Neffe-Skociń ska K, Sionek B, Ś cibisz I, Kołoż yn-Krajewska D (2017) Acid contents and the effect of fermentation condition of Kombucha tea beverages on physicochemical, microbiological and sensory properties. CYTA - J Food 15:601–607. https://doi.org/10.1080/19476337.2017.1321588

Nguyen TA, Nguyen XC (2022) Bacterial Cellulose-Based Biofilm Forming Agent Extracted from Vietnamese Nata-de-Coco Tree by Ultrasonic Vibration Method: Structure and Properties. J Chem 2022:1–10. https://doi.org/10.1155/2022/7502796

Nguyen VT, Flanagan B, Gidley MJ, Dykes GA (2008) Characterization of cellulose production by a Gluconacetobacter xylinus strain from Kombucha. Curr Microbiol 57:449–453. https://doi.org/10.1007/s00284-008-9228-3

Nie W, Zheng X, Feng W, et al (2022) Characterization of bacterial cellulose produced

by Acetobacter pasteurianus MGC-N8819 utilizing lotus rhizome. Lwt 165:. https://doi.org/10.1016/j.lwt.2022.113763

Nurazzi NM, Asyraf MRM, Rayung M, et al (2021) Thermogravimetric analysis properties of cellulosic natural fiber polymer composites: A review on influence of chemical treatments. Polymers (Basel) 13:. https://doi.org/10.3390/polym13162710

Oliver-Ortega H, Geng S, Espinach FX, et al (2021) Bacterial cellulose network from kombucha fermentation impregnated with emulsion-polymerized poly(Methyl methacrylate) to form nanocomposite. Polymers (Basel) 13:1–17. https://doi.org/10.3390/polym13040664

Perna Manrique O, Lanchero RJ, Garrido LV (2018) Effect of the Source of Carbon and Vitamin C Present in Tropical Fruits, on the Production of Cellulose by Glunconacetobacter Xylinus. Indian J Sci Technol 11:1–8. https://doi.org/10.17485/ijst/2018/v11i22/122280

Petrosian A (2021) Production of bacterial cellulose from kombucha SCOBY: optimization of the bioprocess and industrial application. 77

Pham TT, Tran TTA (2023) Evaluation of the Crystallinity of Bacterial Cellulose Produced from Pineapple Waste Solution by Using Acetobacter Xylinum. ASEAN Eng J 13:81–91. https://doi.org/10.11113/aej.V13.18868

Phan ADT, Netzel G, Wang D, et al (2015) Binding of dietary polyphenols to cellulose: Structural and nutritional aspects. Food Chem 171:388–396. https://doi.org/10.1016/j.foodchem.2014.08.118

Photphisutthiphong Y, Vatanyoopaisarn S (2020) The production of bacterial cellulose from organic low-grade rice. Curr Res Nutr Food Sci 8:206–216. https://doi.org/10.12944/CRNFSJ.8.1.19

Phung LT, Kitwetcharoen H, Chamnipa N, et al (2023) Changes in the chemical compositions and biological properties of kombucha beverages made from black teas and pineapple peels and cores. Sci Rep 13:1–20.

https://doi.org/10.1038/s41598-023-34954-7

Potivara K, Phisalaphong M (2019) Development and characterization of bacterial cellulose reinforced with natural rubber. Materials (Basel) 12:. https://doi.org/10.3390/ma12142323

Rabbani FA, Yasin S, Iqbal T, Farooq U (2022) Experimental Study of Mechanical Properties of Polypropylene Random Copolymer and Rice-Husk-Based Biocomposite by Using Nanoindentation. Materials (Basel) 15:1–14. https://doi.org/10.3390/ma15051956

Rahmayetty, Sulaiman F (2023) Wastewater from the Arenga Starch Industry as a Potential Medium for Bacterial Cellulose and Cellulose Acetate Production. Polymers (Basel) 15:1–15. https://doi.org/10.3390/polym15040870

Raiszadeh-Jahromi Y, Rezazadeh-Bari M, Almasi H, Amiri S (2020) Optimization of bacterial cellulose production by Komagataeibacter xylinus PTCC 1734 in a low-cost medium using optimal combined design. J Food Sci Technol 57:2524–2533. https://doi.org/10.1007/s13197-020-04289-6

Ramírez Tapias YA, Di Monte MV, Peltzer MA, Salvay AG (2022) Bacterial cellulose films production by Kombucha symbiotic community cultured on different herbal infusions. Food Chem 372:. https://doi.org/10.1016/j.foodchem.2021.131346

Razali NAM, Sohaimi RM, Othman RNIR, et al (2022) Comparative Study on Extraction of Cellulose Fiber from Rice Straw Waste from Chemo-Mechanical and Pulping Method. Polymers (Basel) 14:. https://doi.org/10.3390/polym14030387

Reiniati I (2017) Bacterial Cellulose Nanocrystals : Production and Application. The University of Western Ontario

Revin V, Liyaskina E, Nazarkina M, et al (2018) Cost-effective production of bacterial cellulose using acidic food industry by-products. Brazilian J Microbiol 49:151–159. https://doi.org/10.1016/j.bjm.2017.12.012

Roberts RJ, Rowe RC, York P (1994) The Poisson's ratio of microcrystalline cellulose.

Int J Pharm 105:177–180. https://doi.org/10.1016/0378-5173(94)90463-4

Ryngajłło M, Jacek P, Cielecka I, et al (2019) Effect of ethanol supplementation on the transcriptional landscape of bionanocellulose producer Komagataeibacter xylinus E25. Appl Microbiol Biotechnol 103:6673–6688. https://doi.org/10.1007/s00253-019-09904-x

Said Azmi SNN, Samsu Z 'Asyiqin, Mohd Asnawi ASF, et al (2023) The production and characterization of bacterial cellulose pellicles obtained from oil palm frond juice and their conversion to nanofibrillated cellulose. Carbohydr Polym Technol Appl 5:100327. https://doi.org/10.1016/j.carpta.2023.100327

Samuel OS, Adefusika AM (2019) Influence of Size Classifications on the Structural and Solid-State Characterization of Cellulose Materials. In: Pascual R, Martín MEE (eds) Cellulose. IntechOpen

Sardjono SA, Suryanto H, Aminnudin, Muhajir M (2019) Crystallinity and morphology of the bacterial nanocellulose membrane extracted from pineapple peel waste using high-pressure homogenizer. In: AIP Conference Proceedings. AIP Publishing, pp 080015-1-080015–5

Schrecker ST, Gostomski PA (2005) Determining the water holding capacity of microbial cellulose. Biotechnol Lett 27:1435–1438. https://doi.org/10.1007/s10529-005-1465-y

Shahidi F, Dissanayaka CS (2023) Phenolic-protein interactions: insight from in-silico analyses – a review. Food Prod Process Nutr 5:. https://doi.org/10.1186/s43014-022-00121-0

Sharma C, Bhardwaj NK, Pathak P (2021) Static intermittent fed-batch production of bacterial nanocellulose from black tea and its modification using chitosan to develop antibacterial green packaging material. J Clean Prod 279:123608. https://doi.org/10.1016/j.jclepro.2020.123608

Shevchuk A, Megías-Pérez R, Zemedie Y, Kuhnert N (2020) Evaluation of carbohydrates and quality parameters in six types of commercial teas by

targeted statistical analysis. Food Res Int 133:109122. https://doi.org/10.1016/j.foodres.2020.109122

Shim E, Kim HR (2019) Coloration of bacterial cellulose using in situ and ex situ methods. Text Res J 89:1297–1310. https://doi.org/10.1177/0040517518770673

Shu CH (2007) Fungal Fermentation for Medicinal Products. In: Yang S-T (ed) Bioprocessing for Value-Added Products from Renewable Resources: New Technologies and Applications. Elsevier B.V., Amsterdam; Boston, pp 447–463

Sinamo KN, Ginting S, Pratama S (2022) Effect of sugar concentration and fermentation time on secang kombucha drink. IOP Conf Ser Earth Environ Sci 977:. https://doi.org/10.1088/1755-1315/977/1/012080

Singhsa P, Narain R, Manuspiya H (2018) Physical structure variations of bacterial cellulose produced by different Komagataeibacter xylinus strains and carbon sources in static and agitated conditions. Cellulose 25:1571–1581. https://doi.org/10.1007/s10570-018-1699-1

Son H, Heo M, Kim Y, Lee S (2001) Optimization of fermentation conditions for the production of bacterial cellulose by a newly isolated Acetobacter . Biotechnol Appl Biochem 33:1–5. https://doi.org/10.1042/ba20000065

Srivastava S, Mathur G (2022) Komagataeibacter saccharivorans strain BC-G1: an alternative strain for production of bacterial cellulose. Biologia (Bratisl) 77:3657–3668. https://doi.org/10.1007/s11756-022-01222-4

Suryanto H, Muhajir M, Sutrisno TA, et al (2019) The Mechanical Strength and Morphology of Bacterial Cellulose Films: The Effect of NaOH Concentration. IOP Conf Ser Mater Sci Eng 515:. https://doi.org/10.1088/1757-899X/515/1/012053

Tabaii MJ, Emtiazi G (2016) Comparison of bacterial cellulose production among different strains and fermented media. Appl Food Biotechnol 3:35–41. https://doi.org/10.22037/afb.v3i1.10582

Tang W, Jia S, Jia Y, Yang H (2010) The influence of fermentation conditions and post-treatment methods on porosity of bacterial cellulose membrane. World J

Microbiol Biotechnol 26:125–131. https://doi.org/10.1007/s11274-009-0151-y

Teixeira SRZ, Dos Reis EM, Apati GP, et al (2019) Biosynthesis and functionalization of bacterial cellulose membranes with cerium nitrate and silver nanoparticles. Mater Res 22:1–13. https://doi.org/10.1590/1980-5373-MR-2019-0054

Teoh AL, Heard G, Cox J (2004) Yeast ecology of Kombucha fermentation. Int J Food Microbiol 95:119–126. https://doi.org/10.1016/j.ijfoodmicro.2003.12.020

Thegreencreator.com (2022) Thai Tea: made from scratch. https://thegreencreator.com/thai-tea/. Accessed 8 Aug 2024

Theppakorn T, Luthfiyyah A, Ploysri K (2014) Comparison of the Composition and Antioxidant Capacities of Green Teas Produced From the Assam and the Chinese Varieties Cultivated in Thailand. J Microbiol Biotechnol food Sci 3:364–370

Thielemans K, De Bondt Y, Comer L, et al (2023) Decreasing the Crystallinity and Degree of Polymerization of Cellulose Increases Its Susceptibility to Enzymatic Hydrolysis and Fermentation by Colon Microbiota. Foods 12:1100. https://doi.org/10.3390/foods12051100

Thorat MN, Dastager SG (2018) High yield production of cellulose by a: Komagataeibacter rhaeticus PG2 strain isolated from pomegranate as a new host. RSC Adv 8:29797–29805. https://doi.org/10.1039/c8ra05295f

Trevino-Garza MZ, Guerrero-Medina AS, González-Sánchez RA, et al (2020) Production of Microbial Cellulose Films from Green Tea (Camellia Sinensis) Kombucha with Various Carbon Sources. MDPI Coat 10:1–14. https://doi.org/doi:10.3390/coatings10111132

Treviño-Garza MZ, Guerrero-Medina AS, González-Sánchez RA, et al (2020) Production of microbial cellulose films from green tea (Camellia sinensis) kombucha with various carbon sources. Coatings 10:1–14. https://doi.org/10.3390/coatings10111132

Tsouko E, Kourmentza C, Ladakis D, et al (2015) Bacterial cellulose production from industrial waste and by-product streams. Int J Mol Sci 16:14832–14849.

https://doi.org/10.3390/ijms160714832

Tureck BC, Hackbarth HG, Neves EZ, et al (2021) Obtaining and characterization of bacterial cellulose synthesized by Komagataeibacter hansenii from alternative sources of nitrogen and carbon. Rev Mater 26:. https://doi.org/10.1590/S1517-707620210004.1392

U˘gurel C, Ö˘güt H (2024) Optimization of Bacterial Cellulose Production by Komagataeibacter rhaeticus K23. fibers 12:1–16. https://doi.org/https://doi.org/10.3390/fib12030029

Ul-Islam M, Khan T, Park JK (2012) Water holding and release properties of bacterial cellulose obtained by in situ and ex situ modification. Carbohydr Polym 88:596–603. https://doi.org/10.1016/j.carbpol.2012.01.006

Ullah MW, Manan S, Kiprono S, Islam MU (2019) Synthesis , Structure , and Properties of Bacterial Cellulose. In: Huang J, Dufresne A, Lin N (eds) Nanocellulose: From Fundamentals to AdvancedMaterials, first. Wiley-VCHVerlag GmbH& Co. KGaA, pp 81–114

Vasconcellos VM, Farinas CS (2018) The effect of the drying process on the properties of bacterial cellulose films from gluconacetobacter hansenii. Chem Eng Trans 64:145–150. https://doi.org/10.3303/CET1864025

Villarreal-Soto SA, Beaufort S, Bouajila J, et al (2018) Understanding Kombucha Tea Fermentation: A Review. J Food Sci 83:580–588. https://doi.org/10.1111/1750-3841.14068

Vohra B, Fazry S, Sairi F, Othman BA (2019) Effects of medium variation and fermentation time towards the pH level and ethanol content of Kombucha. In: AIP Conference Proceedings

Volova TG, Prudnikova S V., Kiselev EG, et al (2022) Bacterial Cellulose (BC) and BC Composites: Production and Properties. Nanomaterials 12:. https://doi.org/10.3390/nano12020192

Waghmare PR, Patil SM, Jadhav SL, et al (2018) Utilization of agricultural waste

biomass by cellulolytic isolate Enterobacter sp. SUK-Bio. Agric Nat Resour 52:399–406. https://doi.org/10.1016/j.anres.2018.10.019

Wang B, Rutherfurd-Markwick K, Naren N, et al (2023a) Microbiological and Physico-Chemical Characteristics of Black Tea Kombucha Fermented with a New Zealand Starter Culture. Foods 12:. https://doi.org/10.3390/foods12122314

Wang B, Rutherfurd-Markwick K, Zhang XX, Mutukumira AN (2022a) Kombucha: Production and Microbiological Research †. Foods 11:1–18. https://doi.org/10.3390/foods11213456

Wang C, Han J, Pu Y, Wang X (2022b) Tea (Camellia sinensis): A Review of Nutritional Composition, Potential Applications, and Omics Research. Appl Sci 12:1–20. https://doi.org/10.3390/app12125874

Wang G, Liu J, Liu X, et al (2023b) Oxidation-resistant vitamin C/MXene foam via surface hydrogen bonding for stable electromagnetic interference shielding in air ambient. Appl Surf Sci 610:155396. https://doi.org/10.1016/j.apsusc.2022.155396

Wang J, Tavakoli J, Tang Y (2019) Bacterial cellulose production , properties and applications with di ff erent culture methods – A review. Carbohydr Polym 219:63–76. https://doi.org/10.1016/j.carbpol.2019.05.008

Wang SS, Han YH, Chen JL, et al (2018) Insights into bacterial cellulose biosynthesis from different carbon sources and the associated biochemical transformation pathways in Komagataeibacter sp. W1. Polymers (Basel) 10:. https://doi.org/10.3390/polym10090963

Wang T, Wang J, Han D, et al (2024) Elucidating the adsorption mechanisms of yeast extract on trimethylamine and dimethylamine based on multi-spectroscopic techniques and molecular docking. J Mol Liq 405:125087. https://doi.org/10.1016/j.molliq.2024.125087

Wang W, Khabazian S, Roig-Sanchez S, et al (2021) Carbons derived from alcohol-treated bacterial cellulose with optimal porosity for Li–O2 batteries. Renew Energy 177:209–215. https://doi.org/10.1016/j.renene.2021.05.059

Wang YY, Zhao XQ, Li DM, et al (2023c) Review on the strategies for enhancing mechanical properties of bacterial cellulose. J Mater Sci 58:15265–15293. https://doi.org/10.1007/s10853-023-08803-x

Wen W, Hu M, Gao Y, et al (2024) Effect of Soy Protein Products on Growth and Metabolism of Bacillus subtilis, Streptococcus lactis, and Streptomyces clavuligerus. Foods 13:. https://doi.org/10.3390/foods13101525

Wu JM, Liu RH (2013) Cost-effective production of bacterial cellulose in static cultures using distillery wastewater. J Biosci Bioeng 115:284–290. https://doi.org/10.1016/j.jbiosc.2012.09.014

Wu LM, Tong DS, Zhao LZ, et al (2014) Fourier transform infrared spectroscopy analysis for hydrothermal transformation of microcrystalline cellulose on montmorillonite. Appl Clay Sci 95:74–82. https://doi.org/10.1016/j.clay.2014.03.014

Yamano H, Miyagawa K (1997) Buffer Capacity Curves of Green Tea Extracts Using a Personal Computer with Numerically Treated Online Software. Food Sci Technol Int Tokyo 3:69–73. https://doi.org/10.3136/fsti9596t9798.3.69

Yanti NA, Ahmad SW, Muhiddin NH (2018) Evaluation of inoculum size and fermentation period for bacterial cellulose production from sago liquid waste. J Phys Conf Ser 1116:. https://doi.org/10.1088/1742-6596/1116/5/052076

Yao H, Dai Q, You Z (2015) Fourier Transform Infrared Spectroscopy characterization of aging-related properties of original and nano-modified asphalt binders. Constr Build Mater 101:1078–1087. https://doi.org/10.1016/j.conbuildmat.2015.10.085

Yilmaz M, Goksungur Y (2024) Optimization of Bacterial Cellulose Production from Waste Figs by Komagataeibacter xylinus. Fibers 12:1–18. https://doi.org/10.3390/fib12030029

Zeng M, Laromaine A, Roig A (2014) Bacterial cellulose films: influence of bacterial strain and drying route on film properties. Cellulose 21:4455–4469. https://doi.org/10.1007/s10570-014-0408-y

Zeng X, Liu J, Chen J, et al (2011) Screening of the common culture conditions affecting crystallinity of bacterial cellulose. J Ind Microbiol Biotechnol 38:1993–1999. https://doi.org/10.1007/s10295-011-0989-5

Zhang H, Chen C, Yang J, et al (2022) Effect of Culture Conditions on Cellulose Production by a Komagataeibacter xylinus Strain. Macromol Biosci 22:. https://doi.org/10.1002/mabi.202100476

Zhang K, Huang J, Wang D, et al (2024) Covalent polyphenols-proteins interactions in food processing: formation mechanisms, quantification methods, bioactive effects, and applications. Front Nutr 11:1–15. https://doi.org/10.3389/fnut.2024.1371401

Zhao ZJ, Sui YC, Wu HW, et al (2018) Flavour chemical dynamics during fermentation of kombucha tea. Emirates J Food Agric 30:732–741. https://doi.org/10.9755/ejfa.2018.v30.i9.1794

Zheng D, Zhang Y, Guo Y, Yue J (2019) Isolation and characterization of nanocellulose with a novel shape from walnut (Juglans Regia L.) shell agricultural waste. Polymers (Basel) 11:. https://doi.org/10.3390/polym11071130

Zheng G, Su H, Cheng Y (2023) Role of Carbon Dioxide, Ammonia, and Organic Acids in Buffering Atmospheric Acidity: The Distinct Contribution in Clouds and Aerosols. Environ Sci Technol 57:12571–12582. https://doi.org/10.1021/acs.est.2c09851

Zubaidah E, Ifadah RA, Afgani CA (2019) Changes in chemichal characteristics of kombucha from various cultivars of snake fruit during fermentation. IOP Conf Ser Earth Environ Sci 230:. https://doi.org/10.1088/1755-1315/230/1/012098

Zywicka A, Peitler D, Rakoczy R, et al (2015) The Effect of Different Agitation Modes on Bacterial Cellulose Synthesis. Acta Sci Pol Zootech 14:137–150